Wavelet FDTD Methods and Applications in Nano-Photonics

Wolfgang Freude, Masafumi Fujii*,
Christian Koos, Jan-Michael Brosi, Ayan Maitra,
Christopher G. Poulton[†], Jin Wang, Juerg Leuthold

Institute of High-Frequency and Quantum Electronics (IHQ), University of Karlsruhe, Germany
*Department of Electrical, Electronic and System Engineering, University of Toyama, Japan
[†]Now with Max-Planck Research Group for Optics, Inform. & Photonics, Univ. of Erlangen-Nuremberg, Germany

Universität Karlsruhe (TH)
Institut für Hochfrequenztechnik und Quantenelektronik (IHQ)
http://www.ihq.uni-karlsruhe.de

The 386th Wilhelm and Else Heraeus Seminar: Computational Nano-Photonics
February 26-28, 2007, Bad Honnef, Germany

Acknowledgements

Many thanks to all who have contributed to the content presented here:

Masafumi Fujii
Jan-Michael Brosi
Christopher G. Poulton
Felix Glöckler
Christian Koos
Ayan Maitra
Jin Wang
Jürg Leuthold

We acknowlege support of

- Center for Functional Nanostructures (CFN) of the Deutsche Forschungsgemeinschaft (DFG) within Projects A3.1 and A4.4
- DFG Priority Program SP 1113 "Photonic Crystals"
- DFG Research Training Group 786 "Mixed Fields and Nonlinear Interactions"
- Deutsche Telekom Stiftung
- National Institute of Information and Communications Technology (NICT), Japan
- Scientific Research Grant in Aid from the Japan Society for the Promotion of Science (JSPS)

Outline

- Wavelets
  What are they good for?
- Finite-differences in time-domain
  Yee's leapfrog algorithm
  Numerical dispersion, stability and accuracy
  Higher-order finite-differences
  Method of weighted residuals: Collocation
- Wavelet FDTD
  Numerical dispersion, stability and accuracy
  What should be further done?
  Dispersive and nonlinear media
- Application examples in nano-photonics
  Waveguide roughness
  Slow light in a photonic crystal with disorder
  Four-wave mixing in a microring resonator
  Switching of a Bragg grating
- Summary and further reading

Outline

- Wavelets
  - What are they good for? Notation
- Finite-differences in time-domain
  - Yee's leapfrog algorithm
  - Numerical dispersion, stability and accuracy
  - Higher-order finite-differences
  - Method of weighted residuals: Collocation
- Wavelet FDTD
  - Numerical dispersion, stability and accuracy
  - What should be further done?
  - Dispersive and nonlinear media
- Application examples in nano-photonics
  - Waveguide roughness
  - Slow light in a photonic crystal with disorder
  - Four-wave mixing in a microring resonator
  - Switching of a Bragg grating
- Summary and further reading

Correlation, Convolution and Inner Product

Convolution:

$$v(t) * w(t) = \int_{-\infty}^{+\infty} v(t) \; w\underbrace{(t' - t)}_{\downarrow} \, \mathrm{d}t = \int_{-\infty}^{+\infty} \bar{v}(f) \, \bar{w}(f) \, \mathrm{e}^{\mathrm{j}\, 2\pi f t'} \, \mathrm{d}f$$

Correlation:

$$v(t) \otimes w(t) = \int_{-\infty}^{+\infty} v(t) \, w^* \overbrace{(t - t')}^{\uparrow} \, \mathrm{d}t = \int_{-\infty}^{+\infty} \bar{v}(f) \, \bar{w}^*(f) \, \mathrm{e}^{\mathrm{j}\, 2\pi f t'} \, \mathrm{d}f$$

Inner product:

$$\langle w(t) | v(t) \rangle = \int_{-\infty}^{+\infty} v(t) \, w^*(t) \, \mathrm{d}t \qquad = \int_{-\infty}^{+\infty} \bar{v}(f) \, \bar{w}^*(f) \, \mathrm{d}f$$

Fourier Transform

$$\breve{v}(f) = \left\langle e^{+j\,2\pi f t} \,\middle|\, v(t) \right\rangle = \int_{-\infty}^{+\infty} v(t)\, e^{-j\,2\pi f t}\, dt$$

$$v(t) = \left\langle e^{-j\,2\pi f t} \,\middle|\, \breve{v}(f) \right\rangle = \int_{-\infty}^{+\infty} \breve{v}(f)\, e^{+j\,2\pi f t}\, df$$

Outline

- Wavelets
  What are they good for? Fourier and uncertainty
- Finite-differences in time-domain
  Yee's leapfrog algorithm
  Numerical dispersion, stability and accuracy
  Higher-order finite-differences
  Method of weighted residuals: Collocation
- Wavelet FDTD
  Numerical dispersion, stability and accuracy
  What should be further done?
  Dispersive and nonlinear media
- Application examples in nano-photonics
  Waveguide roughness
  Slow light in a photonic crystal with disorder
  Four-wave mixing in a microring resonator
  Switching of a Bragg grating
- Summary and further reading

Fourier Transform and Uncertainty

A well localized time function $v_s(t) = \frac{1}{\sqrt{s}} v(t/s)$ (small s) has a widespread Fourier spectrum $\breve{v}_s(f) = \sqrt{s}\, \breve{v}(sf)$:

$$\breve{v}_s(f) = \int_{-\infty}^{+\infty} \underbrace{\frac{1}{\sqrt{s}} v(t/s)}_{v_s(t)} \mathrm{e}^{-\mathrm{j}\, 2\pi f t}\, \mathrm{d}t = \sqrt{s}\, \breve{v}(sf),$$

Energy conservation: $W_t = \int_{-\infty}^{+\infty} |v_s(t)|^2 \,\mathrm{d}t = \int_{-\infty}^{+\infty} |\breve{v}_s(f)|^2 \,\mathrm{d}f = W_f$

Expected location in time and frequency domain:

$$\bar{t} = \frac{1}{W_t} \int_{-\infty}^{+\infty} t\, |v_s(t)|^2 \,\mathrm{d}t\,, \qquad \bar{f} = \frac{1}{W_f} \int_{-\infty}^{+\infty} f\, |\breve{v}_s(f)|^2 \,\mathrm{d}f$$

Location variances in time and frequency domain:

$$\sigma_t^2 = \frac{1}{W_t} \int_{-\infty}^{+\infty} (t - \bar{t})^2\, |v_s(t)|^2 \,\mathrm{d}t\,, \qquad \sigma_f^2 = \frac{1}{W_f} \int_{-\infty}^{+\infty} (f - \bar{f})^2\, |\breve{v}_s(f)|^2 \,\mathrm{d}f$$

Uncertainty of time and frequency spread: $\sigma_t^2\, (2\pi\sigma_f)^2 \geq \frac{1}{4}$

Fourier Transform, Uncertainty and Compact Support

Uncertainty of time and angular frequency spread: $\sigma_t^2\,\sigma_\omega^2 \geq \frac{1}{4}$

Gaussian wave function: zero mean, $\omega = 2\pi f$, $\int_{-\infty}^{+\infty} v_s(t)\,\mathrm{d}t = 1$:

$$v(t) = \frac{1}{\sqrt{2\pi\sigma^2}}\,\mathrm{e}^{-\frac{t^2}{2\sigma^2}}, \qquad \breve{v}(f) = \mathrm{e}^{-\frac{\omega^2}{2/\sigma^2}} = \mathrm{e}^{-\frac{\omega^2}{2\sigma'^2}}, \qquad \sigma^2\sigma'^2 = 1$$

Variances of location probabilities in time and spectrum:

$$\sigma_t^2 = \frac{1}{W_t}\int_{+\infty}^{+\infty} t^2\,v^2(t)\,\mathrm{d}t = \frac{\sigma^2}{2}, \qquad \sigma_\omega^2 = \frac{1}{W_\omega}\int_{+\infty}^{+\infty} \omega^2\,\breve{v}^2(f)\,\mathrm{d}\omega = \frac{1/\sigma^2}{2}$$

Minimum location uncertainty (Gaussian wave function): $\sigma_t^2\,\sigma_\omega^2 = \frac{1}{4}$

Compact support: If $v(t) \neq 0\ \forall t \in [a, b]$ has compact support, then $\breve{v}(f)$ cannot have compact support included in $[-c, +c]$:

$$v(t) \overset{?}{=} \int_{-c}^{+c} \mathrm{d}f\,\breve{v}(f)\,\mathrm{e}^{\mathrm{j}\,2\pi f t} = \int_a^b \mathrm{d}t'\,v(t') \underbrace{\int_{-c}^{+c} \mathrm{d}f\,\mathrm{e}^{\mathrm{j}\,2\pi f(t'-t)}}_{\underset{c\to\infty}{=}\ \delta(t'-t)} \neq v(t)$$

Short-Time Fourier Transform

Fourier transform measures similarity of signal $v(t)$ with harmonic function localized in frequency f':

$$\bar{v}(f') = \left\langle \mathrm{e}^{\mathrm{j}\,2\pi f' t} \middle| v(t) \right\rangle = \int_{-\infty}^{+\infty} v(t)\, \mathrm{e}^{-\mathrm{j}\,2\pi f' t}\, \mathrm{d}t$$

Gabor transform measures similarity of signal $v(t)$ with a window $w(t-t')\,\mathrm{e}^{\mathrm{j}\,2\pi f' t}$ localized at time t' and frequency f' ($\widehat{=}$ similarity of windowed signal $v(t)\,w(t-t')$ with harmonic function):

$$\bar{v}(t', f') = \left\langle w(t-t')\,\mathrm{e}^{\mathrm{j}\,2\pi f' t} \middle| v(t) \right\rangle = \int_{-\infty}^{+\infty} v(t)\, w^*(t-t')\, \mathrm{e}^{-\mathrm{j}\,2\pi f' t}\, \mathrm{d}t$$

$$= \left\langle \mathrm{e}^{\mathrm{j}\,2\pi f' t} \middle| v(t)\, w^*(t-t') \right\rangle = \int_{-\infty}^{+\infty} v(t)\, w^*(t-t')\, \mathrm{e}^{-\mathrm{j}\,2\pi f' t}\, \mathrm{d}t$$

Spread of Gabor window in time and frequency σ_t, σ_f is fixed and *independent* of its position in time and frequency $t' = \bar{t}$, $f' = \bar{f}$.

Further functions to which a signal may be compared?

Short-Time Fourier Trafo (STFT) — Contin. Wavelet Trafo (CWT)

Gabor "atom" (1946) is finite-length window $w(t)$ at $t = t'$ multiplied with impulse response of a zero-width bandpass at $f = f'$ (uncertainty rectangles $\sigma_t\,\sigma_\omega \geq \frac{1}{2}$):

$$w_{t',f'}(t) = w(t - t')\,\mathrm{e}^{\mathrm{j}\,2\pi f' t}, \qquad \breve{v}(t', f') = \int_{-\infty}^{+\infty} v(t)\,w^*(t - t')\,\mathrm{e}^{-\mathrm{j}\,2\pi f' t}\,\mathrm{d}t$$

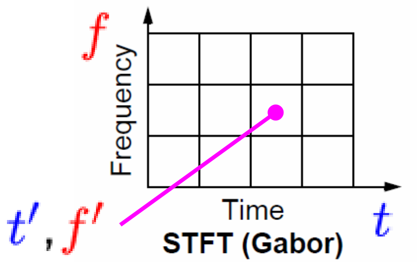

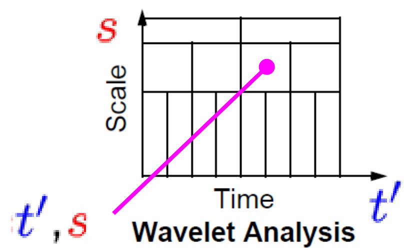

Wavelet $\psi(t)$ is function with $\int_{-\infty}^{+\infty} \psi(t)\,\mathrm{d}t = 0$ ($\breve{\psi}(0) = 0$). Dilated with scale factor s, translated by t' $\rightarrow$ wavelet trafo $\hat{v}(t', s)$ of $v(t)$:

$$\psi_{t'}^{s}(t) = \frac{1}{\sqrt{s}}\,\psi\Big(\frac{t - t'}{s}\Big), \qquad \hat{v}(t', s) = \int_{-\infty}^{+\infty} v(t)\,\frac{1}{\sqrt{s}}\,\psi^*\Big(\frac{t - t'}{s}\Big)\,\mathrm{d}t$$

Outline

- Wavelets
  - What are they good for? Haar wavelet
- Finite-differences in time-domain
  - Yee's leapfrog algorithm
  - Numerical dispersion, stability and accuracy
  - Higher-order finite-differences
  - Method of weighted residuals: Collocation
- Wavelet FDTD
  - Numerical dispersion, stability and accuracy
  - What should be further done?
  - Dispersive and nonlinear media
- Application examples in nano-photonics
  - Waveguide roughness
  - Slow light in a photonic crystal with disorder
  - Four-wave mixing in a microring resonator
  - Switching of a Bragg grating
- Summary and further reading

The Shape of Wavelets — Haar Wavelet and Scaling Function

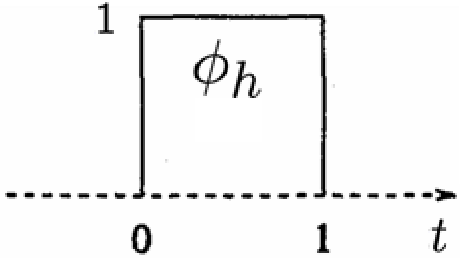

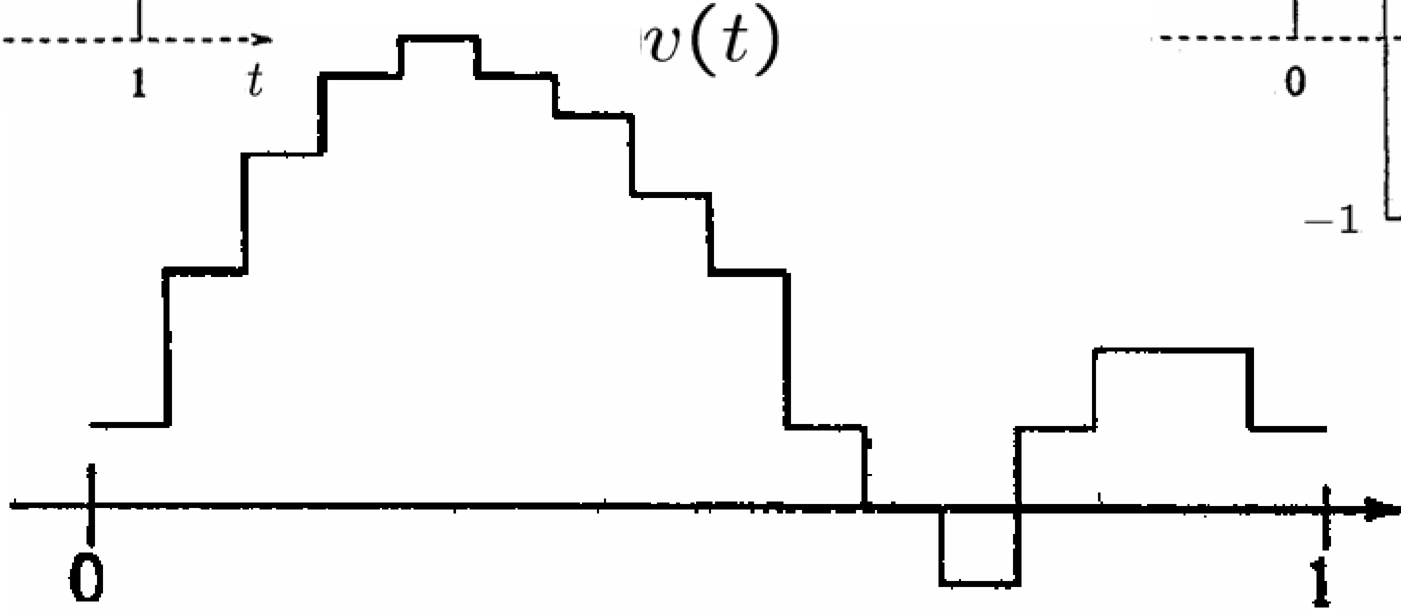

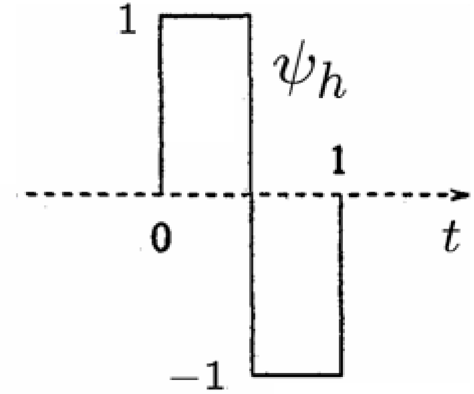

Wavelet $\psi(t)$ dilated and translated: $\psi_{t'}^{s}(t) = \frac{1}{\sqrt{s}}\,\psi\left(\frac{t-t'}{s}\right)$

Not sufficient, DC part is missing:

Scaling function $\phi(t)$ dilated and translated: $\phi_{t'}^{s}(t) = \frac{1}{\sqrt{s}}\,\phi\left(\frac{t-t'}{s}\right)$

Outline

- Wavelets
  What are they good for? Wavelet transform
- Finite-differences in time-domain
  Yee's leapfrog algorithm
  Numerical dispersion, stability and accuracy
  Higher-order finite-differences
  Method of weighted residuals: Collocation
- Wavelet FDTD
  Numerical dispersion, stability and accuracy
  What should be further done?
  Dispersive and nonlinear media
- Application examples in nano-photonics
  Waveguide roughness
  Slow light in a photonic crystal with disorder
  Four-wave mixing in a microring resonator
  Switching of a Bragg grating
- Summary and further reading

Continuous Wavelet Transform — "Mother" of Wavelets

Wavelet $\psi(t)$ ("ondelette", small wave) is waveform of limited duration with average value of zero ($\widehat{=}$ impulse response of "bandpass").

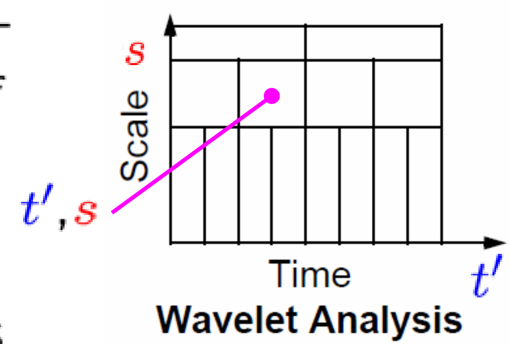

Wavelet $\psi(t)$ dilated with scale factor $s \neq 0$, translated by t' → wavelet transform $\hat{v}(t', s)$ is correlation of $v(t)$ with BP impulse response:

$$\psi_{t'}^{s}(t) = \frac{1}{\sqrt{s}}\,\psi\Big(\frac{t-t'}{s}\Big), \qquad \hat{v}(t', s) = \int_{-\infty}^{+\infty} v(t)\,\frac{1}{\sqrt{s}}\,\psi^{*}\Big(\frac{t-t'}{s}\Big)\,\mathrm{d}t$$

Wavelet transform is complete and energy conserving if $\psi(t)$ with:

- Admissibility condition $0 < C_\psi := \int_0^\infty \Big|\frac{1}{\sqrt{f}}\,\breve{\psi}(f)\Big|^2 \mathrm{d}f < \infty$
- Zero mean (convergence!) $\int_{-\infty}^{+\infty} \psi(t)\,\mathrm{d}t = 0, \quad \breve{\psi}(0) = 0$
- Normalization $\big\|\psi(t)\big\|^2 := \int_{-\infty}^{+\infty} |\psi(t)|^2\,\mathrm{d}t = 1$

Continuous Wavelet Transform (CWT) for "Mother" Wavelet $\psi(t)$

Wavelet transform $\widehat{v}(t', s)$ of $v(t)$ is cross-correlation ($\otimes$) with dilated (scaled) impulse response $\psi^s(t) = \frac{1}{\sqrt{s}}\,\psi\big(\frac{t}{s}\big)$ of a band-pass:

$$\widehat{v}(t', s) = \int_{-\infty}^{+\infty} \mathrm{d}t\; v(t)\, \frac{1}{\sqrt{s}}\, \psi^*\Big(\frac{t - t'}{s}\Big) = v(t) \otimes \frac{1}{\sqrt{s}}\, \psi\Big(\frac{t}{s}\Big)$$

Bandpass, because Fourier transform $\breve{\psi}^s(f)$ of $\psi^s(t) = \frac{1}{\sqrt{s}}\,\psi(\frac{t}{s})$ is

$$\breve{\psi}^s(f) = \int_{-\infty}^{+\infty} \frac{1}{\sqrt{s}}\, \psi\Big(\frac{t}{s}\Big)\, \mathrm{e}^{-\mathrm{j}\,2\pi f t}\, \mathrm{d}t = \sqrt{s}\, \breve{\psi}(s f),$$

and because of $\int_{-\infty}^{+\infty} \psi(t)\, \mathrm{d}t = 0$ or $\breve{\psi}(0) = 0$: The DC component $f = 0$ of the transfer function disappears → oscillation around time axis → naming "wavelet",

$$\breve{\psi}^s(0) = \int_{-\infty}^{+\infty} \frac{1}{\sqrt{s}}\, \psi\Big(\frac{t}{s}\Big)\, \mathrm{d}t = 0\,.$$

CWT: Correlation with dilated (scaled) impulse responses $\frac{1}{\sqrt{s}}\,\psi(\frac{t}{s})$ of hypothetical *band-pass* filters $\sqrt{s}\, \breve{\psi}(s f)$.

Inverse Continuous Wavelet Transform (ICWT) for Mother $\psi(t)$

Wavelet transform $\widehat{v}(t',s)$ of $v(t)$ is cross-correlation ($\otimes$) with dilated (scaled) impulse response $\psi^s(t) = \frac{1}{\sqrt{s}}\,\psi\big(\frac{t}{s}\big)$ of a band-pass:

$$\widehat{v}(t',s) = \int_{-\infty}^{+\infty} \mathrm{d}t_1\; v(t_1)\,\frac{1}{\sqrt{s}}\,\psi^*\Big(\frac{t_1-t'}{s}\Big) = v(t_1)\otimes\frac{1}{\sqrt{s}}\,\psi\Big(\frac{t_1}{s}\Big)$$

Inverse wavelet transform $v(t)$ of $\widehat{v}(t',s)$ is double integral:

$$v(t) = \frac{1}{C_\psi}\int_0^\infty \frac{1}{s^2}\,\mathrm{d}s\int_{-\infty}^{+\infty}\mathrm{d}t'\;\widehat{v}(t',s)\,\frac{1}{\sqrt{s}}\,\psi\Big(\frac{t-t'}{s}\Big),$$

$$0 < C_\psi := \int_0^\infty \Big|\frac{1}{\sqrt{f}}\,\breve{\psi}(f)\Big|^2\mathrm{d}f = \int_0^\infty \Big|\frac{1}{\sqrt{s}}\,\breve{\psi}(sf)\Big|^2\mathrm{d}s < \infty$$

Energy conservation ("Parceval") between time and WT domain:

$$1 = \int_{-\infty}^{+\infty}\mathrm{d}t\;|v(t)|^2 = \frac{1}{C_\psi}\int_0^\infty\frac{\mathrm{d}s}{s^2}\int_{-\infty}^{+\infty}\mathrm{d}t'\;|\widehat{v}(t',s)|^2 \qquad (s\neq 0)$$

ICWT proof by substituting $\widehat{v}(t',s)$, $\delta(x-x_0) = \int_{-\infty}^{+\infty} \mathrm{e}^{\pm\mathrm{j}\,2\pi(x-x_0)y}\,\mathrm{d}y$,

$$\frac{1}{\sqrt{s}}\,\psi^*\Big(\frac{t_1-t'}{s}\Big) = \int_{-\infty}^{+\infty}\mathrm{d}f_1\;\sqrt{s}\;\breve{\psi}^*(sf_1)\,\mathrm{e}^{\mathrm{j}\,2\pi f_1 t'}\,\mathrm{e}^{-\mathrm{j}\,2\pi f_1 t_1}\,.$$

Scaling Function is Aggregation (“Father”) of Wavelets

When CWT $\hat{g}(t', s)$ is known only for $s < s_0$, to recover $g(t)$ we need complimentary information corresponding to $\hat{g}(t', s)$ for $s > s_0$.

Inverse wavelet transform $v(t)$ of $\hat{v}(t', s)$ then splits in two parts:

$$v(t) = \overbrace{\frac{1}{C_\psi} \int_0^{s_0} \frac{1}{s^2} \mathrm{d}s \underbrace{\int_{-\infty}^{+\infty} \mathrm{d}t' \, \hat{v}(t', s) \, \frac{1}{\sqrt{s}} \psi\Big(\frac{t - t'}{s}\Big)}_{(\cdots)}}^{v_{\mathrm{BP}}(t)} + \overbrace{\frac{1}{C_\psi} \int_{s_0}^{\infty} \frac{1}{s^2} \mathrm{d}s \, (\cdots)}^{v_{\mathrm{LP}}(t)}$$

Meaning of $v_{\mathrm{LP}}(t)$:

$$v(t) = v_{\mathrm{BP}}(t) + v_{\mathrm{LP}}(t) = \frac{1}{C_\psi} \int_{-\infty}^{+\infty} \mathrm{d}t_1 \, v(t_1) \int_{-\infty}^{+\infty} \mathrm{d}f_1 \, \mathrm{e}^{-\mathrm{j}\,2\pi f_1 (t_1 - t)}$$

$$\times \left[\int_0^{s_0 f_1} \frac{\mathrm{d}f}{f} \left| \breve{\psi}(f) \right|^2 + \underbrace{\int_{s_0 f_1}^{\infty} \frac{\mathrm{d}f}{f} \left| \breve{\psi}(f) \right|^2}_{=: \left| \sqrt{s_0} \, \breve{\phi}(s_0 f_1) \right|^2} \right]$$

Scaling function $\phi^s(t) = \frac{1}{\sqrt{s}} \phi\left(\frac{t}{s}\right)$ *defined* as aggregation of wavelets $\psi^s(t)$ at scales $s > s_0$. Its FT has arbitrary phase.

Meaning of Scaling Function

Computation of $v_{\mathrm{LP}}(t)$:

$$\left|\sqrt{s_0}\,\bar{\phi}(s_0 f_1)\right|^2 := \int_{s_0 f_1}^{\infty} \left|\frac{1}{\sqrt{f}}\,\bar{\psi}(f)\right|^2 \mathrm{d}f = \int_{s_0}^{\infty} \left|\frac{1}{\sqrt{s}}\,\bar{\psi}(s f_1)\right|^2 \mathrm{d}s\,,$$

$$v_{\mathrm{LP}}(t) = \frac{1}{C_\psi} \int_{-\infty}^{+\infty} \mathrm{d}t_1\, v(t_1) \int_{-\infty}^{+\infty} \mathrm{d}f_1\, \mathrm{e}^{-\mathrm{j}\,2\pi f_1 (t_1 - t)} \int_{s_0 f_1}^{\infty} \frac{\mathrm{d}f}{f} \left|\bar{\psi}(f)\right|^2$$

Substituting scaling function $\frac{1}{\sqrt{s_0}}\,\phi\left(\frac{t}{s_0}\right)$ for last integral:

$$v_{\mathrm{LP}}(t) = \frac{1}{C_\psi} \int_{-\infty}^{+\infty} \mathrm{d}t_1\, v(t_1) \int_{-\infty}^{+\infty} \mathrm{d}f_1\, \mathrm{e}^{-\mathrm{j}\,2\pi f_1 (t_1 - t)} \left|\sqrt{s_0}\,\bar{\phi}(s_0 f_1)\right|^2,$$

$$\sqrt{s_0}\,\bar{\phi}(s_0 f_1) = \int_{-\infty}^{+\infty} \mathrm{d}t_i\, \frac{1}{\sqrt{s_0}}\,\phi\left(\frac{t_i}{s_0}\right) \mathrm{e}^{-\mathrm{j}\,2\pi f_1 t_i}\,, \qquad i = 2, 3$$

Substituting $\int_{-\infty}^{+\infty} \mathrm{d}f_1\, \mathrm{e}^{-\mathrm{j}\,2\pi f_1 (t_1 - t - t_2 + t_3)} = \delta(t_1 - t - t_2 + t_3)$, integrating over t_3 and substituting $t' = t_1 - t_2$:

$$v_{\mathrm{LP}}(t) = \frac{1}{C_\psi} \int_{-\infty}^{+\infty} \mathrm{d}t' \underbrace{\int_{-\infty}^{+\infty} \mathrm{d}t_1\, v(t_1)\, \frac{1}{\sqrt{s_0}}\,\phi^*\left(\frac{t_1 - t'}{s_0}\right)}_{=:\ \bar{v}(t', s_0)} \frac{1}{\sqrt{s_0}}\,\phi\left(\frac{t - t'}{s_0}\right)$$

Scaling Function as Low-Pass Impulse Response

From admissibility condition $0 < C_\psi := \int_0^\infty \left|\frac{1}{\sqrt{f}}\,\breve{\psi}(f)\right|^2 \mathrm{d}f < \infty$,

$$\lim_{f_1\to 0}\left|\sqrt{s_0}\,\breve{\phi}(s_0 f_1)\right|^2 = \lim_{f_1\to 0}\int_{s_0 f_1}^\infty \left|\frac{1}{\sqrt{f}}\,\breve{\psi}(f)\right|^2 \mathrm{d}f = C_\psi \qquad \rightsquigarrow$$

Scaling function is impulse response of *low-pass* filter, $\left|\breve{\phi}(0)\right|^2 \neq 0$.

Normalization of scaling function:

$$\int_{-\infty}^{+\infty} \phi(t)\,\mathrm{d}t = 1 \qquad \left(\text{wavelet: } \int_{-\infty}^{+\infty} \psi(t)\,\mathrm{d}t = 0\right)$$

Scaling function transform $\bar{v}(t', s)$ is cross-correlation with dilated (scaled) impulse response $\frac{1}{\sqrt{s_0}}\,\phi(\frac{t}{s_0})$ of a hypothetical *low-pass* filter $\sqrt{s_0}\,\breve{\phi}(s_0 f)$:

$$\bar{v}(t', s_0) = \int_{-\infty}^{+\infty} v(t_1)\,\frac{1}{\sqrt{s_0}}\,\phi^*\left(\frac{t_1 - t'}{s_0}\right)\mathrm{d}t_1 = v(t_1) \otimes \frac{1}{\sqrt{s_0}}\,\phi\left(\frac{t_1}{s_0}\right)$$

Wavelet and Scaling Function Transform

$v(t) = v_{\text{BP}}(t) + v_{\text{LP}}(t)$, BP and LP parts take form of a convolution:

$$v_{\text{BP}}(t) = \frac{1}{C_\psi} \int_0^{s_0} \frac{\mathrm{d}s}{s^2} \underbrace{\int_{-\infty}^{+\infty} \mathrm{d}t' \, \widehat{v}(t', s) \, \frac{1}{\sqrt{s}} \, \psi\Big(\frac{t - t'}{s}\Big)}_{\widehat{v}(t', s) \, * \, \frac{1}{\sqrt{s}} \, \psi\left(\frac{t'}{s}\right)}$$

$$v_{\text{LP}}(t) = \frac{1}{C_\psi} \underbrace{\int_{-\infty}^{+\infty} \mathrm{d}t' \, \bar{v}(t', s_0) \, \frac{1}{\sqrt{s_0}} \, \phi\Big(\frac{t - t'}{s_0}\Big)}_{\bar{v}(t', s_0) \, * \, \frac{1}{\sqrt{s_0}} \, \phi\left(\frac{t'}{s_0}\right)}$$

Wavelet and scaling function transform are cross-correlations ($\otimes$) with dilated (scaled) impulse responses of BP and LP filters:

$$\widehat{v}(t', s) = \int_{-\infty}^{+\infty} v(t_1) \, \frac{1}{\sqrt{s}} \, \psi^*\Big(\frac{t_1 - t'}{s}\Big) \, \mathrm{d}t_1 = v(t_1) \otimes \frac{1}{\sqrt{s}} \, \psi\Big(\frac{t_1}{s}\Big)$$

$$\bar{v}(t', s) = \int_{-\infty}^{+\infty} v(t_1) \, \frac{1}{\sqrt{s}} \, \phi^*\Big(\frac{t_1 - t'}{s}\Big) \, \mathrm{d}t_1 = v(t_1) \otimes \frac{1}{\sqrt{s}} \, \phi\Big(\frac{t_1}{s}\Big)$$

Moments of a Wavelet

2D CWT $\widehat{v}(t', s)$ of 1D function $v(t)$, 4D transform for 2D signal.

Desirable: Fast decay of $\widehat{v}(t', s)$ wrt to small scales s (fine details)

Moments of a wavelet (from admissibility condition $\rightarrow M_0 = 0$):

$$M_p = \int_{-\infty}^{+\infty} t^p \, \psi(t) \, \mathrm{d}t$$

Taylor expansion of $v(t)$ for $t' = 0$, pth derivative $v^{(0)}(t)$:

$$\widehat{v}(t', s) = \int_{-\infty}^{+\infty} v(t_1) \, \frac{1}{\sqrt{s}} \, \psi^*\Big(\frac{t_1 - t'}{s}\Big) \, \mathrm{d}t_1 = \int_{-\infty}^{+\infty} v(t_2 + t') \, \frac{1}{\sqrt{s}} \, \psi^*\Big(\frac{t_2}{s}\Big) \, \mathrm{d}t_2 \, ,$$

$$\widehat{v}(0, s) = \sum_{p'=0}^{p} \frac{1}{\sqrt{s}} \, \frac{v^{(p')}(0)}{p'!} \int_{-\infty}^{+\infty} (s\, t)^{p'} \, \psi^*(t) \, s \, \mathrm{d}t$$

$$= \frac{1}{\sqrt{s}} \left[\sum_{p'=0}^{p} \frac{v^{(p')}(0)}{p'!} \, M_{p'}^* \, s^{p'+1} + \mathcal{O}\big(s^{p+2}\big) \right]$$

Smallness of CWT: $M_{p' \le p} = 0$ (or $\lll$) $\rightsquigarrow$ $\widehat{v}(t', s) \propto s^{p+2}$, approx. order $p \rightsquigarrow$ polyn. $v(t) = \sum_{p'=0}^{p} v_{p'} \, t^{p'}$ has $\widehat{v}(t', s) = 0$, ψ-support $\geq 2p - 1$.

CWT Example

Wavelet $\frac{1}{\sqrt{s}}\psi\left(\frac{t-t'}{s}\right)$ is localized near $t = t'$. The FT $\breve{\psi}(f)$ of $\psi(t)$ be localized near $f = f'$. Because of

$$\sqrt{s}\,\breve{\psi}(sf) = \int_{-\infty}^{+\infty} \frac{1}{\sqrt{s}}\,\psi\left(\frac{t}{s}\right) \mathrm{e}^{-\mathrm{j}\,2\pi f t}\,\mathrm{d}t\,,$$

spectrum of wavelet $\sqrt{s}\,\breve{\psi}(sf)$ is localized near $f = f'/s$.

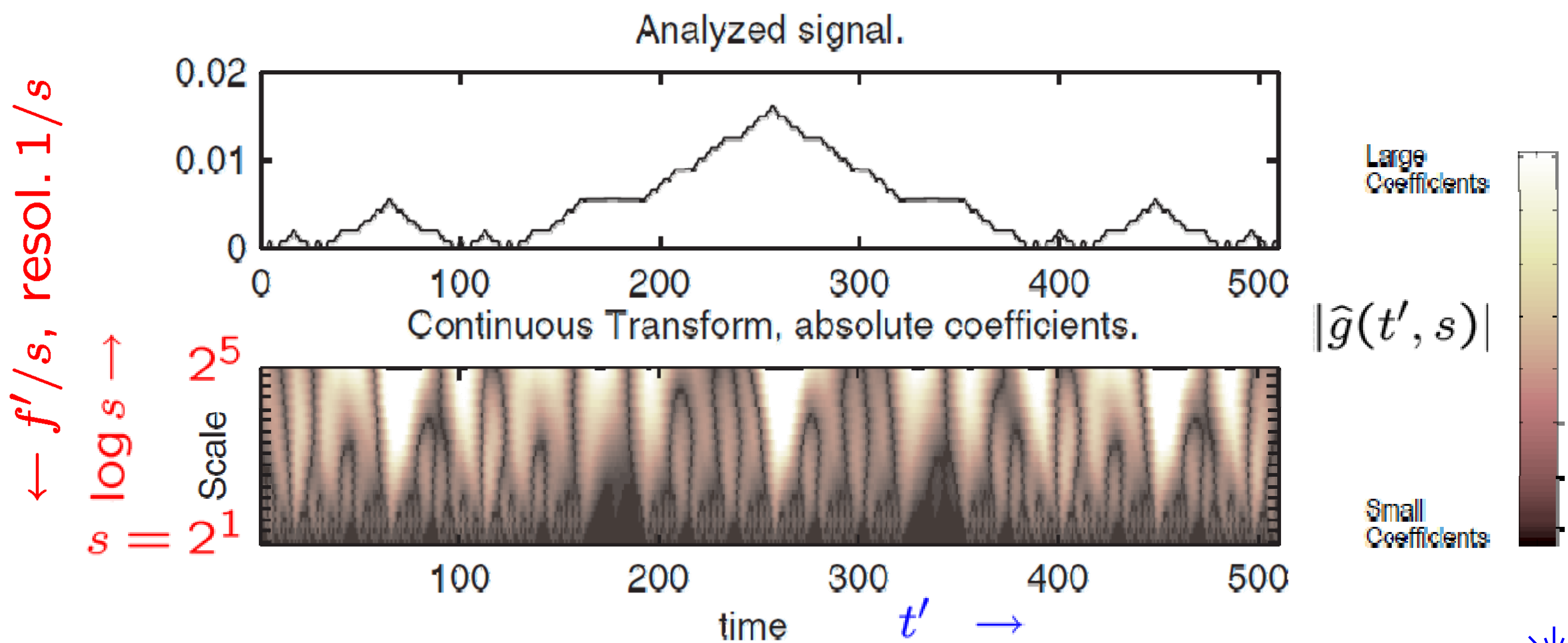

Outline

- Wavelets
  - What are they good for? Discrete wavelet transform
- Finite-differences in time-domain
  - Yee's leapfrog algorithm
  - Numerical dispersion, stability and accuracy
  - Higher-order finite-differences
  - Method of weighted residuals: Collocation
- Wavelet FDTD
  - Numerical dispersion, stability and accuracy
  - What should be further done?
  - Dispersive and nonlinear media
- Application examples in nano-photonics
  - Waveguide roughness
  - Slow light in a photonic crystal with disorder
  - Four-wave mixing in a microring resonator
  - Switching of a Bragg grating
- Summary and further reading

Discrete Wavelet Transform (DWT)

Wavelet representation of $v(t)$ is higly redundant (2D *integral*):

$$v(t) = \frac{1}{C_\psi} \int_0^\infty \frac{\mathrm{d}s}{s^2} \int_{-\infty}^{+\infty} \mathrm{d}t' \, \hat{v}(t', s) \, \frac{1}{\sqrt{s}} \, \psi\Big(\frac{t - t'}{s}\Big)$$

Admissibility: $0 < C_\psi := \int_0^\infty |\frac{1}{\sqrt{f}} \, \breve{\psi}(f)|^2 \, \mathrm{d}f < \infty$

Energy conservation ("Parceval") between time and WT domain:

$$1 = \int_{-\infty}^{+\infty} \mathrm{d}t \, |v(t)|^2 = \frac{1}{C_\psi} \int_0^\infty \frac{\mathrm{d}s}{s^2} \int_{-\infty}^{+\infty} \mathrm{d}t' \, |\hat{v}(t', s)|^2 \qquad (s \neq 0)$$

Conjecture: Double integral can be replaced by double sum, usually "dyadic" wavelets (scale $s = 2^j$, resolution 2^{-j}):

$$\psi_k^j(t) := 2^{-j/2} \, \psi\left(2^{-j} \, t - k\Delta t\right) \quad \text{for} \quad s = 2^j, \;\; t' = 2^j k\Delta t \,, \;\; (j, k) \in \mathbb{Z}$$

Discrete wavelet representation of $v(t)$ with orthonormal wavelets $\int_{-\infty}^{+\infty} \mathrm{d}t \, \psi_k^j(t) \, \psi_{k'}^{j'*}(t) = \delta_{j,j'} \, \delta_{k,k'}$ (no redundancy):

$$v(t) = \sum\nolimits_{j,k} \hat{v}_k^j \, \psi_k^j(t), \qquad \hat{v}_k^j = \int_{-\infty}^{+\infty} \mathrm{d}t \, v(t) \, \psi_k^{j*}(t)$$

Discrete Wavelet Transform (DWT) Removes Redundancy

"Dyadic" orthonormal wavelets ($s = 2^j,\ t' = 2^j k \Delta t$):

$$\psi_k^j(t) := 2^{-j/2}\,\psi(2^{-j}\,t - k\Delta t), \qquad \int_{-\infty}^{+\infty} \mathrm{d}t\ \psi_k^j(t)\,\psi_{k'}^{j'*}(t) = \delta_{j,j'}\,\delta_{k,k'}$$

Wavelet coefficients $\hat{v}_k^j$ in expansion $v(t) = \sum_{j,k} \hat{v}_k^j\,\psi_k^j(t)\ \forall\,(j,k) \in \mathbb{Z}$:

$$\int_{-\infty}^{+\infty} \mathrm{d}t\ v(t)\,\psi_{k'}^{j'*}(t) = \sum_{j,k} \hat{v}_k^j \underbrace{\int_{-\infty}^{+\infty} \mathrm{d}t\ \psi_k^j(t)\,\psi_{k'}^{j'*}(t)}_{=\delta_{j,j'}\,\delta_{k,k'}} = \hat{v}_{k'}^{j'} \qquad \blacksquare$$

Wavelet coefficient $\hat{v}_k^j$ gives correlation of signal $v(t)$ with wavelet $\psi_k^j(t)$ shifted to $t' = 2^{-j/2} k \Delta t$, i. e., with impulse response of constant-Q band-pass filters (width $2^j \Delta f_j = \Delta f_\mathrm{C}$ near $2^j f_j = f_\mathrm{C}$):

$$2^{j/2}\,\breve{\psi}(2^j f) \quad \bullet\!\!-\!\!\circ \quad 2^{-j/2}\,\psi(2^{-j}\,t), \qquad Q_j = \frac{f_j}{\Delta f_j} = \frac{2^j f_\mathrm{C}}{2^j \Delta f_\mathrm{C}} = \frac{f_\mathrm{C}}{\Delta f_\mathrm{C}}$$

If the wavelet is a matched filter to $\breve{v}(f)$:

$$\breve{\psi}_k^{j*}(f) = \breve{v}(f) \;\rightarrow\; \psi_k^{j*}(t) = v(t) \;\rightarrow\; \hat{v}_k^j = \int_{-\infty}^{+\infty} \mathrm{d}t\ |v(t)|^2 = 1$$

Replacing an Infinite Set of Wavelets by one Scaling Function

$$\phi_k^j(t) := 2^{-j/2}\,\phi(2^{-j}\,t - k\Delta t), \qquad \psi_k^j(t) := 2^{-j/2}\,\psi(2^{-j}\,t - k\Delta t)$$

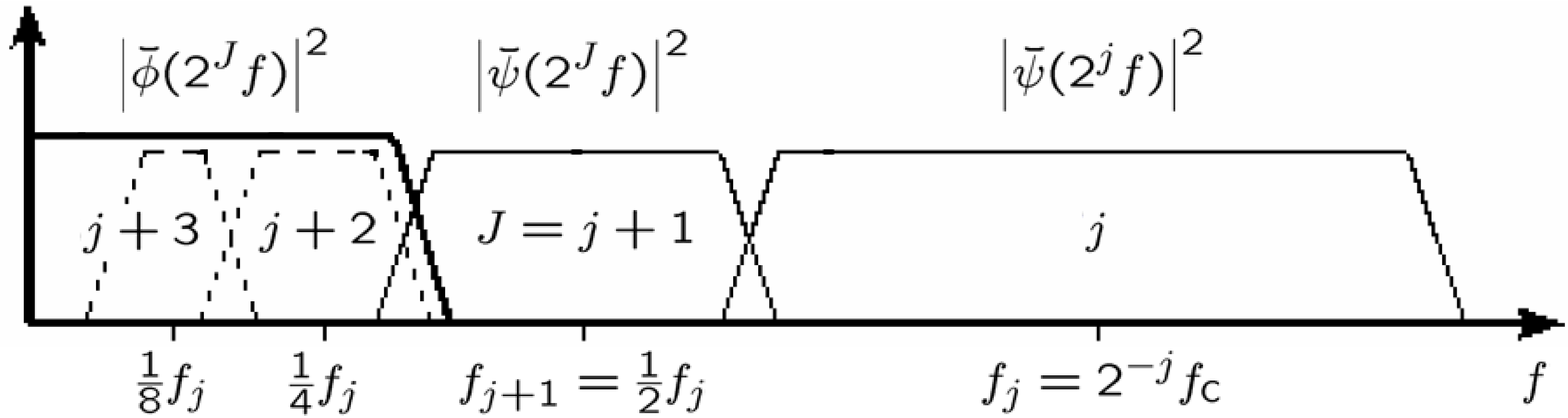

Expansion of non-bandlimited signal $\hat{v}(t)$ $(v_k^j \neq 0\ \forall j < J)$:

$$v(t) = \underbrace{\overbrace{\sum_{j=-\infty}^{J} \underbrace{\sum_{k=-\infty}^{+\infty} \hat{v}_k^j\,\psi_k^j(t)}_{\text{BP detail } D^j(t)}}^{v_\mathrm{BP}(t)}}_{\text{all BP details up to } D^J(t)} + \underbrace{\overbrace{\sum_{k=-\infty}^{+\infty} \underbrace{\sum_{j=J+1}^{+\infty} \hat{v}_k^j\,\psi_k^j(t)}_{\bar{v}_k^J\,\phi_k^J(t)}}^{v_\mathrm{LP}(t)}}_{\text{LP approximation } A^J(t)}$$

Bandlimited Signal $v(t),\ \breve{v}(f > B) = 0$

$$\phi_k^j(t) := 2^{-j/2}\,\phi(2^{-j}t - k\Delta t), \qquad \psi_k^j(t) := 2^{-j/2}\,\psi(2^{-j}t - k\Delta t)$$

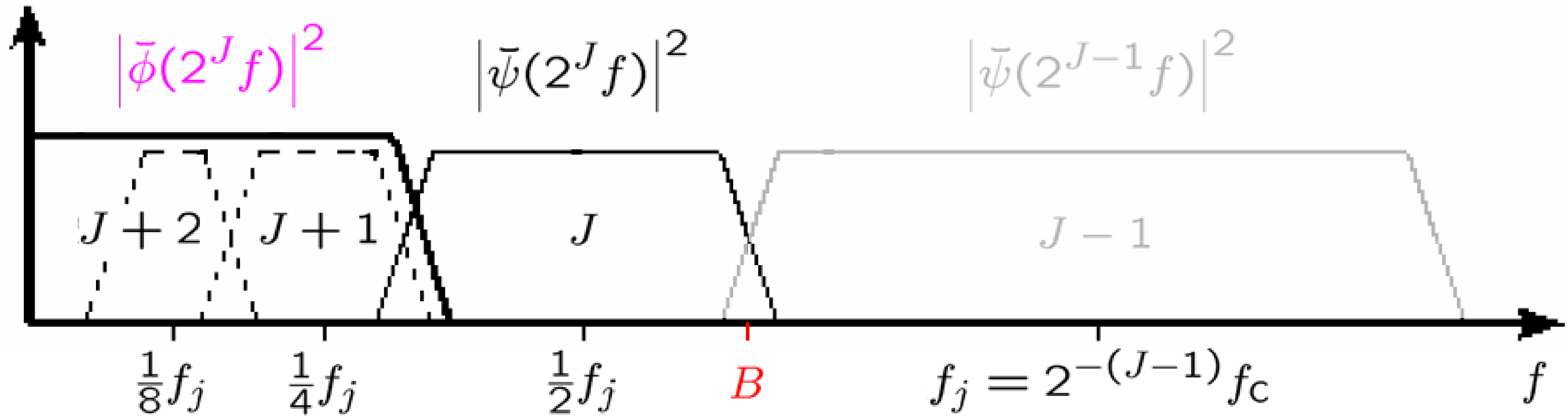

Expansion of bandlimited signal $v(t)$ ($B \mathrel{\widehat{=}} J$):

$$v(t) = \sum_{k=-\infty}^{+\infty} \hat{v}_k^J\,\psi_k^J(t) + \sum_{k=-\infty}^{+\infty} \bar{v}_k^J\,\phi_k^J(t) = \sum_{k=-\infty}^{+\infty} \bar{v}_k^{J-1}\,\phi_k^{J-1}(t)$$

$$= \sum_{k=-\infty}^{+\infty} \hat{v}_k^J\,\psi_k^J(t) + \sum_{k=-\infty}^{+\infty} \hat{v}_k^{J+1}\,\psi_k^{J+1}(t) + \sum_{k=-\infty}^{+\infty} \bar{v}_k^{J+1}\,\phi_k^{J+1}(t)$$

skinny $\phi^J =$ fat $\psi^{J+1} +$ fat ϕ^{J+1}, skinny $\phi^{J-1} =$ fat $\psi^J +$ fat ϕ^J

Outline

- Wavelets
  - What are they good for? Multiresolution analysis
- Finite-differences in time-domain
  - Yee's leapfrog algorithm
  - Numerical dispersion, stability and accuracy
  - Higher-order finite-differences
  - Method of weighted residuals: Collocation
- Wavelet FDTD
  - Numerical dispersion, stability and accuracy
  - What should be further done?
  - Dispersive and nonlinear media
- Application examples in nano-photonics
  - Waveguide roughness
  - Slow light in a photonic crystal with disorder
  - Four-wave mixing in a microring resonator
  - Switching of a Bragg grating
- Summary and further reading

Multiresolution Analysis (MRA)

$$\phi_k^j(t) := 2^{-j/2}\,\phi(2^{-j}\,t - k\Delta t), \qquad \psi_k^j(t) := 2^{-j/2}\,\psi(2^{-j}\,t - k\Delta t)$$

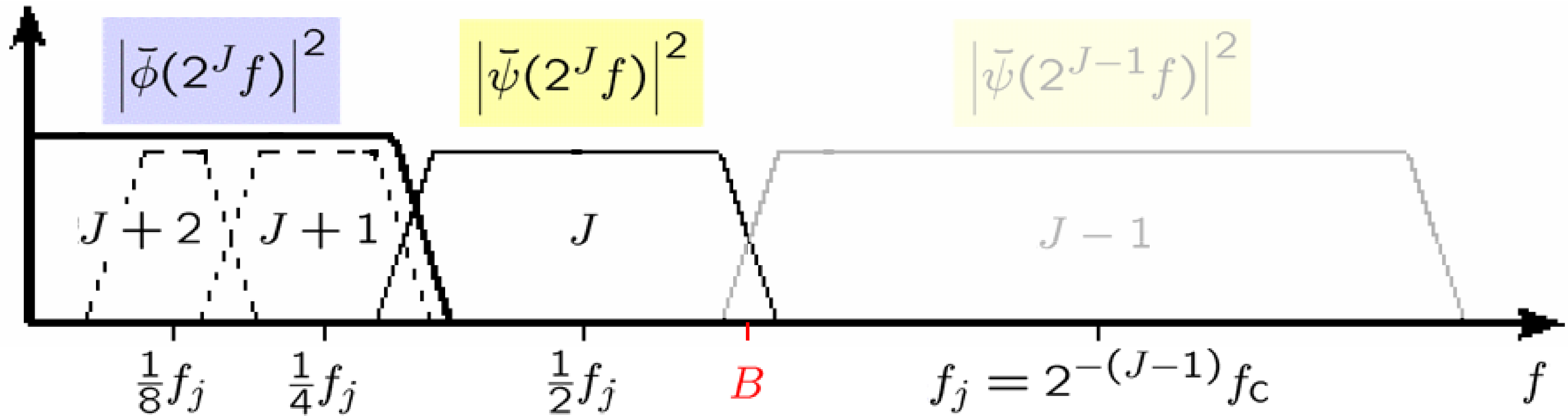

Signal space V_{J-1} has orthogonal subspaces, $V_{J-1} = V_J \oplus W_J$, etc.

"Average" (LP) V_J spanned by orthonormal scaling fct base $\phi_k^J(t)$

"Detail" (BP) W_J spanned by orthonormal wavelet base $\psi_k^J(t)$

Refinement (scaling) relations given by discrete "filters" h_k, g_k:

$$\phi_k^j(t) = \sum_{k'=-\infty}^{+\infty} h_{k'}\, \phi_{2k+k'}^{j-1}(t)\,, \qquad \psi_k^j(t) = \sum_{k'=-\infty}^{+\infty} g_{k'}\, \phi_{2k+k'}^{j-1}(t)$$

Multiresolution Analysis (MRA)

Expansion of bandlimited signal $v(t)$ $(B \mathrel{\widehat{=}} J)$:

$$v(t) = A^J(t) + D^J(t) = \sum_{k=-\infty}^{+\infty} a_k^J \, \phi_k^J(t) + \sum_{k=-\infty}^{+\infty} d_k^J \, \psi_k^J(t)$$

Usual notation of averages (approximations) a_k^j and details d_k^j:

$$a_k^j := \bar{v}_k^j = \int_{-\infty}^{+\infty} \mathrm{d}t \, \phi_k^{j*}(t) \, v(t), \qquad d_k^j := \hat{v}_k^j = \int_{-\infty}^{+\infty} \mathrm{d}t \, \psi_k^{j*}(t) \, v(t)$$

Recursion for averages and details using refinement relations:

$$\phi_k^j(x) = \sum_{k'} h_{k'} \, \phi_{2k+k'}^{j-1}(t) \qquad \psi_k^j(x) = \sum_{k'} g_{k'} \, \phi_{2k+k'}^{j-1}(t)$$

$$a_k^j = \sum_{k'} h_{k'}^* \, a_{2k+k'}^{j-1} \qquad d_k^j = \sum_{k'} g_{k'}^* \, a_{2k+k'}^{j-1}$$

Filtering A^J, D^J with complex conjugate filters h_k^*, g_k^* leads to A^{J+1}, D^{J+1} at larger scale $J+1$. Finite-length signals $k \in [1, K]$: "Filter bank iteration" with scaling / wavelet filters leaves number of coefficients constant (decimation factor 2 in subscript $2k+k'$).

FWT and Inverse FWT (IFWT, Reconstruction)

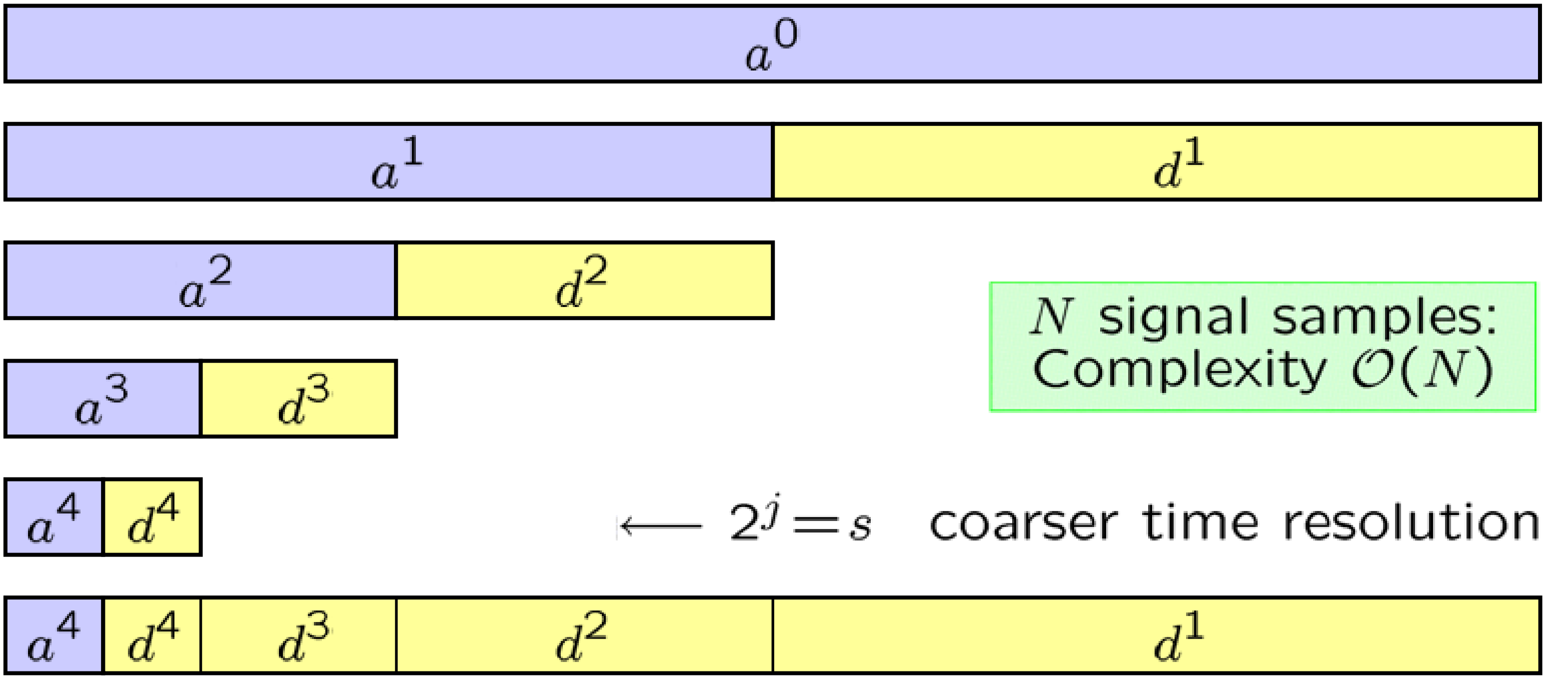

Reconstruction of bandlimited signal $v(t)$ $(B \mathrel{\widehat{=}} J = 1)$:

$$v(t) = \sum_{k=-\infty}^{+\infty} a_k^{J-1} \, \phi_k^{J-1}(t) = \sum_{k=-\infty}^{+\infty} a_k^{J} \, \phi_k^{J}(t) + \sum_{k=-\infty}^{+\infty} d_k^{J} \, \psi_k^{J}(t)$$

$$= \sum_{k=-\infty}^{+\infty} a_k^{J+3} \, \phi_k^{J+3}(t) + \sum_{j=J}^{J+3} \sum_{k=-\infty}^{+\infty} d_k^{j} \, \psi_k^{j}(t)$$

Outline

- Wavelets
  What are they good for? Daubechies wavelets
- Finite-differences in time-domain
  Yee's leapfrog algorithm
  Numerical dispersion, stability and accuracy
  Higher-order finite-differences
  Method of weighted residuals: Collocation
- Wavelet FDTD
  Numerical dispersion, stability and accuracy
  What should be further done?
  Dispersive and nonlinear media
- Application examples in nano-photonics
  Waveguide roughness
  Slow light in a photonic crystal with disorder
  Four-wave mixing in a microring resonator
  Switching of a Bragg grating
- Summary and further reading

MRA with Daubechies Wavelet D3 (Dp or db$p$, p moments vanish)

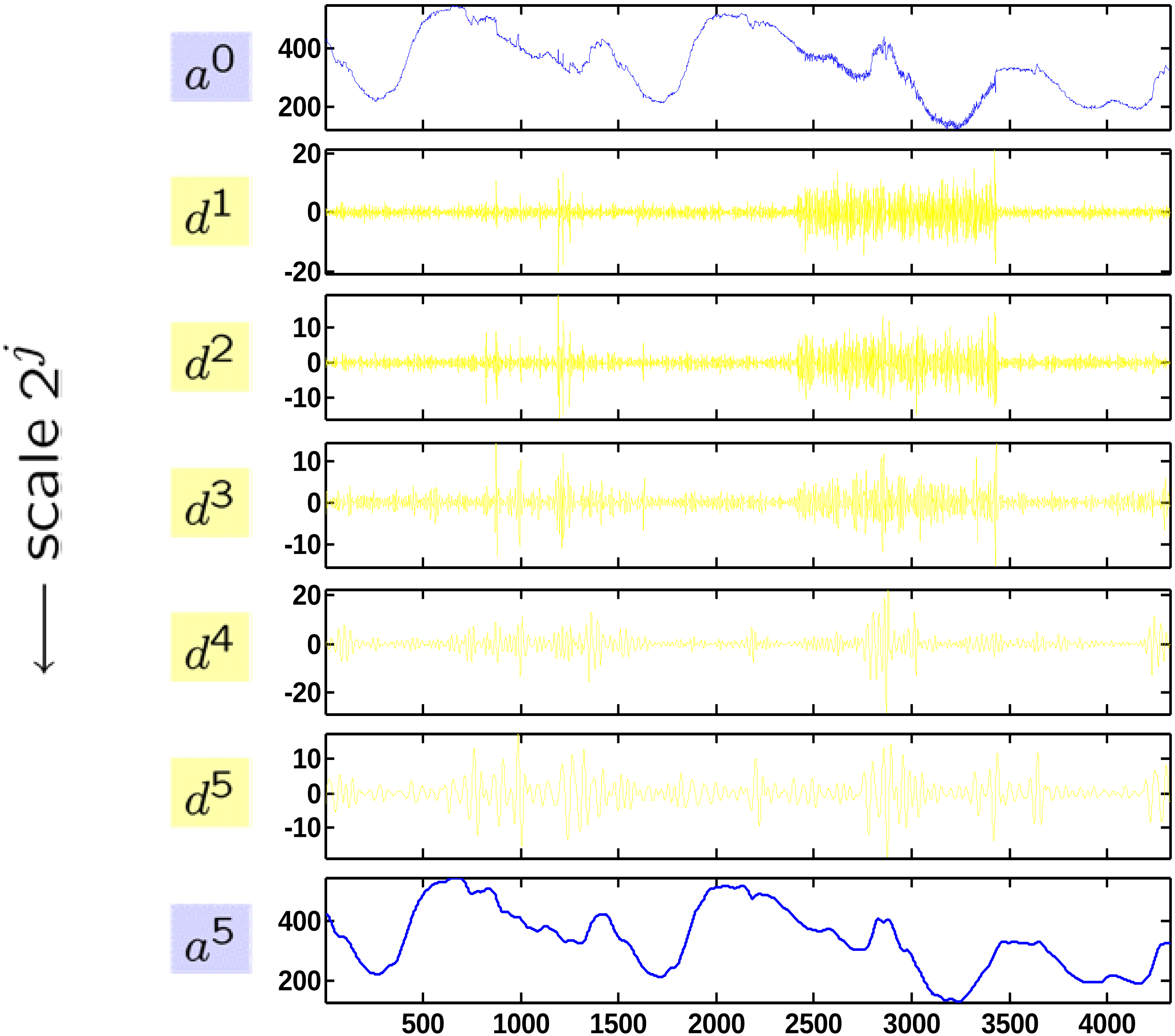

support $[0, 2p-1]$

$\phi(t)$

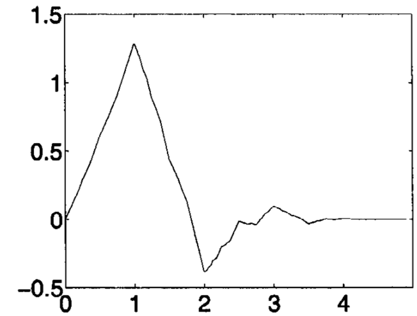

$\psi(t)$

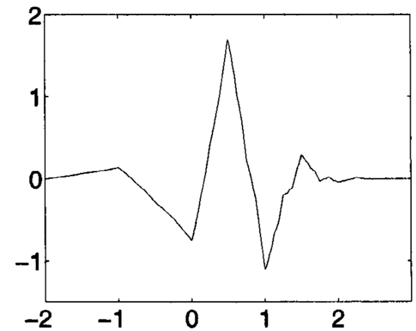

support $[-(p-1), p]$

D3 (db3)

Daubechies Wavelets Dp — Cascade Algorithm

Recursion for $\phi^{\mathrm{D}p}$ with known filter $h_k^{\mathrm{D}p}$. Start with Haar scaling function $\phi_h \,\widehat{=}\, \phi^{\mathrm{D}1} = \phi^{(0)}$, iterate refinement equation:

$$\phi^{(i+1)}(t) = 2^{1/2} \sum_{k'=0}^{p-1} h_{k'}^{\mathrm{D}p}\, \phi^{(i)}(2t - k'\Delta t), \qquad i = 0, 1, 2, \ldots,$$

$$\psi^{\mathrm{D}p}(t) = 2^{1/2} \sum_{k'=-(p-2)}^{1} g_{k'}^{\mathrm{D}p}\, \phi^{\mathrm{D}p}(2t - k'\Delta t), \qquad g_k^{\mathrm{D}p} = (-1)^{1-k} h_{1-k}^{\mathrm{D}p}$$

p wavelet moments vanish, good convergence for details if $j \to -\infty$:

$$M_p = \int_{-\infty}^{+\infty} t^p\, \psi^{\mathrm{D}p}(t)\,\mathrm{d}t \quad \rightsquigarrow \quad d_k^j := \hat{v}_k^j \propto 2^{(p+2)j}$$

- Wavelet suppresses polynomial parts in $v(t)$ up to degree p.
- Support for $\psi^{\mathrm{D}p}, \psi^{\mathrm{D}p}$ is $2p - 1$, i. e.,
- filter coefficients are $h_0^{\mathrm{D}p}, h_1^{\mathrm{D}p}, \ldots, h_{2p-1}^{\mathrm{D}p}$.
- Wavelets and scaling functions orthogonal in all combinations

Outline

- Wavelets
  - What are they good for? Deslauriers-Dubuc
- Finite-differences in time-domain
  - Yee's leapfrog algorithm
  - Numerical dispersion, stability and accuracy
  - Higher-order finite-differences
  - Method of weighted residuals: Collocation
- Wavelet FDTD
  - Numerical dispersion, stability and accuracy
  - Summary, and what should be done further
  - Dispersive and nonlinear media
- Application examples in nano-photonics
  - Waveguide roughness
  - Slow light in a photonic crystal with disorder
  - Four-wave mixing in a microring resonator
  - Switching of a Bragg grating
- Summary and further reading

Deslauriers-Dubuc Interpolating Scaling Function

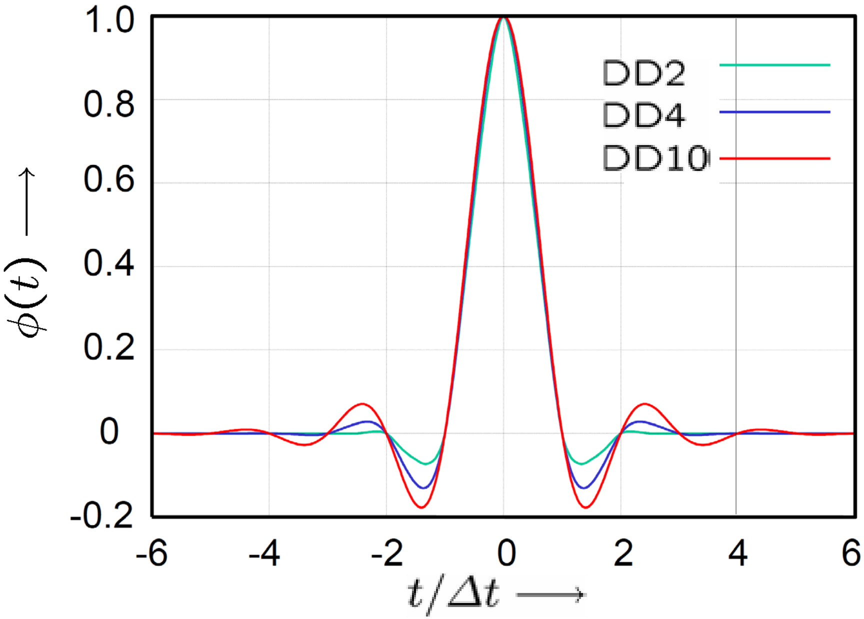

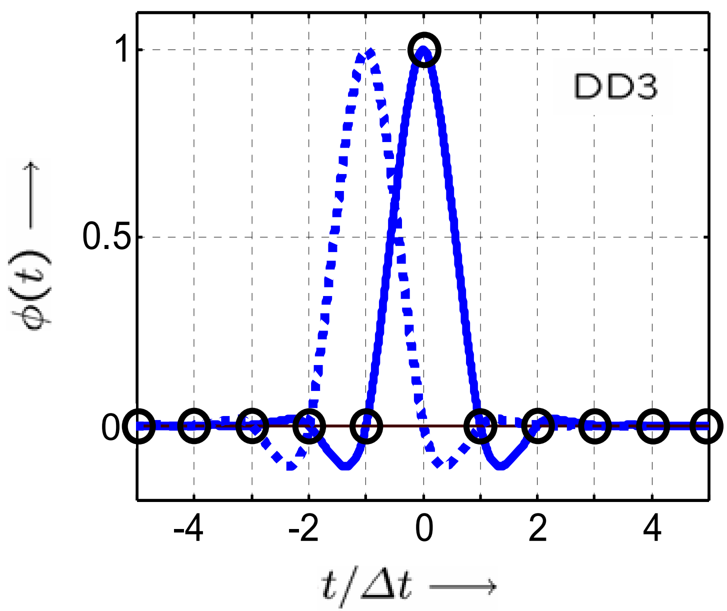

Interpolating function $\phi(t)$ recovers $v(t)$ from sampling $\{v(k\Delta t)\}_{k\in\mathbb{Z}}$.

Deslauriers-Dubuc $\phi^{\mathrm{DDp}}(t)$: has degree $L = 2p-1$, compact support $[-L, L]$, decomposes polynomial of degree L, is derived from (real) Daubechies scaling functions $\phi^{\mathrm{Dp}}(t)$ by correlation:

$$\phi^{\mathrm{DDp}}(t) = \int_{-\infty}^{+\infty} \mathrm{d}t' \, \phi^{\mathrm{Dp}}(t') \, \phi^{\mathrm{Dp}}(t' - t), \quad v(t) = \sum_{k=-\infty}^{+\infty} v(k\Delta t) \, \phi^{\mathrm{DDp}}(t - k\Delta t)$$

Deslauriers, G.; Dubuc, S.: Symmetric iterative interpolation processes. Constr. Approx. 5 (1989) 49–68

Deslauriers-Dubuc Interpolating Wavelets

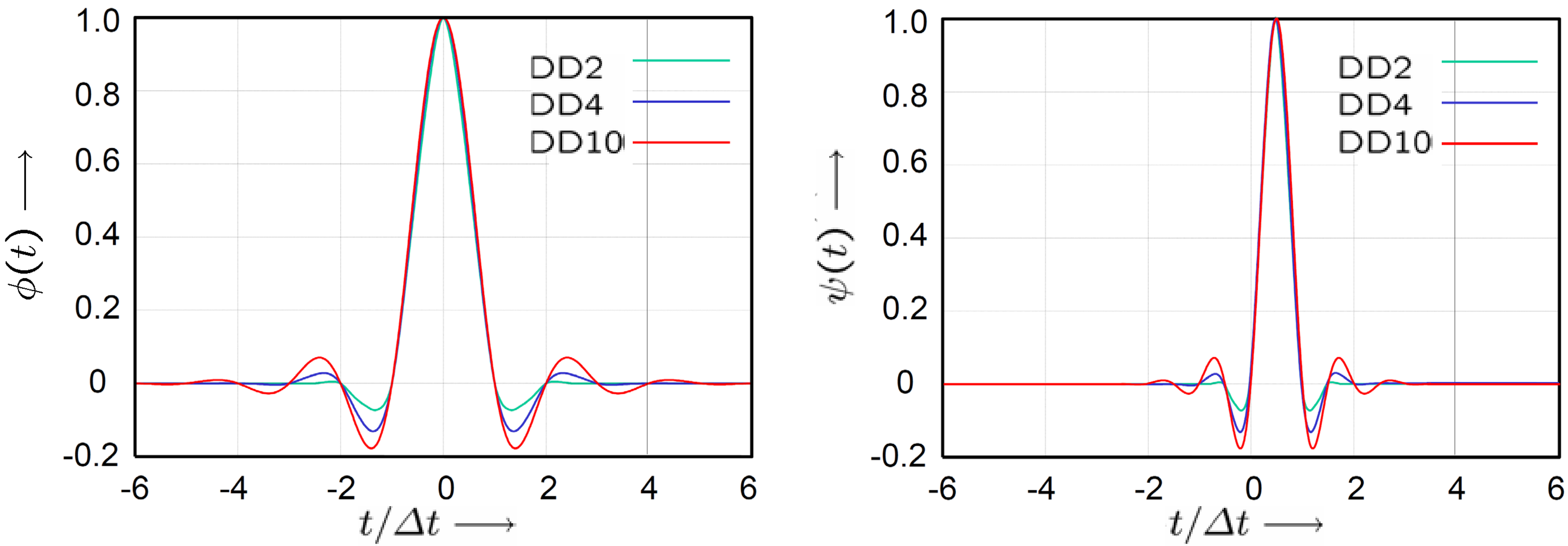

Refinement (scaling) relations given by discrete "filters" $h_k^{\mathrm{DD}p}$:

$$\phi(t) = \sum_{k=-\infty}^{+\infty} h_k^{\mathrm{DD}p}\, \phi(2t - k\Delta t), \quad \psi(t) = \phi(2t - \Delta t)$$

no true wavelet, no vanishing moments

Deslauriers-Dubuc filter by correlating Daubechies wavelet $h_k^{\mathrm{D}p}$:

$$h_k^{\mathrm{DD}p} = \sum_{k'=-\infty}^{+\infty} h_{k'}^{\mathrm{D}p}\, h_{k'-k}^{\mathrm{D}p}, \qquad \text{symmetry: } h_{-k}^{\mathrm{DD}p} = h_k^{\mathrm{DD}p}$$

Deslauriers-Dubuc Wavelets and Duals

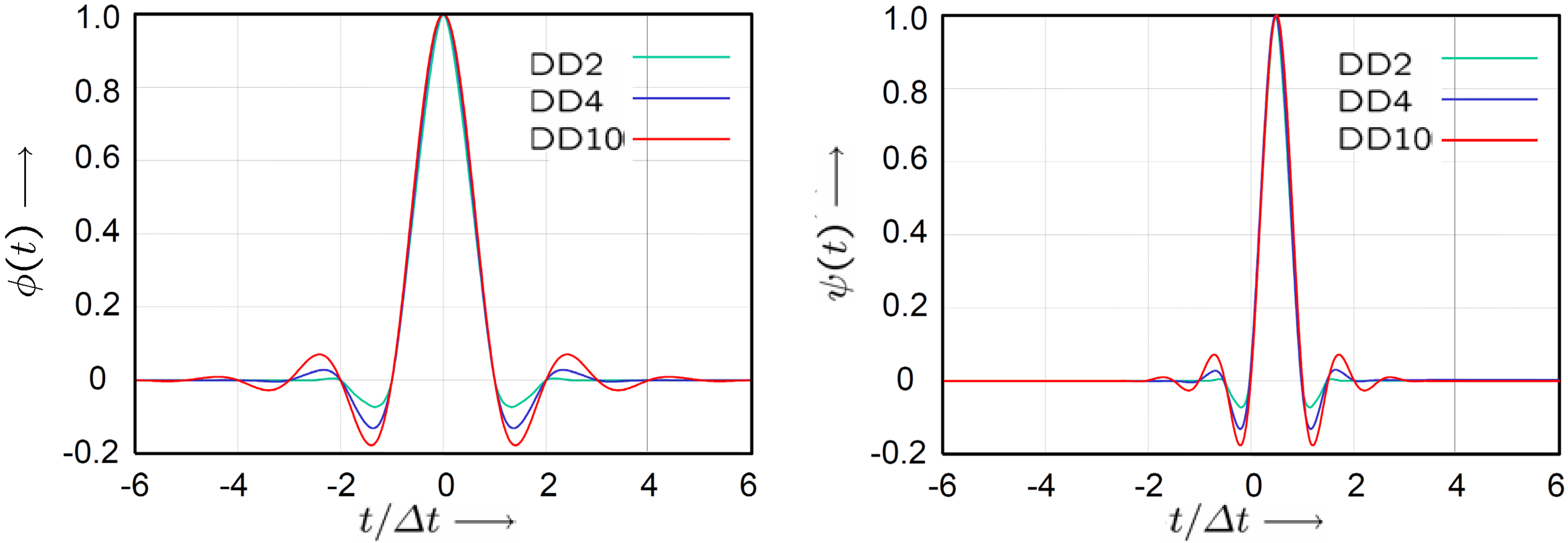

Orthogonality:

$$\int_{-\infty}^{+\infty} \mathrm{d}t\ \phi_k^j(t)\,\tilde{\phi}_{k'}^{j'}(t) = \delta_{j,j'}\,\delta_{k,k'}, \qquad \int_{-\infty}^{+\infty} \mathrm{d}t\ \psi_k^j(t)\,\tilde{\psi}_{k'}^{j'}(t) = \delta_{j,j'}\,\delta_{k,k'}$$

So far: Analyzing fct is $(\cdot)^*$ of synthesizing fct, $\tilde{\phi}_k^j = \phi_k^{j*}$, $\tilde{\psi}_k^j = \psi_k^{j*}$

DD scaling function and "wavelet" are biorthogonal:

$$\tilde{\phi}(t) = \Delta t\,\delta(t), \qquad \tilde{\psi}(t) = \Delta t \sum_{k'=-2p+2}^{2p} (-1)^{k'-1}\,h_{-k'+1}^{\mathrm{DD}p}\,\delta(t - \tfrac{1}{2}k'\Delta t)$$

Deslauriers-Dubuc Wavelets — Biorthogonality

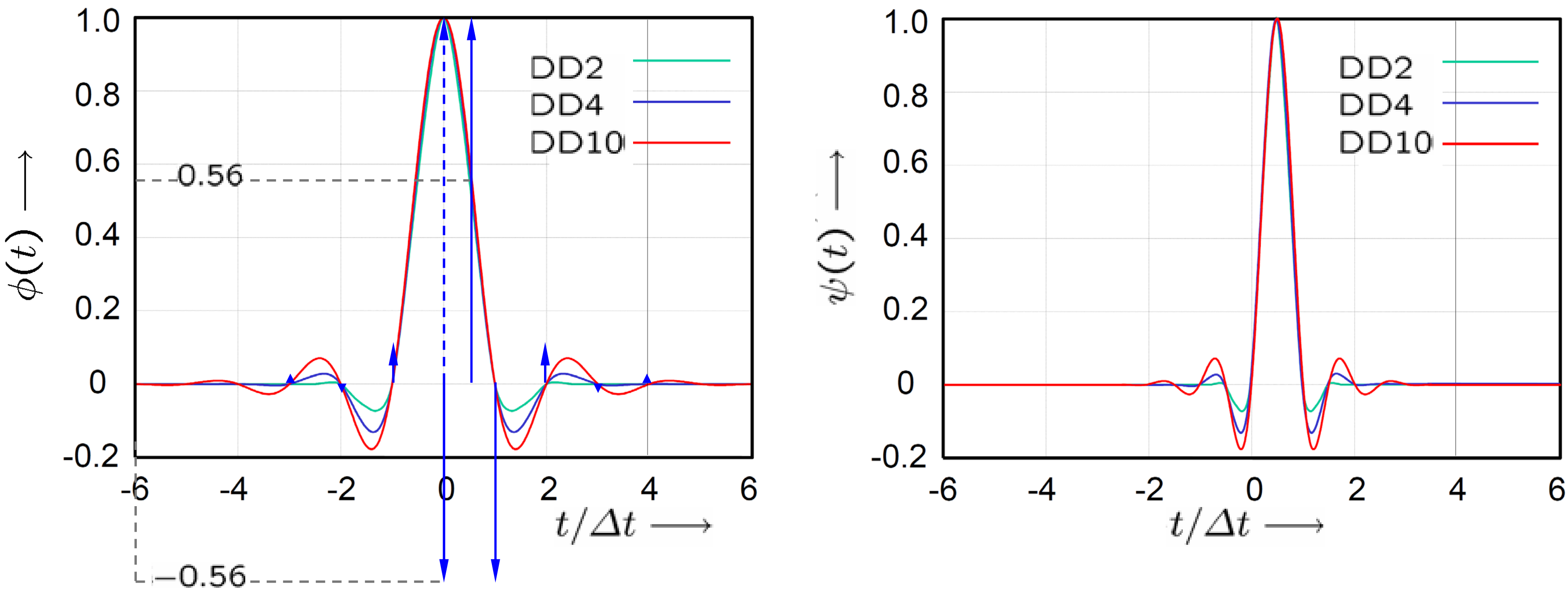

DD scaling function and wavelet are biorthogonal:

$$\tilde{\phi}(t) = \Delta t\,\delta(t), \qquad \tilde{\psi}(t) = \Delta t \sum_{k'=-2p+2}^{2p} (-1)^{k'-1}\, h^{\mathrm{DD}p}_{-k'+1}\,\delta(t - \tfrac{1}{2}k'\Delta t)$$

$$\int_{-\infty}^{+\infty} \mathrm{d}t\ \phi^{j}_{k}(t)\,\tilde{\phi}^{j'}_{k'}(t) = \delta_{j,j'}\,\delta_{k,k'}, \qquad \int_{-\infty}^{+\infty} \mathrm{d}t\ \psi^{j}_{k}(t)\,\tilde{\psi}^{j'}_{k'}(t) = \delta_{j,j'}\,\delta_{k,k'},$$

$$\int_{-\infty}^{+\infty} \mathrm{d}t\ \phi^{j}_{k}(t)\,\tilde{\psi}^{j'}_{k'}(t) = 0, \qquad \int_{-\infty}^{+\infty} \mathrm{d}t\ \psi^{j}_{k}(t)\,\tilde{\phi}^{j'}_{k'}(t) = 0$$

Outline

- Wavelets
  - What are they good for?
- Finite-differences in time-domain
  - Yee's leapfrog algorithm
  - Numerical dispersion, stability and accuracy
  - Higher-order finite-differences
  - Method of weighted residuals: Collocation
- Wavelet FDTD
  - Numerical dispersion, stability and accuracy
  - Summary, and what should be done further
  - Dispersive and nonlinear media
- Application examples in nano-photonics
  - Waveguide roughness
  - Slow light in a photonic crystal with disorder
  - Four-wave mixing in a microring resonator
  - Switching of a Bragg grating
- Summary and further reading

Maxwell´s Fundamental Equations

Ampere's law: $\text{curl}\,\vec{H} = \dfrac{\partial \vec{D}}{\partial t}$, Faraday's law: $\text{curl}\,\vec{E} = -\dfrac{\partial \vec{B}}{\partial t}$

Gauss' law: $\text{div}\,\vec{D} = 0$, $\text{div}\,\vec{B} = 0$

Constitutive: $\vec{D} = \varepsilon_0 \vec{E} + \vec{P}$, $\vec{B} = \mu_0 \vec{H} + \vec{M}$

Electromagnetic waves are described by:

- magnetic and electric field vectors $\vec{H}$ and $\vec{E}$,
- electric displacement $\vec{D}$, electric material polarization $\vec{P}$,
- magnetic induction $\vec{B}$, magnetic material polarization $\vec{M}$

At operating frequencies f, the medium has

- no space charges/currents, is isotropic, linear,
- has a dielectric constant $\varepsilon = \varepsilon_0 \varepsilon_r$, polarisation $\vec{P} = \varepsilon_0(\varepsilon_r - 1)\vec{E}$,
- and a magnetic permeability $\mu = \mu_0 \mu_r$, pol. $\vec{M} = \mu_0(\mu_r - 1)\vec{H}$.
- The vacuum speed of light is $c = 1 / \sqrt{\varepsilon_0 \mu_0}$, and the
- medium phase velocity is $v = c/n$ (refractive index $n = \pm\sqrt{\mu_r \epsilon_r}$).

Sampling, Nyquist Frequency and Interpolation

Sampling function $a(x)$ is self-reciprocal in Fourier space $\tilde{a}(\xi)$:

$$a(x) = X_a \sum_{n=-\infty}^{+\infty} \delta(x - nX_a) = \sum_{n=-\infty}^{+\infty} \exp\left(-\mathrm{j}\, 2\pi\, n \frac{x}{X_a}\right),$$

$$\tilde{a}(\xi) = \sum_{n=-\infty}^{+\infty} \delta(\xi - n\Xi_a), \qquad \Xi_a = 1/X_a$$

Function $\Psi(x)$ assumed to have bandlimited spatial spectrum:

$$\tilde{\Psi}(\xi) = \int_{-\infty}^{+\infty} \Psi(x) \exp(\mathrm{j}\, 2\pi\, \xi x)\, \mathrm{d}x\,, \qquad \tilde{\Psi}(|\xi| > B_x) = 0$$

$\Psi(x)$ sampled with Nyquist frequency B_x at intervals $X_a = 1/B_x$, discrete *complex* $\Psi_a(x) = \Psi(x)\, a(x)$ at positions $x_n = n/B_x$ result.

Reconstruction of $\Psi(x)$ from complex sampled data $\Psi(n/B_x)$ by filtering with ideal lowpass (transm. 1 in band $|\xi| < B_x/2$, 0 outside), i. e., with interpolation recipe (no *linear* interpolation):

$$\Psi(x) = \sum_{n=-\infty}^{+\infty} \Psi(nX_a) \frac{\sin((x - nX_a)\pi B_x)}{(x - nX_a)\pi B_x}, \quad X_a = \frac{1}{B_x}, \quad X_{a1} = \frac{1}{2B_x}$$

Oversampling needed for linear interpolation!

Outline

- Wavelets
  - What are they good for?
- Finite-differences in time-domain
  - Yee's leapfrog algorithm
  - Numerical dispersion, stability and accuracy
  - Higher-order finite-differences
  - Method of weighted residuals: Collocation
- Wavelet FDTD
  - Numerical dispersion, stability and accuracy
  - Summary, and what should be done further
  - Dispersive and nonlinear media
- Application examples in nano-photonics
  - Waveguide roughness
  - Slow light in a photonic crystal with disorder
  - Four-wave mixing in a microring resonator
  - Switching of a Bragg grating
- Summary and further reading

Yee´s Lattice with Cubic Unit Cells of Size $\Delta x \times \Delta y \times \Delta z$

Advantages of Yee algorithm:

- 1st-order DE for $\vec{E}$ *and* $\vec{H}$,
- more robust than 2nd-order wave equation for $\vec{E}$ *or* $\vec{H}$.
- $\vec{E}$ and $\vec{H}$ singularities naturally implemented.

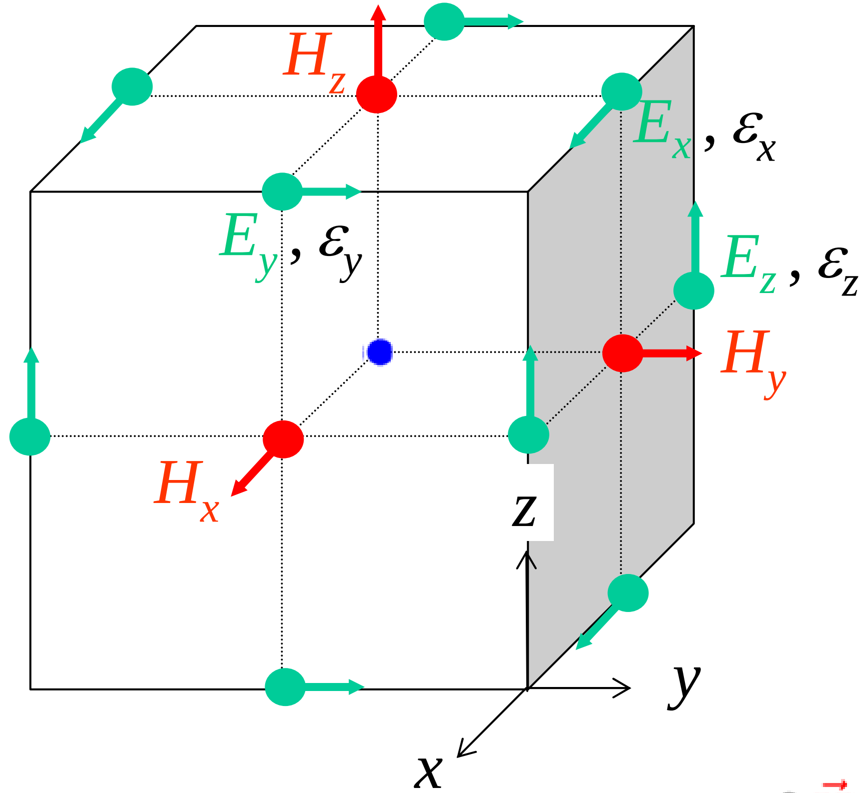

cell centre:
$(i, j, k) \,\widehat{=}\, (i\Delta x, j\Delta y, k\Delta z)$

- Each $\vec{E}$ component surrounded by 4 circulating $\vec{H}$ components
- each $\vec{H}$ component surrounded by 4 circulating $\vec{E}$ components

Faraday: $\text{curl}\,\vec{E} = -\mu \dfrac{\partial \vec{H}}{\partial t}$

Ampere: $\text{curl}\,\vec{H} = \varepsilon \dfrac{\partial \vec{E}}{\partial t}$

Yee, K. S.: Numerical solution of initial boundary value problems involving Maxwell's equations in isotropic media. IEEE Trans. Antennas Propag. AP-14 (1966) 302–307

Finite Differences in Cartesian Coordinates

Centered finite-differences over $\pm\frac{1}{2}\Delta x$, $\pm\frac{1}{2}\Delta t$

at $t = n\Delta t$, $\vec{r} = i\Delta x\,\vec{e}_x + j\Delta y\,\vec{e}_x + k\Delta z\,\vec{e}_z$

for $u(n\Delta t, i\Delta x, j\Delta y, k\Delta z) = u^n_{i,j,k}$:

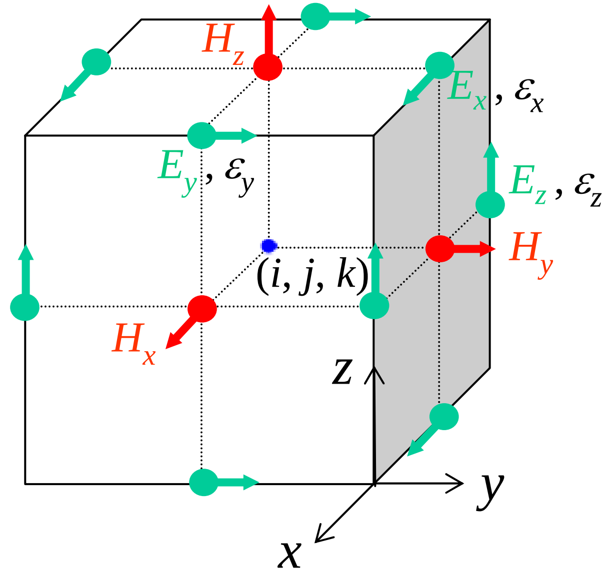

$$\frac{\partial u^n_{i,j,k}}{\partial x} = \frac{u^n_{i+1/2,j,k} - u^n_{i-1/2,j,k}}{\Delta x} + \mathcal{O}(\Delta x^2)$$

$$\frac{\partial u^n_{i,j,k}}{\partial t} = \frac{u^{n+1/2}_{i,j,k} - u^{n-1/2}_{i,j,k}}{\Delta t} + \mathcal{O}(\Delta t^2)$$

- Second-order accurate central differencing to the right and left of observation point (i, j, k) by $\frac{1}{2}\Delta x$.
- Interleaved $\vec{E}$ and $\vec{H}$ components at intervals $\frac{1}{2}\Delta x$.
- Second-order accurate central differencing to the past and future of observation point n by $\frac{1}{2}\Delta t$.
- Interleaved $\vec{E}$ and $\vec{H}$ components at intervals $\frac{1}{2}\Delta t$.
- This leads to a so-called “leapfrog” algorithm.

Central Differences and Discretization

$$\frac{\partial u^n_{i,j,k}}{\partial x} = \frac{u^n_{i+1/2,j,k} - u^n_{i-1/2,j,k}}{\Delta x} + \mathcal{O}(\Delta x^2)$$

$$\frac{\partial u^n_{i,j,k}}{\partial t} = \frac{u^{n+1/2}_{i,j,k} - u^{n-1/2}_{i,j,k}}{\Delta t} + \mathcal{O}(\Delta t^2)$$

Time-space pt: $(n, i, j+1/2, k+1/2)$

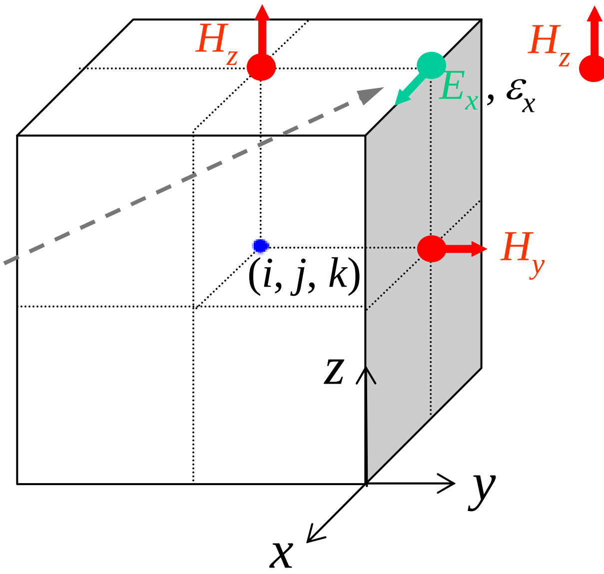

$$\text{curl}\ \vec{H} = \varepsilon \frac{\partial \vec{E}}{\partial t} \quad \rightarrow \quad \text{only } x\text{-component:}$$

$$\frac{\partial E_x}{\partial t} = \frac{1}{\varepsilon_x}\left(\frac{\partial H_z}{\partial y} - \frac{\partial H_y}{\partial z}\right)$$

Discretization:

$$\frac{\partial H_y}{\partial z} \approx \frac{H_y|^n_{i,j+1/2,k+1} - H_y|^n_{i,j+1/2,k}}{\Delta z}$$

$$\frac{\partial H_z}{\partial y} \approx \frac{H_z|^n_{i,j,k+1/2} - H_z|^n_{i,j+1,k+1/2}}{\Delta y}$$

$$\frac{\partial E_x}{\partial t} \approx \frac{E_x|^{n+1/2}_{i,j+1/2,k+1/2} - E_x|^{n-1/2}_{i,j+1/2,k+1/2}}{\Delta t}$$

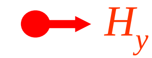

Six Update Equations for Ampere´s and Faraday´s Laws

$$E_x\Big|_{i,j+\frac{1}{2},k+\frac{1}{2}}^{n+\frac{1}{2}} = E_x\Big|_{i,j+\frac{1}{2},k+\frac{1}{2}}^{n-\frac{1}{2}} + \frac{\Delta t}{\varepsilon_{i,j+\frac{1}{2},k+\frac{1}{2}}}\left(\frac{H_z\big|_{i,j,k+\frac{1}{2}}^{n} - H_z\big|_{i,j+1,k+\frac{1}{2}}^{n}}{\Delta y} - \frac{H_y\big|_{i,j+\frac{1}{2},k+1}^{n} - H_y\big|_{i,j+\frac{1}{2},k}^{n}}{\Delta z}\right)$$

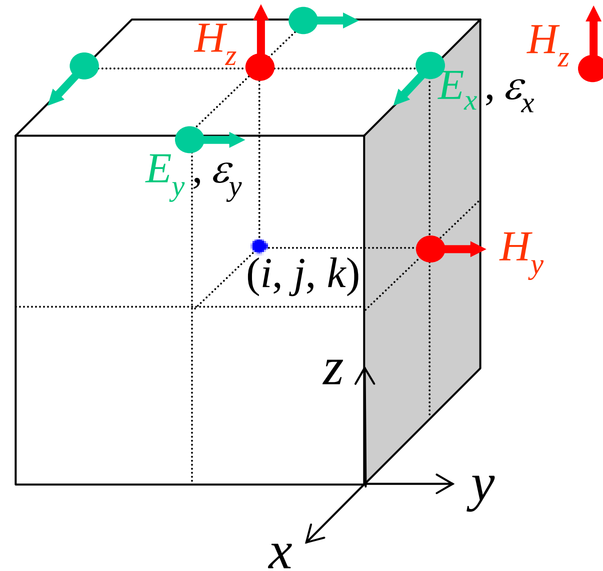

$$\frac{\partial H_z}{\partial t} = -\frac{1}{\mu_z}\left(\frac{\partial E_y}{\partial x} - \frac{\partial E_x}{\partial y}\right)$$

$$H_z\Big|_{i,j,k+\frac{1}{2}}^{n+1} = H_z\Big|_{i,j,k+\frac{1}{2}}^{n} - \frac{\Delta t}{\mu_{i,j,k+\frac{1}{2}}}\left(\frac{E_y\big|_{i+\frac{1}{2},j,k+\frac{1}{2}}^{n+\frac{1}{2}} - E_y\big|_{i-\frac{1}{2},j,k+\frac{1}{2}}^{n+\frac{1}{2}}}{\Delta x} - \frac{E_x\big|_{i,j+\frac{1}{2},k+\frac{1}{2}}^{n+\frac{1}{2}} - E_x\big|_{i,j-\frac{1}{2},k+\frac{1}{2}}^{n+\frac{1}{2}}}{\Delta y}\right)$$

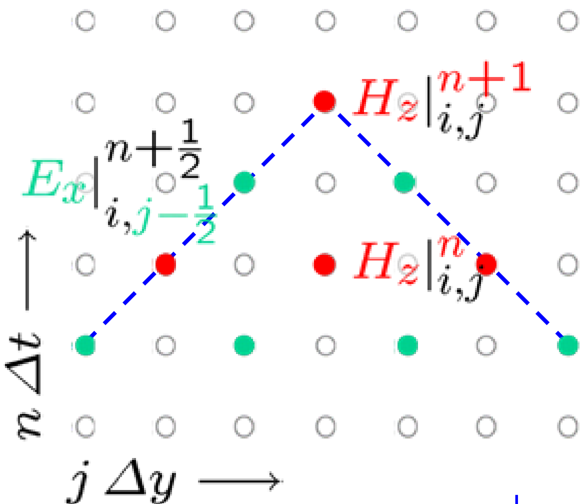

Why Leapfrog?

Leapfrog A game in which players in turn vault with parted legs over others who are bending down.

(New Oxford Dictionary of English. Oxford Univ. Press, New York 1998)

$$H_z\Big|_{i,j,k+1/2}^{\mathbf{n+1}} = H_z\Big|_{i,j,k+1/2}^{\mathbf{n}} - \frac{\Delta t}{\mu_{i,j,k+1/2}}\left(\frac{E_y\big|_{i+1/2,j,k+1/2}^{\mathbf{n+1/2}} - E_y\big|_{i-1/2,j,k+1/2}^{\mathbf{n+1/2}}}{\Delta x} - \frac{E_x\big|_{i,j+1/2,k+1/2}^{\mathbf{n+1/2}} - E_x\big|_{i,j-1/2,k+1/2}^{\mathbf{n+1/2}}}{\Delta y}\right)$$

Arrive at time $\mathbf{n+1}$

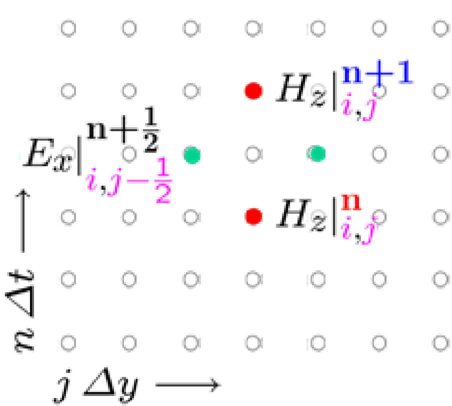

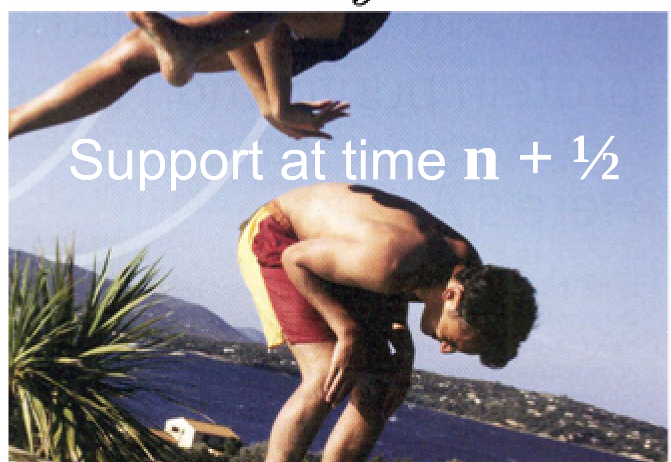

Start at time $\mathbf{n}$

www.stratagene.com

Outline

- Wavelets
  - What are they good for?
- Finite-differences in time-domain
  - Yee's leapfrog algorithm
  - Numerical dispersion, stability and accuracy
  - Higher-order finite-differences
  - Method of weighted residuals: Collocation
- Wavelet FDTD
  - Numerical dispersion, stability and accuracy
  - Summary, and what should be done further
  - Dispersive and nonlinear media
- Application examples in nano-photonics
  - Waveguide roughness
  - Slow light in a photonic crystal with disorder
  - Four-wave mixing in a microring resonator
  - Switching of a Bragg grating
- Summary and further reading

Numerical Dispersion

Maxwell's equations, homogeneous lossless space, parameters $\epsilon = \epsilon_0 \epsilon_r$, $\mu = \mu_0 \mu_r$, $n^2 = \epsilon_r \mu_r$, $c^2 = 1/(\epsilon_0 \mu_0)$, $Z = \sqrt{\mu/\epsilon}$:

$$\mathrm{j}\,\mathrm{curl}\left(\sqrt{\frac{\mu}{\epsilon}}\,\vec{H}\right) = \mathrm{j}\sqrt{\epsilon\mu}\,\frac{\partial}{\partial t}\left(\vec{E}\right), \qquad -\mathrm{curl}\left(\vec{E}\right) = \sqrt{\epsilon\mu}\,\frac{\partial}{\partial t}\left(\sqrt{\frac{\mu}{\epsilon}}\,\vec{H}\right)$$

In compact form, and with $\vec{V} = Z\,\vec{H} + \mathrm{j}\,\vec{E}$:

$$\mathrm{j}\,\mathrm{curl}\left(Z\,\vec{H} + \mathrm{j}\,\vec{E}\right) = \frac{n}{c}\frac{\partial}{\partial t}\left(Z\,\vec{H} + \mathrm{j}\,\vec{E}\right), \qquad \mathrm{j}\,\mathrm{curl}\,\vec{V} = \frac{n}{c}\frac{\partial \vec{V}}{\partial t}$$

Plane wave $\vec{V}(t,\vec{r}\,) = \vec{V}_0 \exp\left[\mathrm{j}\left(\omega_0 t - \vec{k}\cdot\vec{r}\,\right)\right]$ with $|\vec{k}|^2 = (n\omega_0/c)^2$, sampled in time $t = n\Delta t$ and space $\vec{r} = i\,\Delta x\,\vec{e}_x + j\,\Delta y\,\vec{e}_y + k\,\Delta z\,\vec{e}_z$.

Differential operator scheme:

$$\frac{\partial \vec{V}^{n}_{i,j,k}}{\partial t} = \frac{\vec{V}^{n+\frac{1}{2}}_{i,j,k} - \vec{V}^{n-\frac{1}{2}}_{i,j,k}}{\Delta t} = \frac{\mathrm{e}^{\mathrm{j}\,\omega_0\frac{\Delta t}{2}} - \mathrm{e}^{-\mathrm{j}\,\omega_0\frac{\Delta t}{2}}}{\Delta t}\vec{V}^{n}_{i,j,k} = \mathrm{j}\,\omega_0 \frac{\sin\left(\omega_0\frac{\Delta t}{2}\right)}{\omega_0\frac{\Delta t}{2}}\vec{V}^{n}_{i,j,k}$$

Numerical Dispersion

Plane wave $\vec{V}(t,\vec{r}) = \vec{V}_0 \exp\left[\mathrm{j}\left(\omega_0 t - \vec{k}\cdot\vec{r}\right)\right]$ with $|\vec{k}|^2 = (n\omega_0/c)^2$.

Numerical differential operators $(q = x, y, z)$:

$$\partial_t \vec{V}^n_{i,j,k} = \mathrm{j}\,\omega_0 \frac{\sin\left(\omega_0 \frac{\Delta t}{2}\right)}{\omega_0 \frac{\Delta t}{2}} \vec{V}^n_{i,j,k}\,, \qquad \partial_q \vec{V}^n_{i,j,k} = -\mathrm{j}\,k_q \frac{\sin\left(k_q \frac{\Delta q}{2}\right)}{k_q \frac{\Delta q}{2}} \vec{V}^n_{i,j,k}$$

For a plane wave to fulfill the wave equation $\nabla^2 \vec{V} = \frac{n^2}{c^2}\partial_t^2 \vec{V}$:

$$\left(-k_x^2 - k_y^2 - k_z^2\right)\vec{V} = -\frac{n^2}{c^2}\omega_0^2\,\vec{V}\,, \qquad |\vec{k}|^2 = \left(n\frac{\omega_0}{c}\right)^2 = n^2 k_0^2$$

For the numerical wave an equivalent condition must hold:

$$\left(-\mathrm{j}\,k_x \frac{\sin\left(k_x \frac{\Delta x}{2}\right)}{k_x \frac{\Delta x}{2}}\right)^2 + \left(-\mathrm{j}\,k_y \frac{\sin\left(k_y \frac{\Delta y}{2}\right)}{k_y \frac{\Delta y}{2}}\right)^2 + \left(-\mathrm{j}\,k_z \frac{\sin\left(k_z \frac{\Delta z}{2}\right)}{k_z \frac{\Delta z}{2}}\right)^2$$

$$= \frac{n^2}{c^2}\left(-\mathrm{j}\,\omega_0 \frac{\sin\left(\omega_0 \frac{\Delta t}{2}\right)}{\omega_0 \frac{\Delta t}{2}}\right)^2$$

1D Numerical Dispersion Artefact

Numerical wave solves Maxwell's equations if (refractive index n):

$$\left(-\mathrm{j}\,k_x \frac{\sin\left(k_x \frac{\Delta x}{2}\right)}{k_x \frac{\Delta x}{2}}\right)^2 + \left(-\mathrm{j}\,k_y \frac{\sin\left(k_y \frac{\Delta y}{2}\right)}{k_y \frac{\Delta y}{2}}\right)^2 + \left(-\mathrm{j}\,k_z \frac{\sin\left(k_z \frac{\Delta z}{2}\right)}{k_z \frac{\Delta z}{2}}\right)^2$$

1D case, $k_x = k_y = 0$:

$$= \frac{n^2}{c^2}\left(-\mathrm{j}\,\omega_0 \frac{\sin\left(\omega_0 \frac{\Delta t}{2}\right)}{\omega_0 \frac{\Delta t}{2}}\right)^2$$

$$\left(\frac{\sin\left(k_z\,\Delta z/2\right)}{\Delta z/2}\right)^2 = \frac{n^2}{c^2}\left(\frac{\sin\left(\omega_0\,\Delta t/2\right)}{\Delta t/2}\right)^2,$$

$$\sin^2\left(k_z \frac{\Delta z}{2}\right) = \left(\frac{n\Delta z}{c\Delta t}\right)^2 \sin^2\left(\omega_0 \frac{\Delta t}{2}\right),$$

$$\sin\left(\omega_0 \frac{\Delta t}{2}\right) = +\frac{c\Delta t}{n\Delta z} \sin\left(k_z \frac{\Delta z}{2}\right) \quad \left(\text{stability factor } S = \frac{c\Delta t}{n\Delta z}\right),$$

$$\omega_0\,\Delta t = +2\arcsin\left[S \sin\left(k_z \frac{\Delta z}{2}\right)\right],$$

$$n\frac{\omega_0}{c} = \left\{n\Delta z = c\Delta t\right\} = k_z$$

1D Stability and Numerical Dispersion Artefact (refract. index n)

1D case, $k_x = k_y = 0$, stability factor (Courant number) $S = \dfrac{c\Delta t}{n\Delta z}$:

$$\sin\left(\omega_0 \frac{\Delta t}{2}\right) = S \sin\left(k_z \frac{\Delta z}{2}\right) \le S \;\; (0 \le k_z\,\Delta z \le \pi), \qquad \omega_0 = \omega_r + \mathrm{j}\,\omega_i$$

$$\omega_0\,\Delta t = 2\arcsin\left[S \sin\left(k_z \tfrac{\Delta z}{2}\right)\right]$$

Numerical 1D wave (increasing!):

$$\exp\left[+|\omega_i|t\right]\exp\left[\mathrm{j}\,(\omega_r t - k_z z\,)\right]$$

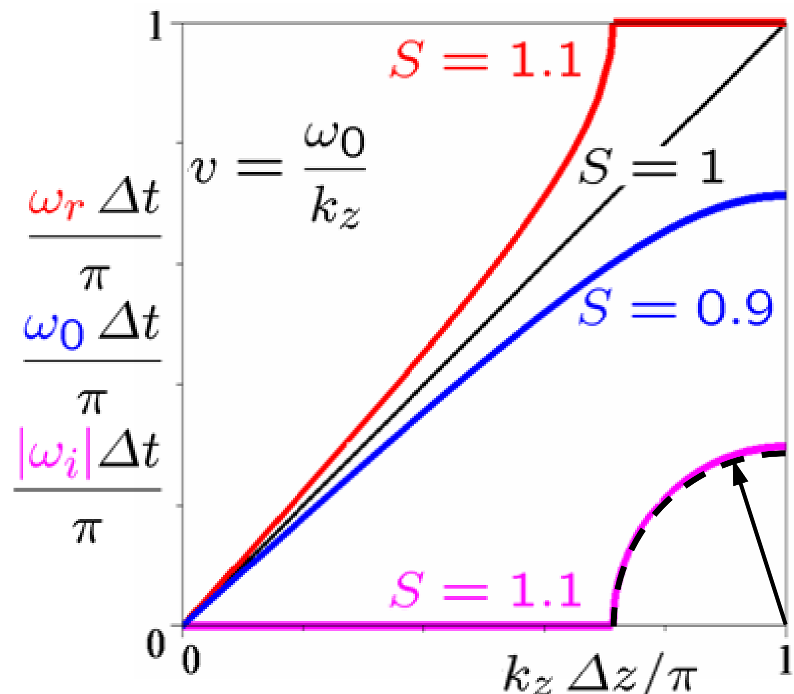

Stability live (2D FDTD): stbl $100\Delta n$ unstbl

Dispersion live (2D FDTD): 0.999 S 0.1 $k_z\Delta z = \pi/2$

3D Stability and Numerical Dispersion

Numerical wave *is* solution of Maxwell's equations if

$$\sin\Big(\omega_0 \frac{\Delta t}{2}\Big) = \frac{c\Delta t}{n} \sqrt{\left(\frac{\sin\big(k_x \frac{\Delta x}{2}\big)}{\Delta x}\right)^2 + \left(\frac{\sin\big(k_y \frac{\Delta y}{2}\big)}{\Delta y}\right)^2 + \left(\frac{\sin\big(k_z \frac{\Delta z}{2}\big)}{\Delta z}\right)^2} \leq 1$$

or if :

$$S = S_{\mathrm{FD2}} := \frac{c}{n}\frac{\Delta t}{\Delta l} = \frac{c\Delta t}{n}\sqrt{\left(\frac{1}{\Delta x}\right)^2 + \left(\frac{1}{\Delta y}\right)^2 + \left(\frac{1}{\Delta z}\right)^2} \leq 1$$

Δl is maximum allowable spatial sampling interval for real propagation constant $\vec{k} = 2\pi\vec{\kappa}$ (spatial frequency $\kappa = n/\lambda$, $k_s \frac{\Delta s}{2} = \frac{\pi}{2}$):

$$\kappa = \frac{n}{\lambda} = \sqrt{\xi^2 + \eta^2 + \zeta^2} = \sqrt{\left(\frac{1}{2\Delta x}\right)^2 + \left(\frac{1}{2\Delta y}\right)^2 + \left(\frac{1}{2\Delta z}\right)^2} = \frac{1}{2\Delta l}$$

Stability limit:

$$\Delta t = \frac{\Delta l}{c/n} = \frac{1}{2f_0}\frac{2\Delta l}{\lambda/n} = \frac{1}{2f_0} \quad \text{for} \quad \Delta l = \frac{\lambda/n}{2} = \frac{1}{2\kappa}$$

3D Plane Wave Dispersion and Accuracy — Choice of Step Sizes

Stability $S = \frac{c}{n}\frac{\Delta t}{\Delta l}$. Keep clear from dangerous $S = 1$, i. e., from

$$\Delta t = \frac{\Delta l}{c/n} = \frac{1}{2f_0}\frac{2\Delta l}{\lambda/n} = \frac{1}{2f_0} \quad \text{for} \quad \Delta l = \frac{\lambda/n}{2} = \frac{1}{2\kappa}.$$

Signal frequency $f_0 = 1/T$ associated with spatial frequency $\kappa = 1/(\lambda/n)$. No temporal detail smaller than period T, no spatial detail smaller than medium wavelength λ/n may be resolved with this specific plane wave. The sampling recipe above yields an exact representation: No dispersion, but risk of global or local instability.

Accuracy Choose a safe $S < 1$. For low dispersion error $< 1\,\%$ ($\arcsin(x) \leq 1.01\,x$) choose $k_s\frac{\Delta s}{2} \leq 0.16\,\frac{\pi}{2} \ll \frac{\pi}{2}$ $(s = x, y, z)$, i. e.,

$$\omega_0\Delta t = 2\arcsin\left(S\,\tfrac{1}{2}k\Delta l\right) \approx S\,k\Delta l \leq S \times 0.16\,\pi \quad (|\vec{k}| = k = 2\pi\kappa),$$

$$\omega_0 \approx \frac{c}{n}k \quad \text{for } S < 1 \text{ and } \Delta t \leq S\,\frac{0.16}{2f_0} \text{ or } \Delta l \leq \frac{0.16}{2\kappa}$$

3D Stability — Intuitive Explanation for $\Delta = \Delta x = \Delta y = \Delta z$

- A numerical value propagates $\sqrt{3}\,\Delta \ldots 3\Delta$ per $3\Delta t$, given the local nature of the spatial difference used in the Yee algorithm, i. e., at a speed $\tilde{v} \geq \tilde{v}_\Delta = \frac{\sqrt{3}\,\Delta}{3\Delta t} = \frac{1}{\sqrt{3}} \frac{\Delta}{\Delta t}$.

Courant: $S = \frac{c}{n} \frac{\Delta t}{\Delta l}$

$S = \frac{v_{\mathrm{wrld}}}{\tilde{v}}$

- If the dispersion of the numerical wave is chosen such that its phase velocity $v > \tilde{v}$ exceeds the slowest speed $\tilde{v}_\Delta$ provided by the algorithm, instability occurs.

- If the dispersion of the numerical wave leads to a phase velocity $v < \tilde{v}$, which is smaller than the slowest algorithm speed $\tilde{v}_\Delta$, the computation is stable.

- For a good accuracy $v \approx v_{\mathrm{wrld}}$ the step sizes

$$\Delta t \leq \frac{1}{2f_0}\,, \quad \Delta l = \left[\left(\frac{1}{\Delta x}\right)^2 + \left(\frac{1}{\Delta y}\right)^2 + \left(\frac{1}{\Delta z}\right)^2\right]^{-\frac{1}{2}} \leq \frac{1}{2\kappa} = \frac{\lambda/n}{2} = \frac{c/n}{2f_0}$$

must be significantly smaller than the Nyquist limit.

Outline

- Wavelets
  - What are they good for?
- Finite-differences in time-domain
  - Yee's leapfrog algorithm
  - Numerical dispersion, stability and accuracy
  - Higher-order finite-differences
  - Method of weighted residuals: Collocation
- Wavelet FDTD
  - Numerical dispersion, stability and accuracy
  - Summary, and what should be done further
  - Summary, and what should be further done
- Application examples in nano-photonics
  - Waveguide roughness
  - Slow light in a photonic crystal with disorder
  - Four-wave mixing in a microring resonator
  - Switching of a Bragg grating
- Summary and further reading

Second-Order Accurate Central Difference

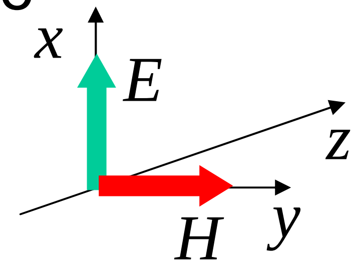

1D wave $E \mathrel{\hat{=}} E_x$ and $H \mathrel{\hat{=}} H_y$:

$$-\varepsilon \frac{\partial E(t,z)}{\partial t} = \frac{\partial H(t,z)}{\partial z} \quad \text{(Ampere)}$$

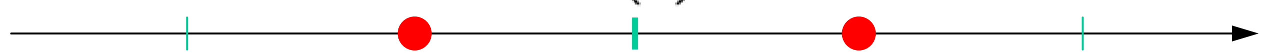

Taylor series expansion:

$$H\left(z+\frac{h}{2}\right) = H(z) + \frac{h}{2}\frac{\partial H(z)}{\partial z} + \frac{1}{2!}\frac{h^2}{4}\frac{\partial^2 H(z)}{\partial z^2} + \frac{1}{3!}\frac{h^3}{8}\frac{\partial^3 H(z)}{\partial z^3} + \dots$$

$$-$$

$$H\left(z-\frac{h}{2}\right) = H(z) - \frac{h}{2}\frac{\partial H(z)}{\partial z} + \frac{1}{2!}\frac{h^2}{4}\frac{\partial^2 H(z)}{\partial z^2} - \frac{1}{3!}\frac{h^3}{8}\frac{\partial^3 H(z)}{\partial z^3} + \dots$$

Second-order accurate central difference:

$$\frac{\partial H(z)}{\partial z} = \frac{1}{h}\left[H\left(z+\frac{h}{2}\right) - H\left(z-\frac{h}{2}\right)\right] + \underbrace{\frac{h^2}{24}\frac{\partial^3 H(z)}{\partial z^3} + \dots}_{\mathcal{O}(h^2)}$$

Fourth-Order Accurate Central Difference

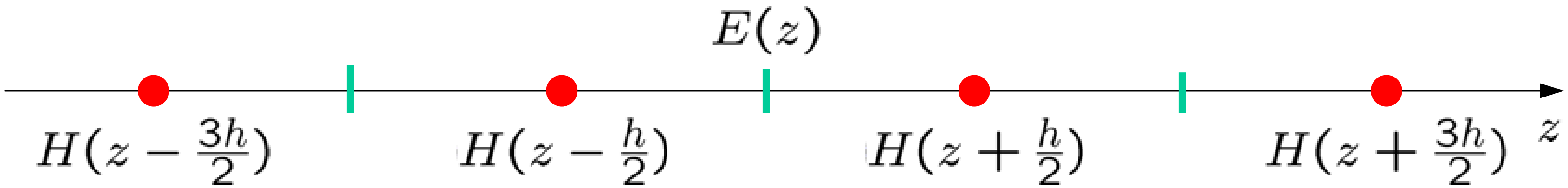

Second-order accurate central difference:

$$27h\frac{\partial H(z)}{\partial z} \approx 27\left[H\left(z+\frac{h}{2}\right) - H\left(z-\frac{h}{2}\right)\right] + \underbrace{\frac{27h^3}{24}\frac{\partial^3 H(z)}{\partial z^3}}_{\text{substitute}}$$

Taylor series expansion:

$$\underbrace{H\left(z+\frac{3h}{2}\right)}_{} \approx \cancel{H(z)} + \frac{3h}{2}\frac{\partial H(z)}{\partial z} + \cancel{\frac{9h^2}{8}\frac{\partial^2 H(z)}{\partial z^2}} + \frac{27h^3}{48}\frac{\partial^3 H(z)}{\partial z^3} + \ldots$$

$$-$$

$$\overbrace{H\left(z-\frac{3h}{2}\right)} \approx \cancel{H(z)} - \frac{3h}{2}\frac{\partial H(z)}{\partial z} + \cancel{\frac{9h^2}{8}\frac{\partial^2 H(z)}{\partial z^2}} - \frac{27h^3}{48}\frac{\partial^3 H(z)}{\partial z^3} + \ldots$$

Fourth-order accurate central difference:

$$\frac{\partial H(z)}{\partial z} = \frac{27}{24h}\left[H\left(z+\frac{h}{2}\right)-H\left(z-\frac{h}{2}\right)\right]+\frac{-1}{24h}\left[H\left(z+\frac{3h}{2}\right)-H\left(z-\frac{3h}{2}\right)\right]+\mathcal{O}(h^4)$$

High-Order Accurate Central Difference

1D wave $E \mathrel{\widehat{=}} E_x$ and $H \mathrel{\widehat{=}} H_y$: $-\varepsilon \dfrac{\partial E(t,z)}{\partial t} = \dfrac{\partial H(t,z)}{\partial z}$ (Ampere)

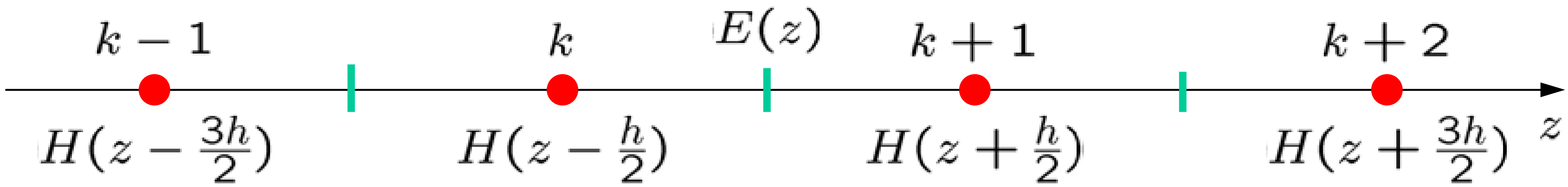

Second-order, $L = 1$:

$$\frac{\partial H(z)}{\partial z} = \frac{H_{k+1} - H_k}{\Delta z} + \mathcal{O}(\Delta z^2)$$

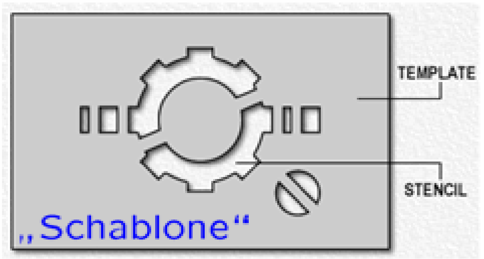

Fourth-order, $L = 2$:

$$\frac{\partial H(z)}{\partial z} = \frac{\frac{27}{24} H_{k+1} - \frac{27}{24} H_k - \frac{1}{24} H_{k+2} + \frac{1}{24} H_{k-1}}{\Delta z} + \mathcal{O}(\Delta z^4)$$

$(2L)$th order, one-sided stencil length L, coefficients $a_{l-1} = -a_{-l}$:

$$\frac{\partial H(z)}{\partial z} = \frac{1}{\Delta z} \sum_{l=-L}^{L-1} a_l H_{k+1+l} + \mathcal{O}(\Delta z^{2L}), \quad \text{terms } H_{k+1-L}, \ldots, H_{k+L}$$

Outline

- Wavelets
  - What are they good for?
- Finite-differences in time-domain
  - Yee's leapfrog algorithm
  - Numerical dispersion, stability and accuracy
  - Higher-order finite-differences
  - Method of weighted residuals: Collocation
- Wavelet FDTD
  - Numerical dispersion, stability and accuracy
  - Summary, and what should be done further
  - Dispersive and nonlinear media
- Application examples in nano-photonics
  - Waveguide roughness
  - Slow light in a photonic crystal with disorder
  - Four-wave mixing in a microring resonator
  - Switching of a Bragg grating
- Summary and further reading

Method of Weighted Residuals

Operator $\mathcal{H}$ (e. g., $\mathcal{H} = \partial/\partial z + \partial/\partial t$), function $G \rightsquigarrow$ exact solution:

$$\mathcal{H} F_{\text{ex}}(z,t) = G(z,t)$$

Seperable basis functions $\phi_k(z)\, h_n(t) \rightsquigarrow$ residual error $R(z,t)$:

$$F(z,t) = \sum_{n=1}^{N} \sum_{k=1}^{K} c_{k,n}\, \phi_k(z)\, h_n(t), \qquad R(z,t) := \mathcal{H} F(z,t) - G(z,t)$$

Weight functions $\tilde{v}_k(z)\, \tilde{u}_n(t)$ force weighted-R integrals to zero:

$$\iint R(z,t)\, \tilde{v}_k(z)\, \tilde{u}_n(t)\, \mathrm{d}z\, \mathrm{d}t \stackrel{!}{=} 0\,, \qquad k = 1,2,\ldots K, \;\; n = 1,2,\ldots N$$

System of $K \times N$ (possibly nonlinear) equations for coefficients $c_{k,n}$

- Petrov-Galerkin: spaces of $\tilde{v}_k, \tilde{u}_n$ different from ϕ_k, h_n
- Bubnov-Galerkin: $\tilde{v}_k = \phi_k^*$, $\tilde{u}_n = h_n^*$,
- Method of moments: injective (1:1) operator $\tilde{v}_k\, \tilde{u}_n = \mathcal{M}(\phi_k^*\, h_n^*)$
- Least squares: $\mathcal{M} = \mathcal{H}$
- Finite elements: compact-support ϕ_k, h_n; $c_{k,n}$(mesh nodes); BG
- Collocation (point matching): $\tilde{v}_k(z) = \delta(z - z_k), \tilde{u}_n(t) = \delta(t - t_n)$

Outline

- Wavelets
  - What are they good for?
- Finite-differences in time-domain
  - Yee's leapfrog algorithm
  - Numerical dispersion, stability and accuracy
  - Higher-order finite-differences
  - Method of weighted residuals: Collocation
- **Wavelet FDTD**
  - Numerical dispersion, stability and accuracy
  - Summary, and what should be done further
  - Dispersive and nonlinear media
- Application examples in nano-photonics
  - Waveguide roughness
  - Slow light in a photonic crystal with disorder
  - Four-wave mixing in a microring resonator
  - Switching of a Bragg grating
- Summary and further reading

Modelling: Wavelet-based FDTD Method

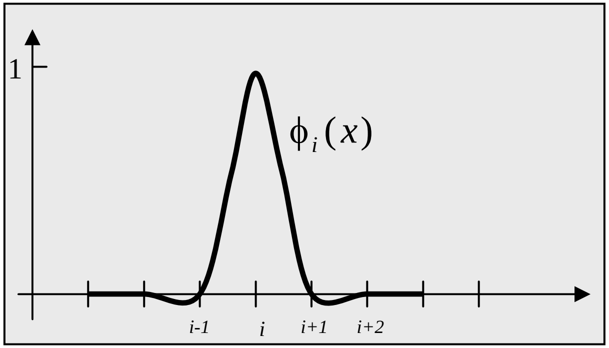

Advantages FDTD:

Time domain solution available

(i.e. pulses / transients can be studied)

Readily extended to include nonlinear materials

Disadvantages FDTD:

Much memory and time are needed for the computation

Promise of interpolating wavelet basis:

Numerical dispersion decreased dramatically

⇒ Coarser grid (less memory)

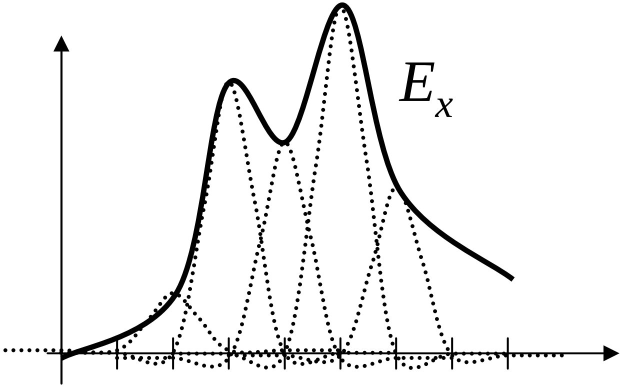

Collocation Method

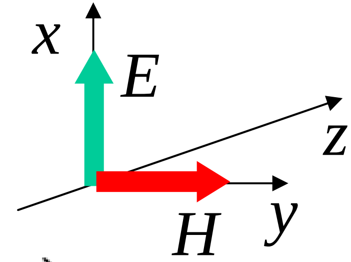

1D wave $E \mathrel{\widehat{=}} E_x$ and $H \mathrel{\widehat{=}} H_y$:

$$-\varepsilon \frac{\partial E(t,z)}{\partial t} = \frac{\partial H(t,z)}{\partial z} \text{ (Ampere)}, \quad -\mu \frac{\partial H(t,z)}{\partial t} = \frac{\partial E(t,z)}{\partial z} \text{ (Faraday)}$$

Spatial DDp MRA & Haar scaling function $\phi_h(t-n\Delta t) \mathrel{\widehat{=}} h_n(t)$:

$$-\varepsilon\frac{\partial}{\partial t}E(t,z) = \sum_{k,n} E^{\phi^{J-1}}_{k,n}\,\phi^{J-1}_k(z)\,h_n(t) \;\Big|\; \iint \mathrm{d}z\,\mathrm{d}t\;\tilde\phi^{J-1}_{k'}(z)\,h_{n'+\frac{1}{2}}(t)$$

scale $J \longrightarrow$

$$= \sum_{k,n} E^{\phi^J}_{k,n}\,\phi^J_k(z)\,h_n(t) + \sum_{k,n} E^{\psi^J}_{k,n}\,\psi^J_k(z)\,h_n(t)$$

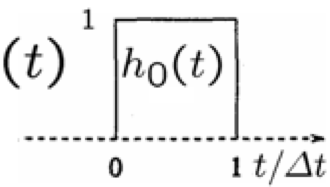

$$= \sum_{k,n} E^{\phi^{J+3}}_{k,n}\,\phi^{J+3}_k(z)\,h_n(t) + \sum_{j=J}^{J+3}\sum_{k,n} E^{\psi^j}_{k,n}\,\psi^j_k(z)\,h_n(t)$$

Spatially and temporarily interleaved $H(t,z)$, $\cdot(t)$ and $\cdot(z)$ omitted:

$$\frac{\partial}{\partial z}H(t,z) = \sum_{k,n} H^{\phi^{J+3}}_{k+\frac{1}{2},n+\frac{1}{2}}\,\phi^{J+3}_{k+\frac{1}{2}}\,h_{n+\frac{1}{2}} + \sum_{j=J}^{J+3}\sum_{k,n} H^{\psi^j}_{k,n+\frac{1}{2}}\,\psi^j_{k+\frac{1}{2}}\,h_{n+\frac{1}{2}}$$

Collocation Method

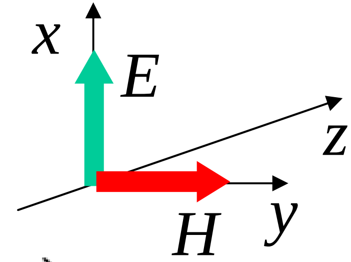

1D wave $E \mathrel{\widehat{=}} E_x$ and $H \mathrel{\widehat{=}} H_y$:

$$-\varepsilon \frac{\partial E(t,z)}{\partial t} = \frac{\partial H(t,z)}{\partial z} \text{ (Ampere)}, \quad -\mu \frac{\partial H(t,z)}{\partial t} = \frac{\partial E(t,z)}{\partial z} \text{ (Faraday)}$$

Spatial DDp MRA & Haar scaling function $\phi_h(t-n\Delta t) \mathrel{\widehat{=}} h_n(t)$:

$$E(t,z) = \sum_{k,n} E_{k,n}^{\phi^{J-1}} \; \phi_k^{J-1}(z)\, h_n(t) \quad \Big| \iint \mathrm{d}z\, \mathrm{d}t\; \tilde{\phi}_{k'}^{J}(z)\, h_{n'+\frac{1}{2}}(t)$$

$$-\varepsilon \frac{\partial}{\partial t} E(t,z) = \sum_{k,n} E_{k,n}^{\phi^J} \; \phi_k^J(z)\, h_n(t) + \sum_{k,n} E_{k,n}^{\psi^J} \; \psi_k^J(z)\, h_n(t)$$

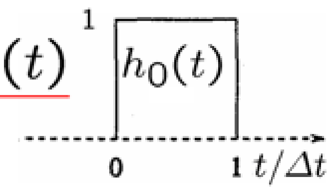

Spatially and temporarily interleaved $H(t,z)$, $\cdot(t)$ and $\cdot(z)$ omitted:

$$\frac{\partial}{\partial z} H(t,z) = \sum_{k,n} H_{k+\frac{1}{2},n+\frac{1}{2}}^{\phi^J} \; \phi_{k+\frac{1}{2}}^{J}\, h_{n+\frac{1}{2}} + \sum_{k,n} H_{k,n+\frac{1}{2}}^{\psi^J} \; \psi_{k+\frac{1}{2}}^{J}\, h_{n+\frac{1}{2}}$$

Force Residual Error to Zero — LHS (Scale J)

Inner product of time functions:

$$T = \int_{-\infty}^{+\infty} \frac{1}{\Delta t} \frac{\mathrm{d}h_n(t)}{\mathrm{d}t} h_{n'+\frac{1}{2}}(t)\,\mathrm{d}t$$

$$= \int_{-\infty}^{+\infty} \left[\delta(t - n\Delta t) - \delta(t-(n+1)\Delta t)\right] h_{n'+\frac{1}{2}}(t)\,\mathrm{d}t / \Delta t$$

$$= h\Big([n-(n'+\tfrac{1}{2})]\Delta t\Big) - h\Big([(n+1)-(n'+\tfrac{1}{2})]\Delta t\Big) / \Delta t$$

$$T = \left(\delta_{n\,n'+1} - \delta_{n\,n'}\right) / \Delta t$$

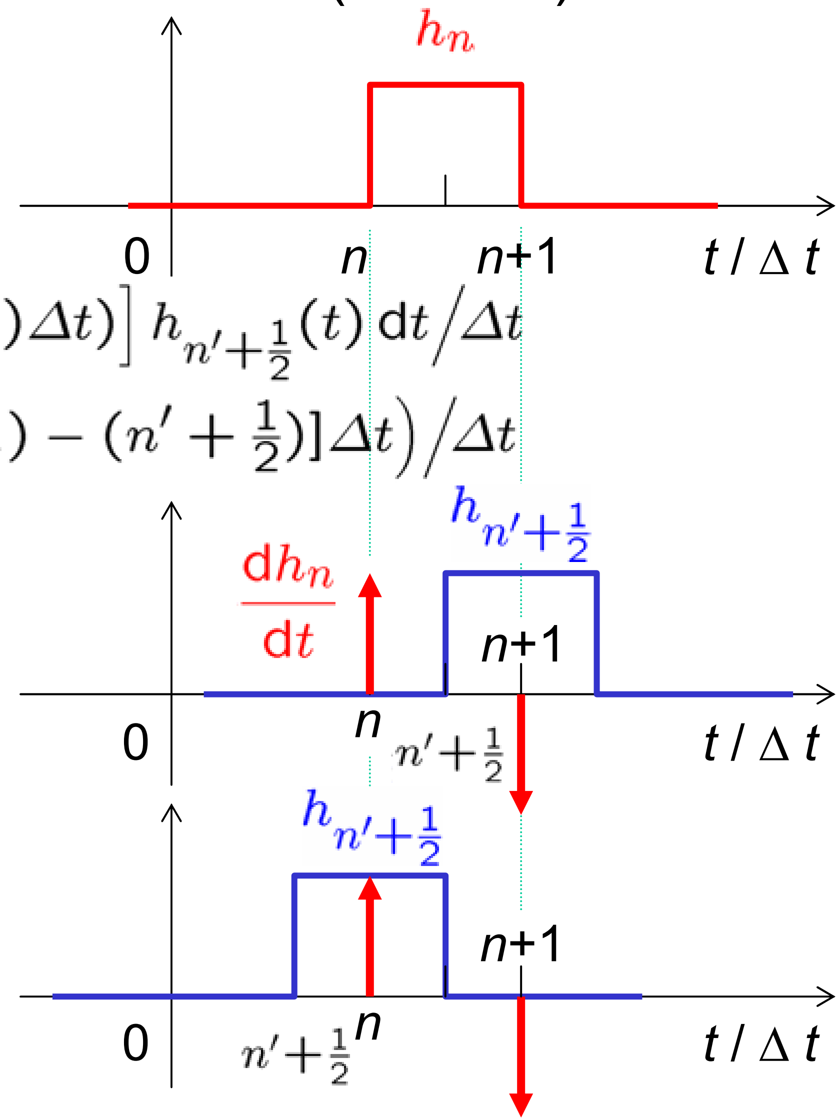

Inner product of spatial functions:

$$\Sigma = \int_{-\infty}^{+\infty} \phi_k^J(z)\,\tilde{\phi}_{k'}^J(z)\,\mathrm{d}t = \delta_{k\,k'}$$

$$\int_{-\infty}^{+\infty} \psi_k^J(z)\,\tilde{\phi}_{k'}^J(z)\,\mathrm{d}t = 0$$

$$\mathrm{LHS} = -\varepsilon_{k'} \frac{E_{k',n'+1}^{\phi^J} - E_{k',n'}^{\phi^J}}{\Delta t}$$

Force Residual Error to Zero — RHS (Scale J)

Inner product of spatial functions:

$$\Sigma = \int_{-\infty}^{+\infty} \frac{1}{\Delta z} \frac{\mathrm{d}\phi^J_{k+1/2}(z)}{\mathrm{d}z} \tilde{\phi}^J_{k'}(z)\,\mathrm{d}z$$

$$= \int_{-\infty}^{+\infty} \frac{\mathrm{d}\phi^J_{k+1/2}(z)}{\mathrm{d}z} \delta(z - k'\Delta z)\,\mathrm{d}z / \Delta z$$

$$\Sigma = \frac{1}{\Delta z} \frac{\mathrm{d}\phi^J_{k+1/2}(z)}{\mathrm{d}z}\bigg|_{k'\Delta z} = a_l^{\phi^J\phi^J} / \Delta z$$

$l = k - k'$

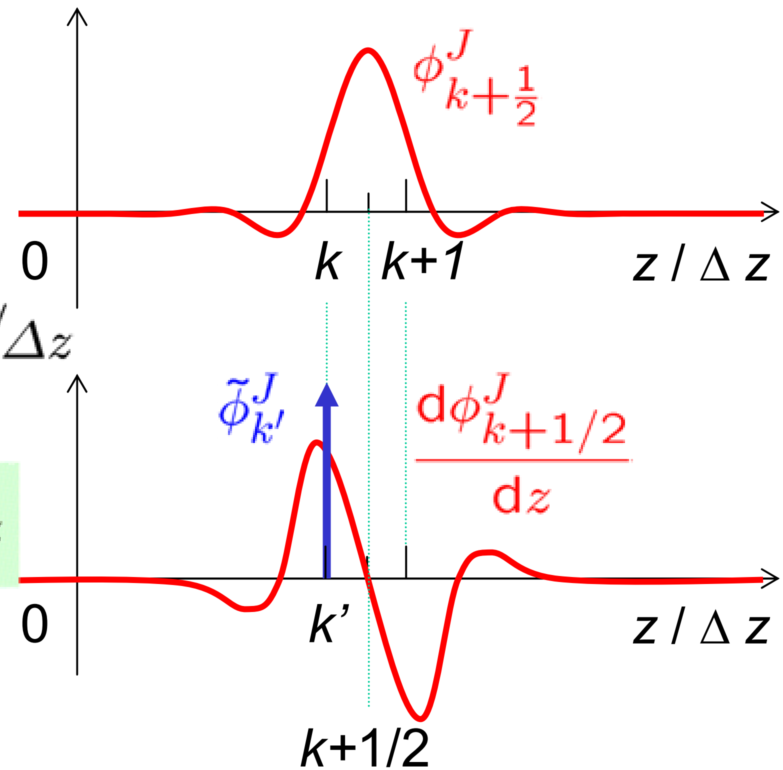

Inner product of time functions:

$$T = \int_{-\infty}^{+\infty} \frac{1}{\sqrt{\Delta t}} h_{n+\frac{1}{2}}(t) \frac{1}{\sqrt{\Delta t}} h_{n'+\frac{1}{2}}(t)\,\mathrm{d}t = \delta_{n\,n'}$$

$$-\varepsilon_{k'} \frac{E^{\phi^J}_{k',n'+1} - E^{\phi^J}_{k',n'}}{\Delta t} = \frac{\sum_l a_l^{\phi^J\phi^J} H^{\phi^J}_{k'+\frac{1}{2}+l,n'+\frac{1}{2}} + \sum_l a_l^{\psi^J\phi^J} H^{\psi^J}_{k'+\frac{1}{2}+l,n'+\frac{1}{2}}}{\Delta z}$$

Outline

- Wavelets
  - What are they good for?
- Finite-differences in time-domain
  - Yee's leapfrog algorithm
  - Numerical dispersion, stability and accuracy
  - Higher-order finite-differences
  - Method of weighted residuals: Collocation
- Wavelet FDTD
  - Numerical dispersion, stability and accuracy
  - Summary, and what should be done further
  - Dispersive and nonlinear media
- Application examples in nano-photonics
  - Waveguide roughness
  - Slow light in a photonic crystal with disorder
  - Four-wave mixing in a microring resonator
  - Switching of a Bragg grating
- Summary and further reading

Comparison of Wavelet DD^p FDTD and Standard FDTD

$$-\varepsilon_{k'} \frac{E^{\phi^J}_{k',n'+1} - E^{\phi^J}_{k',n'}}{\Delta t} = \frac{\sum_l a_l^{\phi^J\phi^J} H^{\phi^J}_{k'+\frac{1}{2}+l,n'+\frac{1}{2}} + \sum_l a_l^{\psi^J\phi^J} H^{\psi^J}_{k'+\frac{1}{2}+l,n'+\frac{1}{2}}}{\Delta z}$$

$$a_l^{\phi^J\phi^J} = \left.\frac{\mathrm{d}\phi^J_{k+\frac{1}{2}}(z)}{\mathrm{d}z}\right|_{z=k'\Delta z} = \left.\frac{\mathrm{d}\phi^J(z)}{\mathrm{d}z}\right|_{z=-(l+\frac{1}{2})\Delta z} \qquad \text{for } l = k-k'\,,\ -L \le l \le L-1$$

Wavelet FDTD: Scaling function only ($a_l^{\psi^J\phi^J} = 0$), $l = -L, \ldots, L-1$, one-sided stencil size $L = 1$, new subscripts ($k' = k+\frac{1}{2}$, $n' = n-\frac{1}{2}$):

$$-\varepsilon_{k+\frac{1}{2}} \frac{E^{\phi^J}_{k+\frac{1}{2},n+\frac{1}{2}} - E^{\phi^J}_{k+\frac{1}{2},n-\frac{1}{2}}}{\Delta t} = \frac{a_0^{\phi^J\phi^J} H^{\phi^J}_{k+1,n} + a_{-1}^{\phi^J\phi^J} H^{\phi^J}_{k,n}}{\Delta z}$$

Standard FDTD with central differences ($H_z|^n_{i,\cdot,k+\frac{1}{2}} = 0$):

$$-\varepsilon_{i,j+\frac{1}{2},k+\frac{1}{2}} \frac{E_x|^{n+\frac{1}{2}}_{i,j+\frac{1}{2},k+\frac{1}{2}} - E_x|^{n-\frac{1}{2}}_{i,j+\frac{1}{2},k+\frac{1}{2}}}{\Delta t} = \frac{H_y|^n_{i,j+\frac{1}{2},k+1} - H_y|^n_{i,j+\frac{1}{2},k}}{\Delta z}$$

2D Stability and Numerical Dispersion for Higher-Order FDTD

Numerical wave *is* solution of Maxwell's equations if

$$\sin\left(\omega_0 \frac{\Delta t}{2}\right) = \frac{c\Delta t}{n}\sqrt{\left(\sum_{l=0}^{L-1} a_l \frac{\sin\left(k_x \frac{\Delta x}{2}(2l+1)\right)}{\Delta x}\right)^2 + \left(\sum_{l=0}^{L-1} a_l \frac{\sin\left(k_z \frac{\Delta z}{2}(2l+1)\right)}{\Delta z}\right)^2} \leq 1$$

or if:

$$S_{\text{HFD}2L} = \left(\sum_{l=0}^{L-1} |a_l|\right) \underbrace{\frac{c\Delta t}{n}\sqrt{\left(\frac{1}{\Delta x}\right)^2 + \left(\frac{1}{\Delta z}\right)^2}}_{S_{\text{FD2}} \text{ for } \Delta t = (\Delta t)_{\text{FD2}}} \leq 1$$

Higher-order scheme for $S_{\text{HFD}2L} = S_{\text{FD2}}$: $\Delta t = (\Delta t)_{\text{FD2}} \Big/ \left(\sum_{l=0}^{L-1} |a_l|\right)$

Stencil	a_0	a_1	a_2	a_3	a_4	a_5	a_6	a_7	$\sum_l \lvert a_l \rvert$
HFD4	1.125	−0.042	0.	0.	0.	0.	0.	0.	1.1667
D2/DD2	1.229	−0.094	0.010	0.	0.	0.	0.	0.	1.3333
HFD6	1.172	−0.065	0.005	0.	0.	0.	0.	0.	1.2417
D4/DD4	1.311	−0.156	0.042	−0.009	0.001	0.000	−0.000	0.	1.5181

2D Numerical Dispersion Error. Stability: $S = \frac{c\Delta t}{n\Delta}\sqrt{D} \leq 1$

FD: Standard 2[nd]-order finite-differences of accuracy order $\mathcal{O}(\Delta^2)$

HFDq: Higher-order FD, $L = q/2$, support $[-L, L]$, accuracy $\mathcal{O}(\Delta^q)$

Dp, DDp: Scaling fct, order $L = 2p - 1$, compact support $[-L, L]$

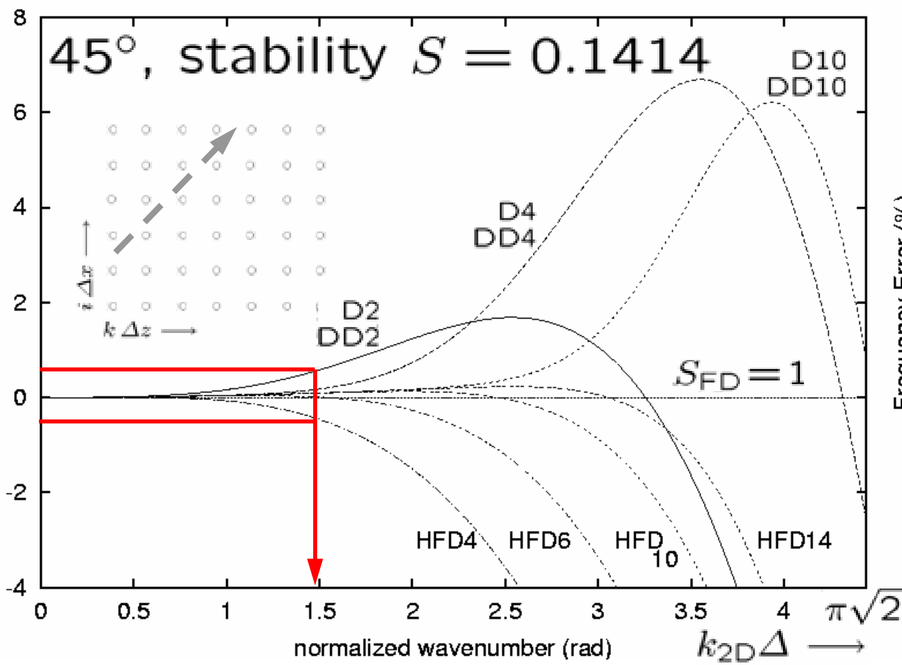

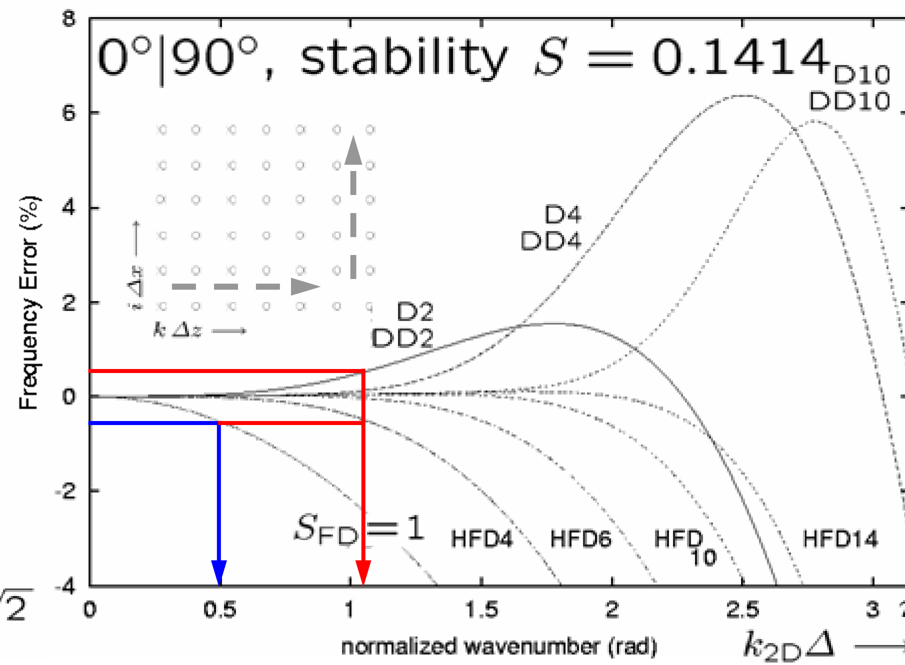

Stencil	a_0	a_1	a_2	a_3	a_4	a_5	a_6	a_7	$\sum_l \lvert a_l \rvert$
HFD4	1.125	−0.042	0.	0.	0.	0.	0.	0.	1.1667
D2/DD2	1.229	−0.094	0.010	0.	0.	0.	0.	0.	1.3333
HFD6	1.172	−0.065	0.005	0.	0.	0.	0.	0.	1.2417
D4/DD4	1.311	−0.156	0.042	−0.009	0.001	0.000	−0.000	0.	1.5181

Same stencil-L

Same accuracy

Outline

- Wavelets
  - What are they good for?
- Finite-differences in time-domain
  - Yee's leapfrog algorithm
  - Numerical dispersion, stability and accuracy
  - Higher-order finite-differences
  - Method of weighted residuals: Collocation
- Wavelet FDTD
  - Numerical dispersion, stability and accuracy
  - Summary, and what should be done further
  - Dispersive and nonlinear media
- Application examples in nano-photonics
  - Waveguide roughness
  - Slow light in a photonic crystal with disorder
  - Four-wave mixing in a microring resonator
  - Switching of a Bragg grating
- Summary and further reading

Summary of Wavelet FDTD

Pros:

- Difference operators basically broader (more coefficients), but detail coefficients may be truncated if fields do not change much in certain regions (less coefficients) $\leadsto$ self-adaptiv
- Static use of $\phi_k^J(t)$ and $\psi_k^j(t)$ for $0 \leq j \leq J$ in a predetermined high-resolution region of space $\leadsto$ simple meshing

Requirements:

- Orthogonality of expansion (synthesizing) functions ϕ, ψ and test (analyzing) functions $\tilde{\phi}$, $\tilde{\psi}$ to avoid solving a system of equations for each time step in a collocation setting
- Vanishing moments of wavelets up to order p assure rapid convergence and effective truncation of expansion with $\mathcal{O}(s^{2+1})$
- Compact support to avoid truncation of difference operators (spurious modes)
- Symmetry of ϕ, ψ and $\tilde{\phi}$, $\tilde{\psi}$, so that mirroring carries over to respective coefficients (but unsymm. Dp with symm. stencil!)

Wavelet Families and their Properties

Property	morl	mexh	meyr	haar	dbN	symN	coifN	biorNr.Nd	rbioNr.Nd	gaus	dmey	cgau	cmor	fbsp	shan
Crude	•	•								•		•	•	•	•
Infinitely regular	•	•	•							•		•	•	•	•
Arbitrary regularity					•	•	•	•	•						
Compactly supported orthogonal				•	•	•	•								
Compactly supported biothogonal								•	•						
Symmetry	•	•	•	•				•	•	•	•	•	•	•	•
Asymmetry					•										
Near symmetry						•	•								
Arbitrary number of vanishing moments					•	•	•	•	•						
Vanishing moments for ϕ							•								
Existence of ϕ			•	•	•	•	•	•	•						
Orthogonal analysis			•	•	•	•	•								
Biorthogonal analysis			•	•	•	•	•	•	•						
Exact reconstruction	≈	•	•	•	•	•	•	•	•	•	≈	•	•	•	•
FIR filters				•	•	•	•	•	•		•				
Continuous transform	•	•	•	•	•	•	•	•	•	•					
Discrete transform			•	•	•	•	•	•	•		•				
Fast algorithm				•	•	•	•	•	•		•				
Explicit expression	•	•		•				For splines	For splines	•		•	•	•	•

Misiti, M.; Misiti, Y.; Oppenheim, G.; Poggi, J.-M.: Wavelet toolbox user's guide, v. 3.1 (MATLAB release 2006b). Natick (MA): The Mathworks Inc. 2006. Page 6-90 ff.
http://www.mathworks.com/access/helpdesk/help/pdf_doc/wavelet/wavelet_ug.pdf

Summary of Wavelet Methods

Daubechies wavelets Dp and Bubnov-Galerkin:

- ✓ ϕ, ψ and $\tilde{\phi}$, $\tilde{\psi}$ are orthogonal
- ■ Moments of ψ up to order p vanish, *could* be self-adaptive
- ✓ Compact support
- ✓ No symmetry, but stencil coefficients are symmetric

Deslauries-Dubuc interpolating wavelets DDp and collocation:

- ✓ ϕ, ψ and $\tilde{\phi}$, $\tilde{\psi}$ are biorthogonal
- ■ Moments of ψ do *not* vanish, self-adaptiveness doubtful
- ✓ Compact support
- ✓ Symmetry
- ■ $\phi^{\mathrm{DD}p}$-stencil coefficients for collocation identical to those with $\phi^{\mathrm{D}p}$ and Bubnov-Galerkin: Methods equivalent!

Summary of Results, And What Should Be Done Further

Results:

- Equivalence of $\phi^{\mathrm{D}p}$-Bubnov-Galerkin and $\phi^{\mathrm{DD}p}$-collocation
- Low dispersion for $\phi^{\mathrm{D}p}/\phi^{\mathrm{DD}p}$ (reduced memory and run time) — but this *may* be equivalent to HFD6
- Equivalence between ϕ and ψ via wavelet transform $\rightsquigarrow$ all dispersion findings also valid for possible MRA

What should be done?

- Chose higher-order time difference operator (relatively simple)
- Try MRA with Daubechies $\phi^{\mathrm{D}p}$ *and* $\psi^{\mathrm{D}p}$
- Chose or invent other wavelets with vanishing moments, observing other requirements

Outline

- Wavelets
  - What are they good for?
- Finite-differences in time-domain
  - Yee’s leapfrog algorithm
  - Numerical dispersion, stability and accuracy
  - Higher-order finite-differences
  - Method of weighted residuals: Collocation
- Wavelet FDTD
  - Numerical dispersion, stability and accuracy
  - Summary, and what should be further done
  - Dispersive and nonlinear media
- Application examples in nano-photonics
  - Waveguide roughness
  - Slow light in a photonic crystal with disorder
  - Four-wave mixing in a microring resonator
  - Switching of a Bragg grating
- Summary and further reading

Dispersive and Nonlinear Media

Lossy and dispersive materials:

- More realistic models (Debye, Lorentz)
- Wave propagation in a plasma

Nonlinear modeling:

- High-power pulses (Kerr, Raman, self-steepening)
- Design of switches
- Design of wavelength converters (e. g., FWM)

Problems and solutions:

- Stability issues
- ABC so far not well established
- PML applicable, also to higher-order FD methods
- Implemented with auxiliary differential equations (ADE)

Fujii, M.; Tahara, M; Sakagami, I; Freude, W.; Russer, P.: High-order FDTD and auxiliary differential equation formulation of optical pulse propagation in 2D Kerr and Raman nonlinear dispersive media. IEEE J. Quantum Electron. 40 (2004) 175–182

Fujii, M.; Omaki, N.; Tahara, M.; Sakagami, I.; Poulton, C.; Freude, W.; Russer, P.: Optimization of nonlinear dispersive APML ABC for the FDTD analysis of optical solitons. IEEE J. Quantum Electron. 41 (2005) 448–454

Fujii, M,; Koos, C.; Poulton, C.; Sakagami, I.; Leuthold, J.; Freude, W.: A simple and rigorous verification technique for nonlinear FDTD algorithm by optical parametric four-wave mixing. Microwave and Optical Technol. Lett. 48 (2006) 88–91

Fujii, M; Koos, C.; Poulton, C.; Leuthold, J.; Freude, W.: Nonlinear FDTD analysis and experimental validation of four-wave mixing in InGaAsP/InP racetrack micro-resonators. IEEE Photon. Technol. Lett. 18 (2006) 361–363

FDTD Analysis of Nonlinear and Dispersive Media

Optical Kerr effect

polarization: $P_K(t) = \varepsilon_0 \; \chi_K^{(3)} \; E^3(t)$ ⇨ finite difference eq.

⇧ const. nonlinear susceptibility

Lorentz dispersion

polarization: $\tilde{P}_L(\omega) = \tilde{\chi}_L(\omega)\tilde{E}(\omega) = \dfrac{\varepsilon_0 \Delta\varepsilon_L \; \omega_L^2}{\omega_L^2 + 2j\delta_L\omega - \omega^2} \tilde{E}(\omega)$

⇩ $\mathcal{F}^{-1}$

$$\omega_L^2 P_L(t) + 2\delta_L \frac{\mathrm{d}P_L(t)}{\mathrm{d}t} + \frac{\mathrm{d}^2 P_L(t)}{\mathrm{d}t^2} = \varepsilon_0 \Delta\varepsilon_L \omega_L^2 E(t)$$

⇨ finite difference eq.

⇨ solved with Yee's leapfrog algorithm

Nonlinear 2D Wavelet FDTD Method for Kerr / Raman Medium

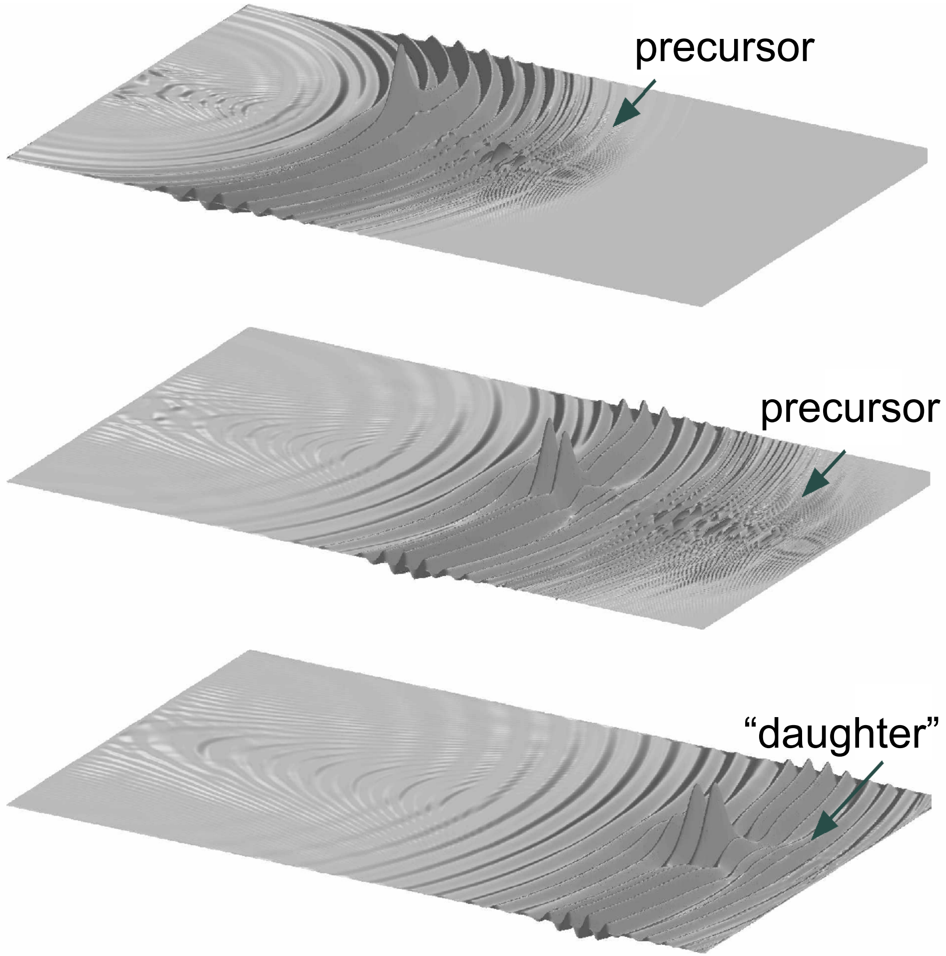

Dual processor version:

Electric field of the 2D pulse in the Kerr and the Raman medium taken at times t = 270, 360 and 450 fs, from top.

High-order DD4 ϕ-scheme with resolution $\Delta x = \Delta z = 0.04$ µm.

REQUIRED COMPUTATIONAL RESOURCES FOR THE 2D ANALYSES

Scheme	Space resolution (μm)	Time step (fs)	Memory (MB)	CPU time (minutes)
FDTD	0.02	0.0472	666	201
DD_4	0.02	0.00943	671	1162
DD_4	0.04	0.0189	193	146
DD_4	0.08	0.0377	60	20

Fujii, M.; Tahara, M.; Sakagami, I.; Freude, W.; Russer, P.: High-order FDTD and auxiliary differential equation formulation of optical pulse propagation in 2D Kerr and Raman nonlinear dispersive media. IEEE J. Quantum Electron. 40 (2004) 175–182

Outline

- Wavelets
  - What are they good for?
- Finite-differences in time-domain
  - Yee's leapfrog algorithm
  - Numerical dispersion, stability and accuracy
  - Higher-order finite-differences
  - Method of weighted residuals: Collocation
- Wavelet FDTD
  - Numerical dispersion, stability and accuracy
  - Summary, and what should be further done
  - Dispersive and nonlinear media
- Application examples in nano-photonics
  - Waveguide roughness
  - Slow light in a photonic crystal with disorder
  - Four-wave mixing in a microring resonator
  - Switching of a Bragg grating
- Summary and further reading

Example for Silicon On Insulator (SOI) Nanophotonic Device

Challenges for numerical modelling:

- High-contrast
  1. Large changes in refractive index prevent approximations
     $\Rightarrow$ vectorial optics needed
- Numerically "large"
  2. Typical problem size
     $8\ \mu m \times 8\ \mu m \times 2\ \mu m$
     $(16\ \lambda \times 16\ \lambda \times 4\ \lambda)$
  3. Grid size in 15 nm ($\sim\lambda$ / 30) range, essential for reliable results
     $\Rightarrow$ Memory requirements for standard FDTD > 2 GB. Instead:
     Wavelet FDTD with memory savings

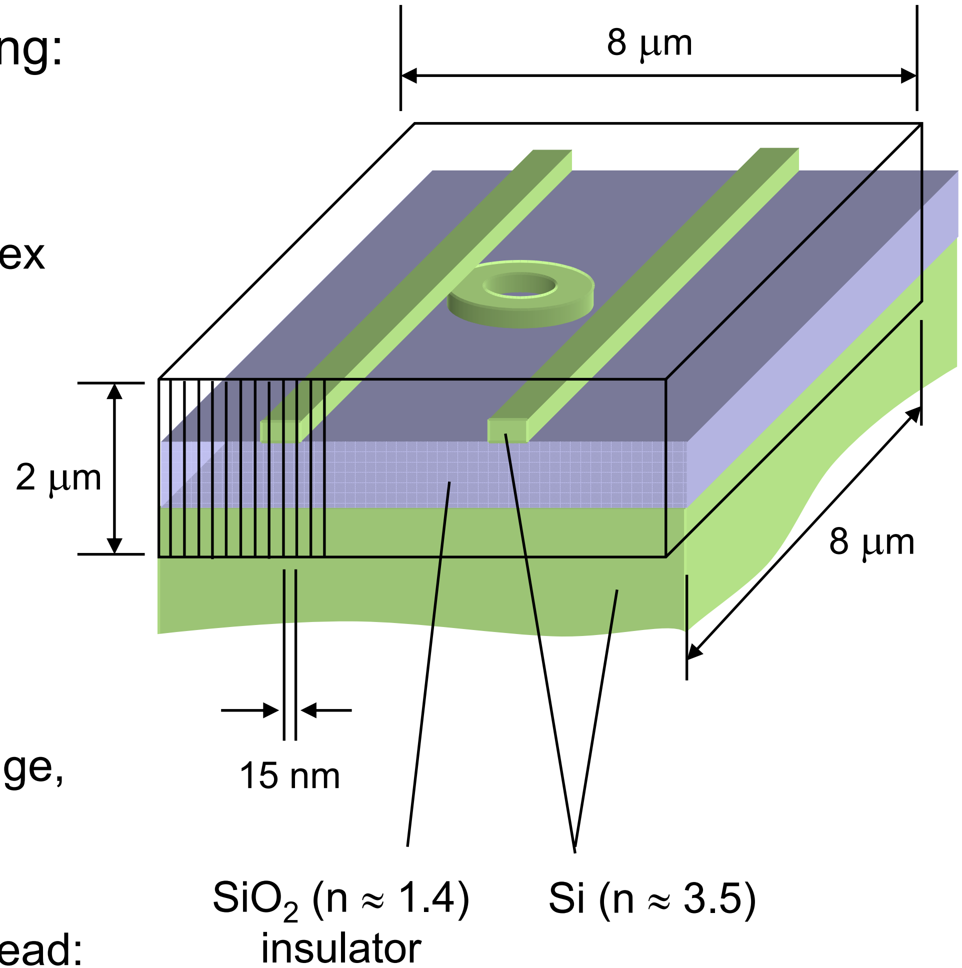

Parallel Computing Efficiency with 3D DD4-Scaling FDTD Code

IBM RS/6000 SP-SMP, distributed memory
256 CPU, 1 GB RAM each
375 MHz clock rate

Computation region:
$8.3 \times 7.1 \times 2.3\ \mu m^3$,
various gridsizes

Timespan:
250 fs

Computation times:
1 **PC** CPU: 110 h
1 *//* CPU: 450 h (× 4)
100 *//* CPU: 5.5 h (÷20)

DD4 scaling function:
$S = 0.2;\ \Delta x = \Delta y = \Delta z = \Delta$

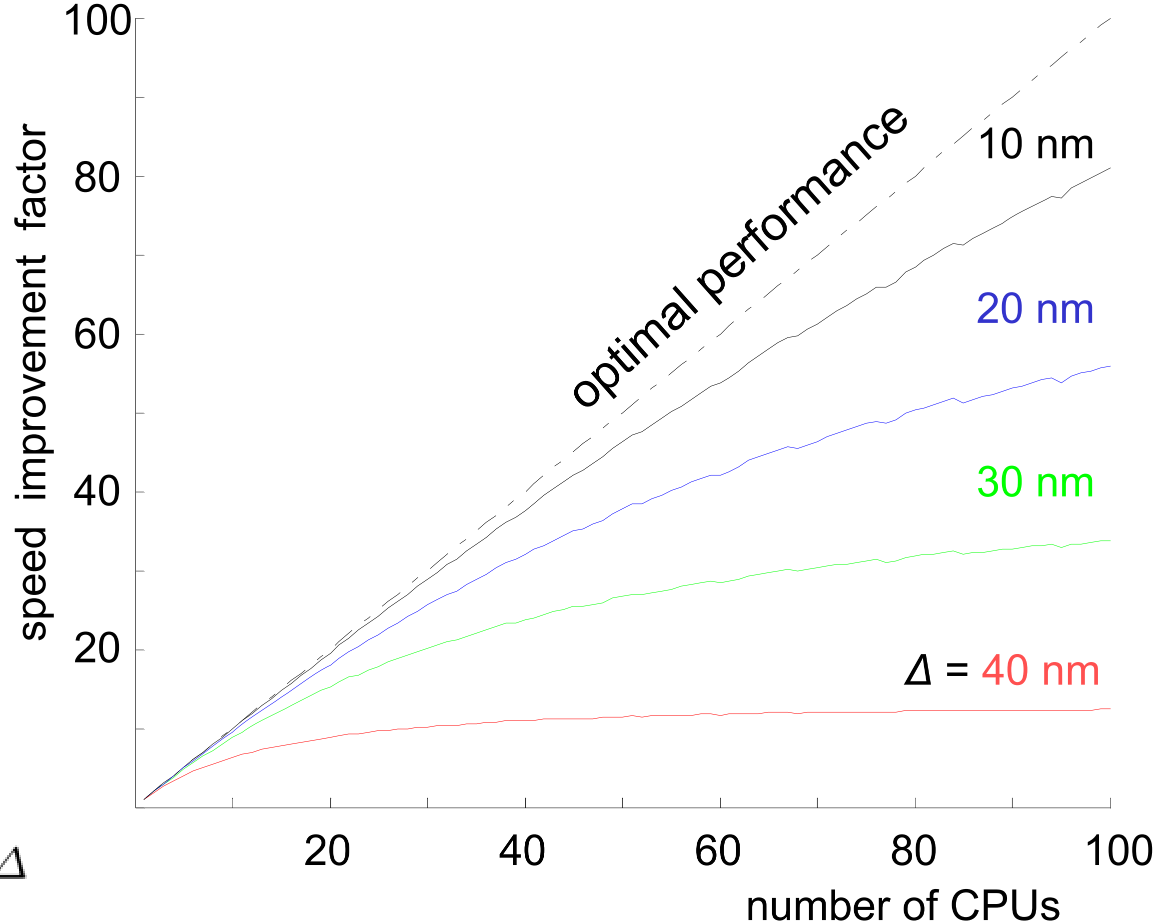

Wang, J.: Efficient techniques for modeling devices in integrated optics. Diploma Thesis, University of Karlsruhe 2003
Glöckler, F.: Efficient techniques for modeling devices in integrated optics. Project Work, University of Karlsruhe 2004

Silicon Nanostrip Waveguide with Sidewall Roughness

Straight 0.365 × 0.365 μm² Si WG, side walls with RMS roughness σ = 10…50 nm

thick glass layer

Si substrate

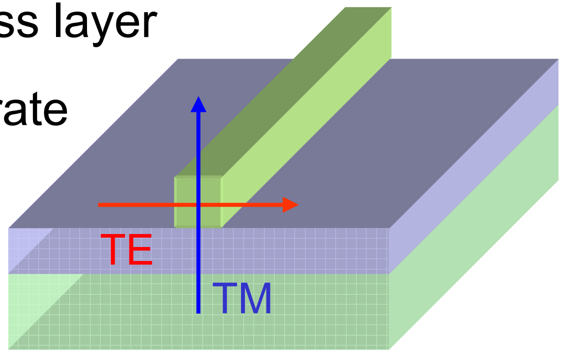

DD4 scaling fct, parallel cluster:
$S = 0.2$; $\Delta x, \Delta y, \Delta z = 10, 20, 50$ nm

w waveguide width

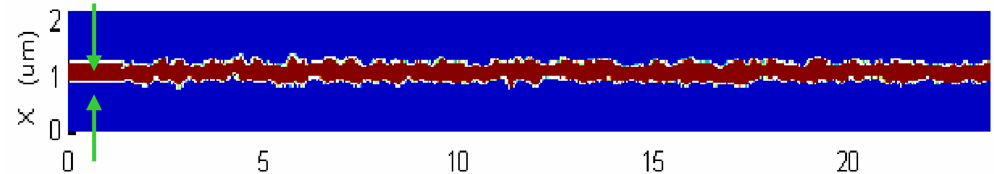

E_x-component (quasi-TE), strong confinement

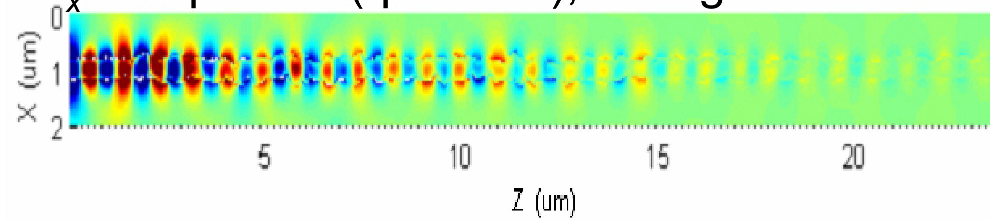

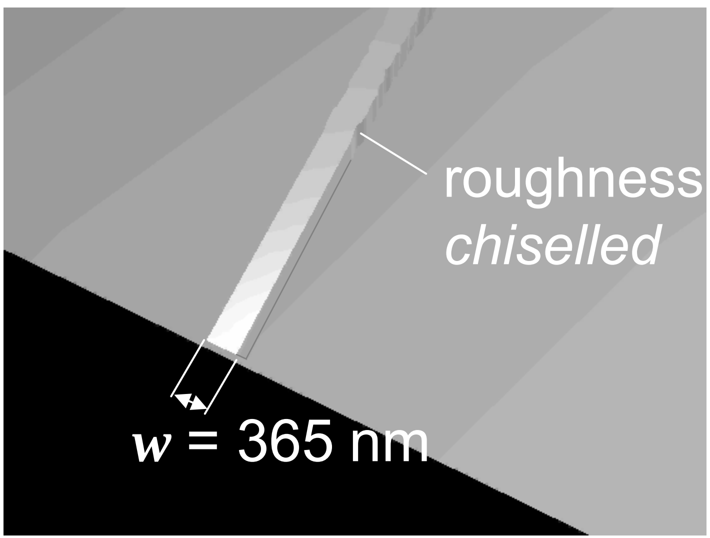

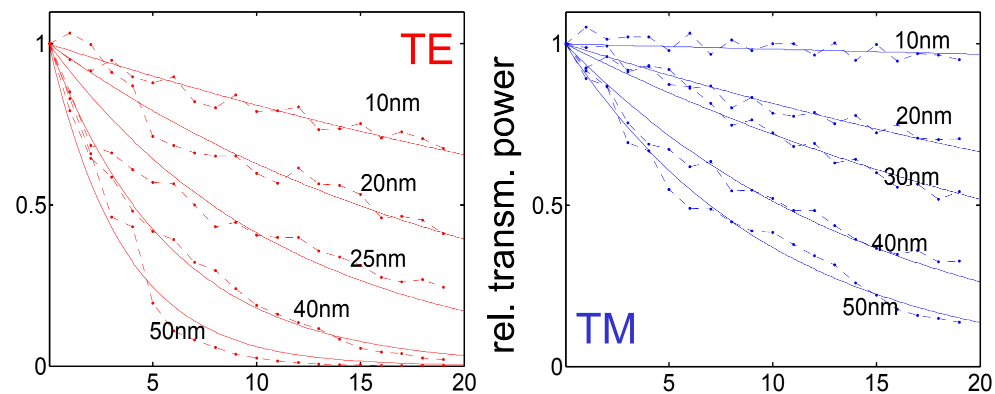

λ = 1.55 μm : propagation distance (μm)

Poulton, C. G.; Koos, C.; Fujii, M.; Pfrang, A.; Schimmel, Th.; Leuthold, J.; Freude, W.: Radiation modes and roughness loss in high index-contrast waveguides. IEEE J. Sel. Topics Quantum Electron. 12 (2006) 1306–1321

Outline

- Wavelets
  - What are they good for?
- Finite-differences in time-domain
  - Yee's leapfrog algorithm
  - Numerical dispersion, stability and accuracy
  - Higher-order finite-differences
  - Method of weighted residuals: Collocation
- Wavelet FDTD
  - Numerical dispersion, stability and accuracy
  - Summary, and what should be further done
  - Dispersive and nonlinear media
- Application examples in nano-photonics
  - Waveguide roughness
  - Slow light in a photonic crystal with disorder
  - Four-wave mixing in a microring resonator
  - Switching of a Bragg grating
- Summary and further reading

PC W1-WG with Radius Disorder

10% radius disorder

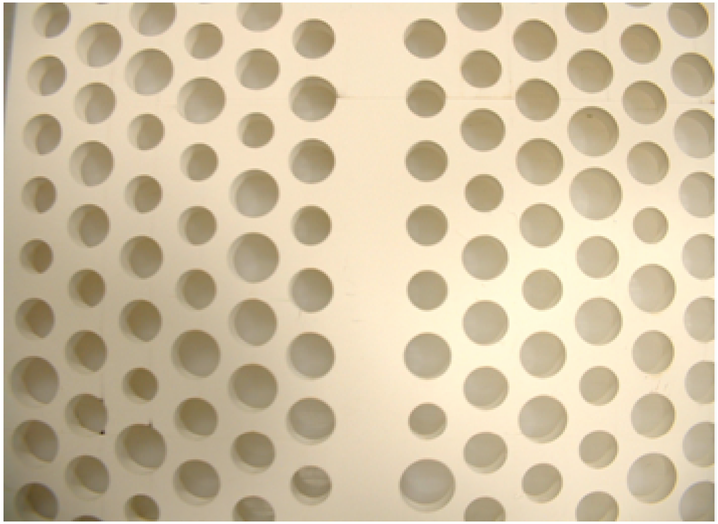

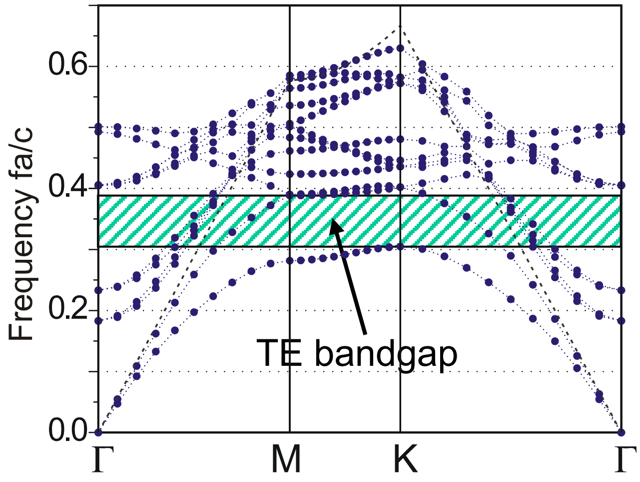

Band diagram for PC without waveguide

Plane wave method, RSoft Bandsolve

Model for Silicon PC with substrate

a = 0.52 µm, r / a = 0.35, h / a = 0.52
n = 3.16 , n_{Sub} = 1.53

PC W1-WG With Radius and Position Disorder

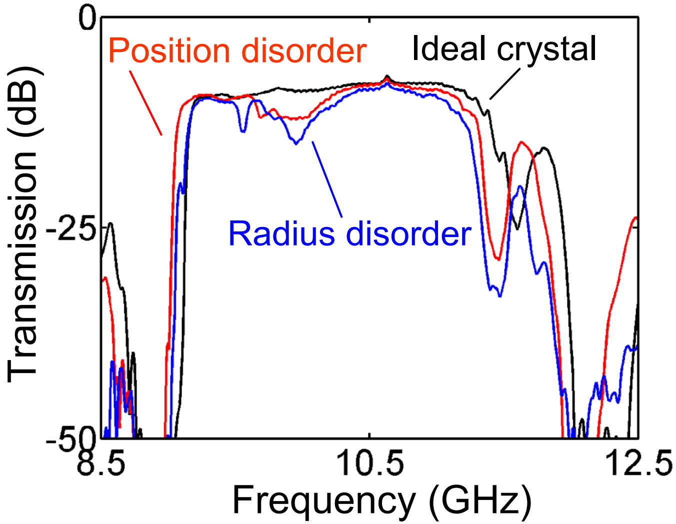

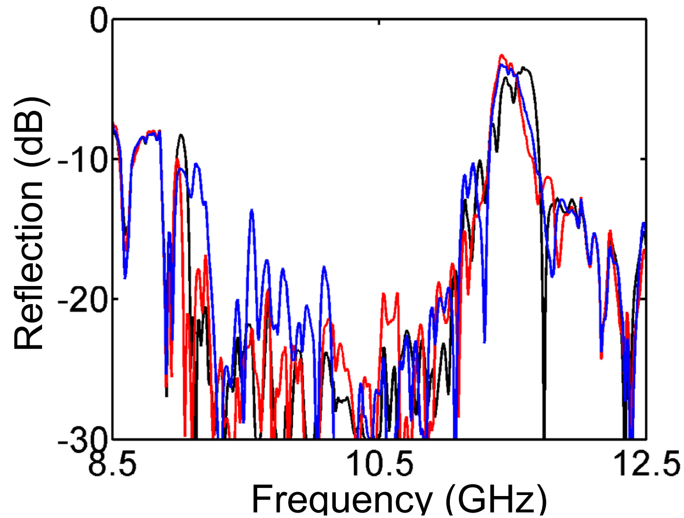

Measurements in upscaled microwave model

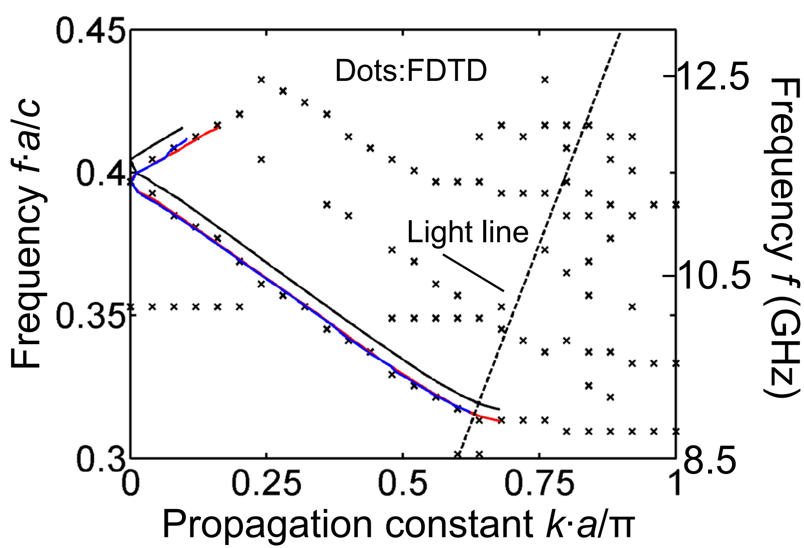

TE (E_x) Field of W1 Defect Waveguide with 10 % Radius Disorder

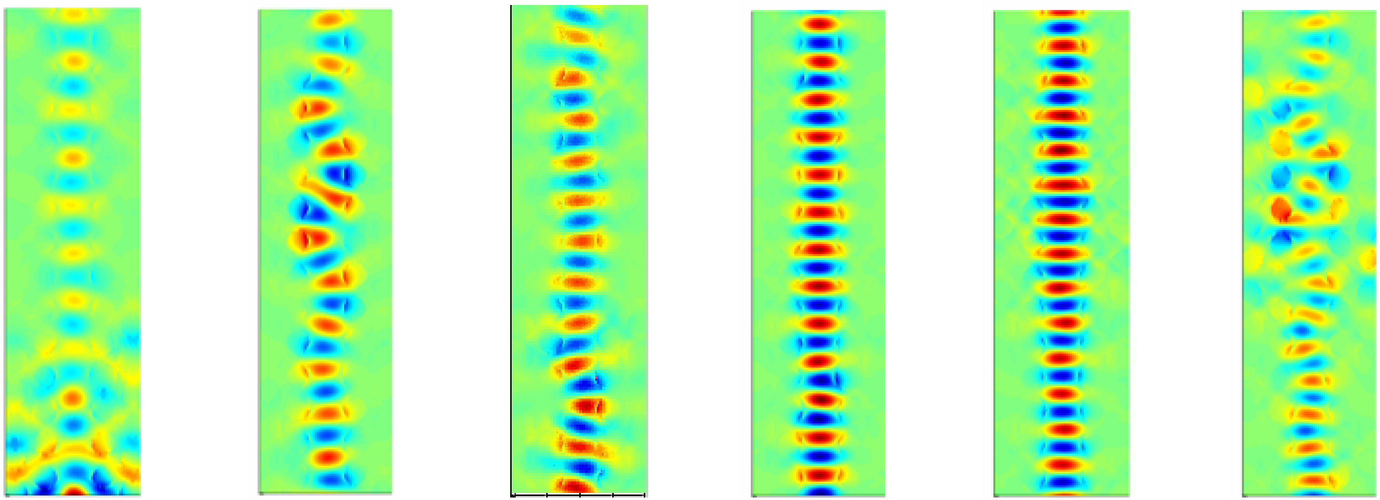

9.05 GHz 9.55 GHz 10.05 GHz 10.55 GHz 11.05 GHz 11.55 GHz

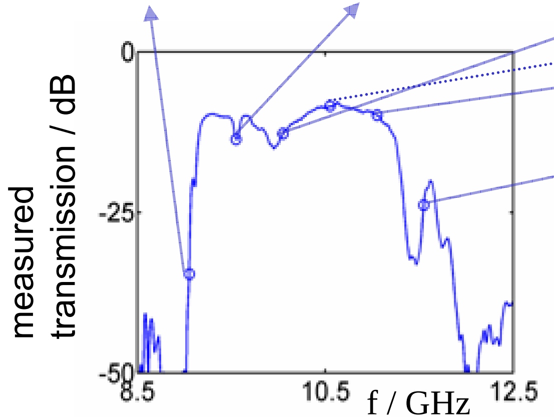

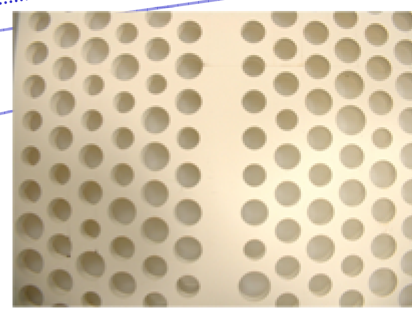

10% radius disorder

Parallel DD4 FDTD:

48 CPU, 3 000 min
$\Delta x,y,z$ = 2 nm (uniform)
→ 23.7 Mio mesh cells!

Duration: 92 pulse widths

Brosi, J.-M.; Leuthold, J.; Freude, W.: Microwave-frequency experiments validate optical simulation tools and demonstrate novel dispersion-tailored photonic crystal waveguides. IEEE J. Lightw. Technol. (2007) (submitted)

Brosi, J.-M.; Freude, W.; Leuthold, J.; Petrov, A. Yu.; Eich, M.: 'Broadband slow light in a photonic crystal line defect waveguide', Technical Digest OSA Topical Meeting on Slow and Fast Light (SL'06), Washington (DC), USA, 23–26 July 2006, Paper MD6

Slow-Light PC Waveguide: Band diagram

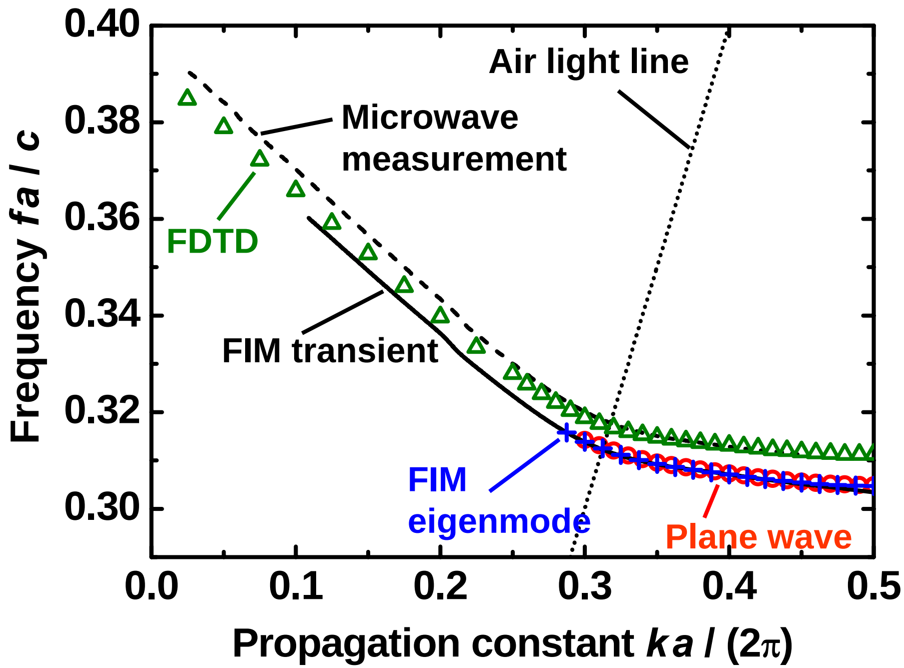

Model for Silicon membrane

a = 0.45 µm, n = 3.16
r / a = 0.25, h / a = 0.6

FDTD: RSoft Fullwave, unit cell with phase cond., ~90 min/point

FIM Eigenmode: CST Microwave Studio, unit cell with phase cond., ~1,5 min/point

FIM Transient: CST Microwave Studio, full structure with pulse exc., ~5 hrs

Plane Wave: MIT MPB, periodically repeated in all directions, ~18 min/point

Microwave Measurement: Upscaled microwave model

Slow-Light PC Waveguide: Group Velocity

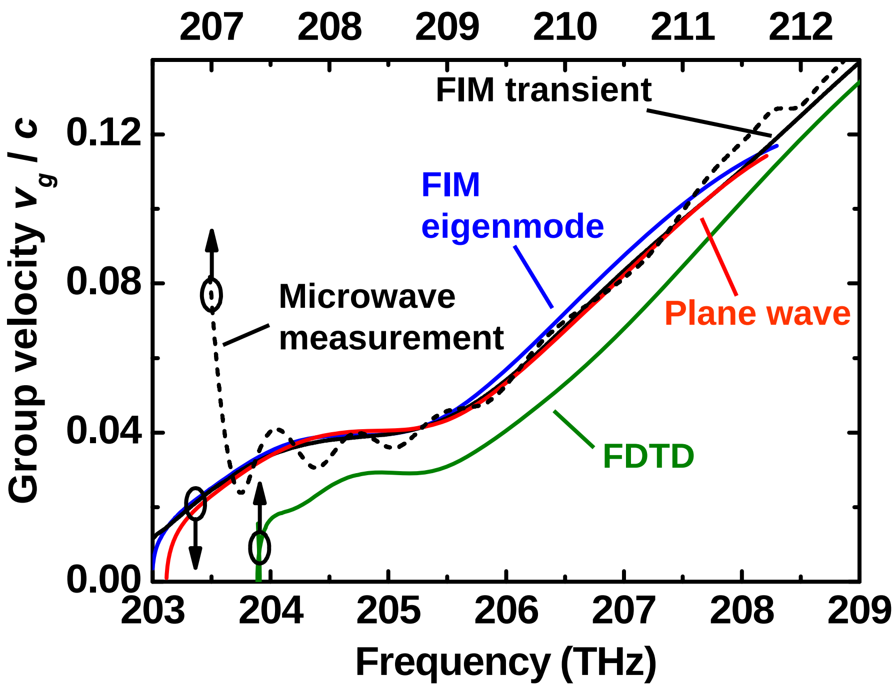

Curves derived from band diagram data

FIM eigenmode, FIM transient and plane wave method agree very well

Results verified with microwave experiments (Frequency offset because of material tolerances)

Outline

- Wavelets
  - What are they good for?
- Finite-differences in time-domain
  - Yee's leapfrog algorithm
  - Numerical dispersion, stability and accuracy
  - Higher-order finite-differences
  - Method of weighted residuals: Collocation
- Wavelet FDTD
  - Numerical dispersion, stability and accuracy
  - Summary, and what should be further done
  - Dispersive and nonlinear media
- **Application examples in nano-photonics**
  - Waveguide roughness
  - Slow light in a photonic crystal with disorder
  - Four-wave mixing in a microring resonator
  - Switching of a Bragg grating
- Summary and further reading

Linear and Nonlinear InP/InGaAsP Micro-Resonator

Resonator structure (2D and 3D)

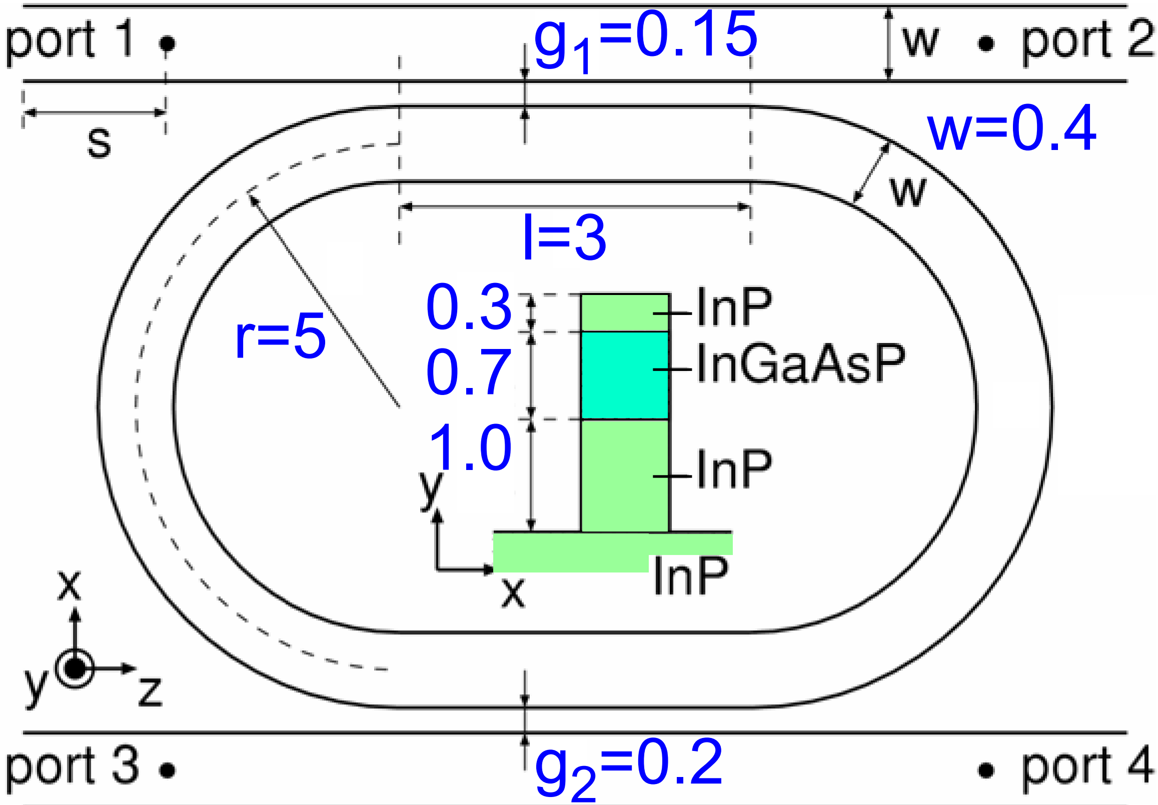

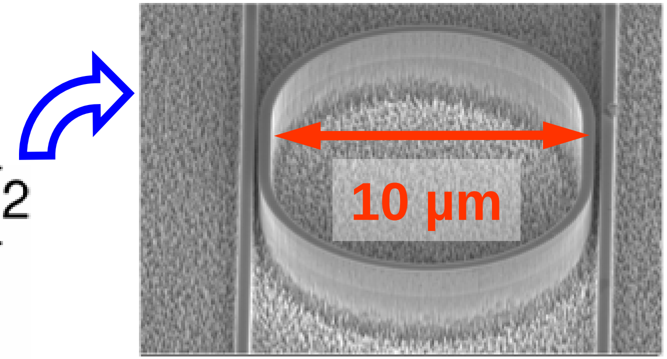

- substrate: InP
- InGaAsP: n = 3.42

  $\chi^{(3)} = 3.8 \times 10^{18}\ \mathrm{m^2/V^2}$
- InP: n = 3.17

  at 1.55 µm
- for 2D analysis:

  n = 3.34 (slab WG)

(all units: µm)

Koos, C.; Fujii, M.; Poulton, C. G.; Steingrueber, R.; Leuthold, J.; Freude, W.: FDTD-modelling of dispersive nonlinear ring resonators: Accuracy studies and experiments. IEEE J. Quantum Electron. 42 (2006) 1215–1223

InP/InGaAsP Micro-Resonator and FWM

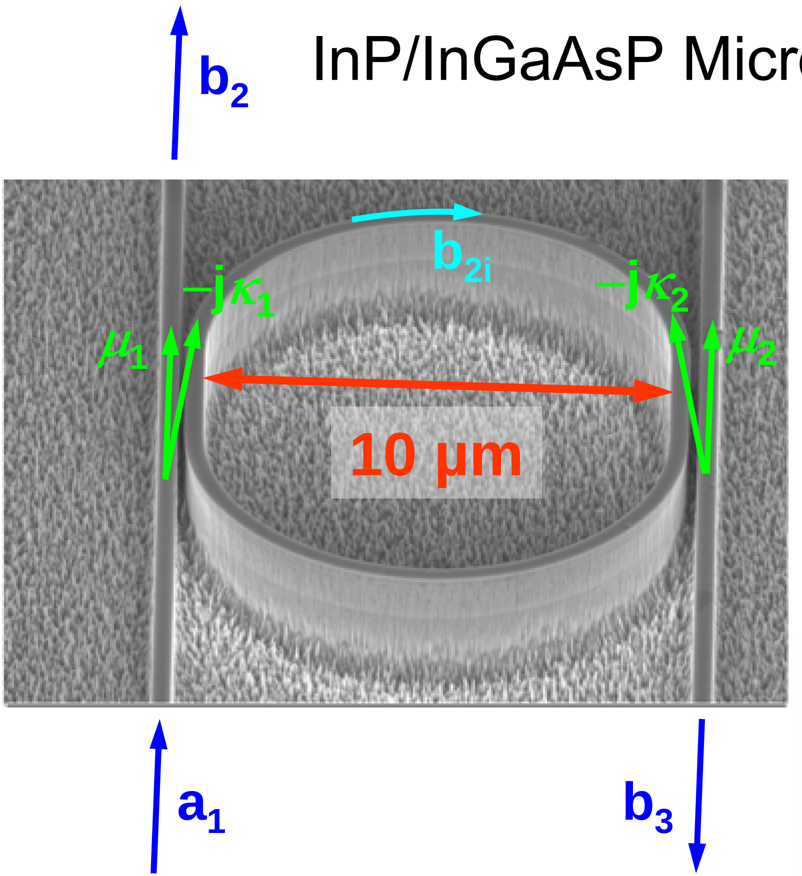

Conversion efficiency improved by resonant field enhancement:

$$\eta_{\mathrm{FWM}} = FE_p^4 \, FE_s^2 \, FE_c^2 \, \gamma_{\mathrm{re}}^2 \left| L_{\mathrm{rt,\,eff}} \right|^2 P_p^2$$

$$FE = \frac{b_{2i}}{a_1} = \frac{\kappa_1}{1 - \rho \mu_1 \mu_2}$$

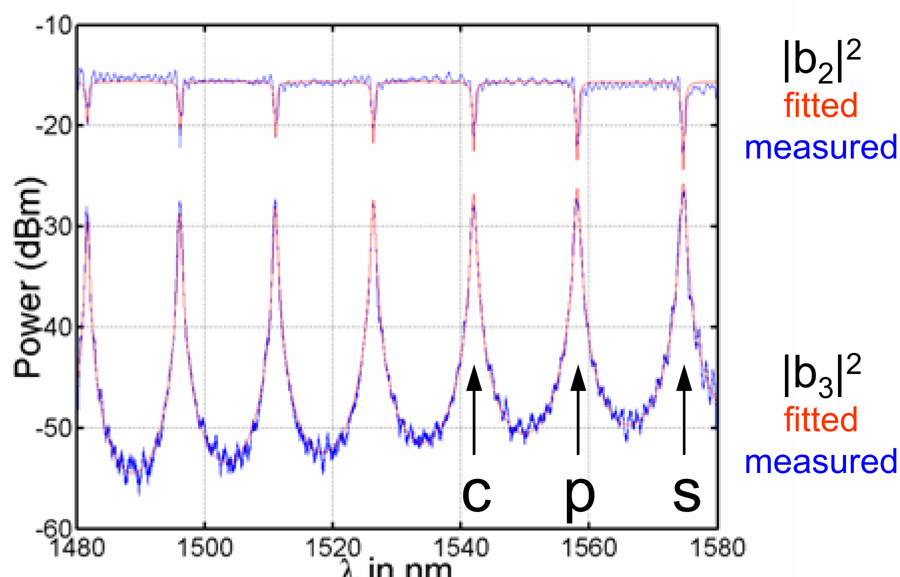

Evaluation of the coupling parameters from transmission fit:

$\kappa_1 = 0.24$ $\rho = 0.92$

$\kappa_2 = 0.13$ $\mathrm{FE} = 2.16$

FWM in Ring Resonators

FWM conversion efficiency is strongly improved by resonant field enhancement:

$$\eta_{\mathrm{FWM}} = FE_p^4 \, FE_s^2 \, FE_c^2 \, \gamma_{\mathrm{re}}^2 \left| L_{\mathrm{rt,\,eff}} \right|^2 P_p^2$$

$$FE = \frac{b_{2i}}{a_1} = \frac{\kappa_1}{1 - \rho\mu_1\mu_2}$$ Field enhancement factor

$$\gamma_{re} \sim \mathrm{Re}\left\{ \iint \left(\chi^{(3)} \vdots \vec{E}\vec{E}\vec{E} \right) \cdot \vec{E}^* \, \mathrm{d}\,x \, \mathrm{d}\,y \right\}$$ Nonlinear Parameter of the ring waveguide

$$L_{\mathrm{rt,\,eff}} \approx L_{\mathrm{rt,geom}} \times \rho^2$$ Effective round-trip length for nonlinear interaction

$$L_{\mathrm{rt,geom}}$$ Geometrical round-trip length of the ring resonator

FWM Experiment

Shift of resonance comb due to heating by pump power

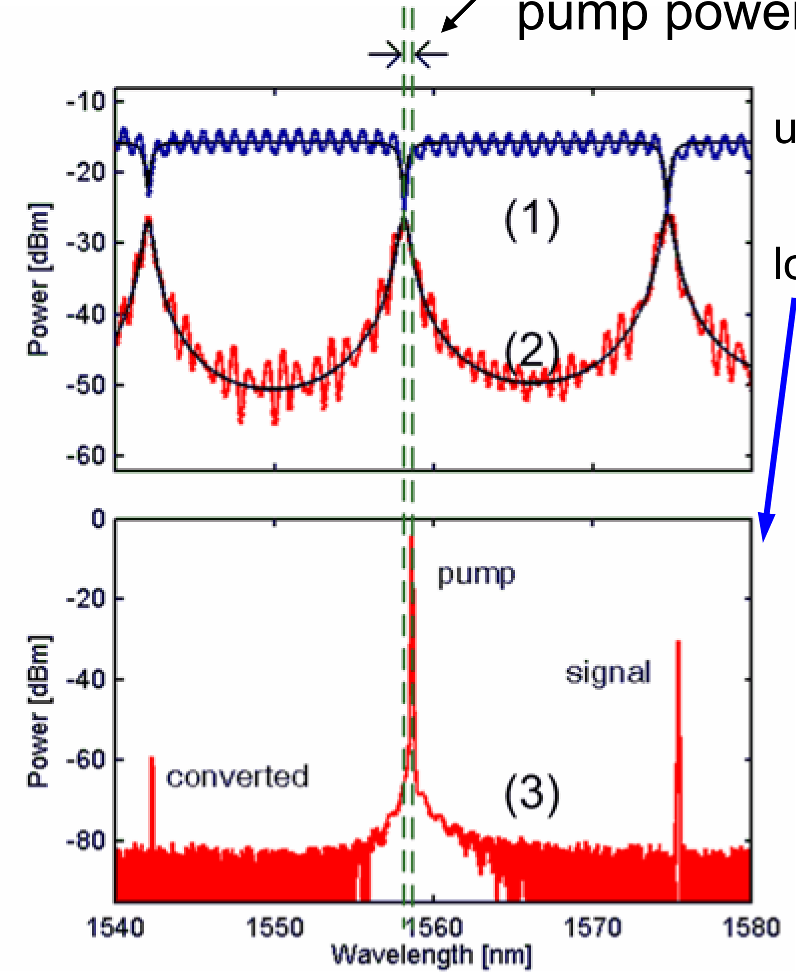

upper part: Linear transmission characteristics

lower part: Output spectrum for nonlinear experiment

FWM conversion efficiency:
η = –32.5 dB for P_P= 13.6 dBm
(measured, pump power on chip**)**

To our knowledge the highest FWM-conversion efficiency measured in passive microrings

Absil et. al., Optics Letters 25, No. 8, April 2000:
“Wavelength conversion in GaAs microring resonators“
measured efficiency: –44.6 dB
predicted efficieny: –8.5 dB

Effective Dielectric Constant Technique Reduces Staircasing

N.Kaneda, et.al, IEEE MTT, vol.45, No.9, Sep. 1997
S.Yu, R.Mittra, IEEE MWCL, vol.11, No.1, Jan. 2001

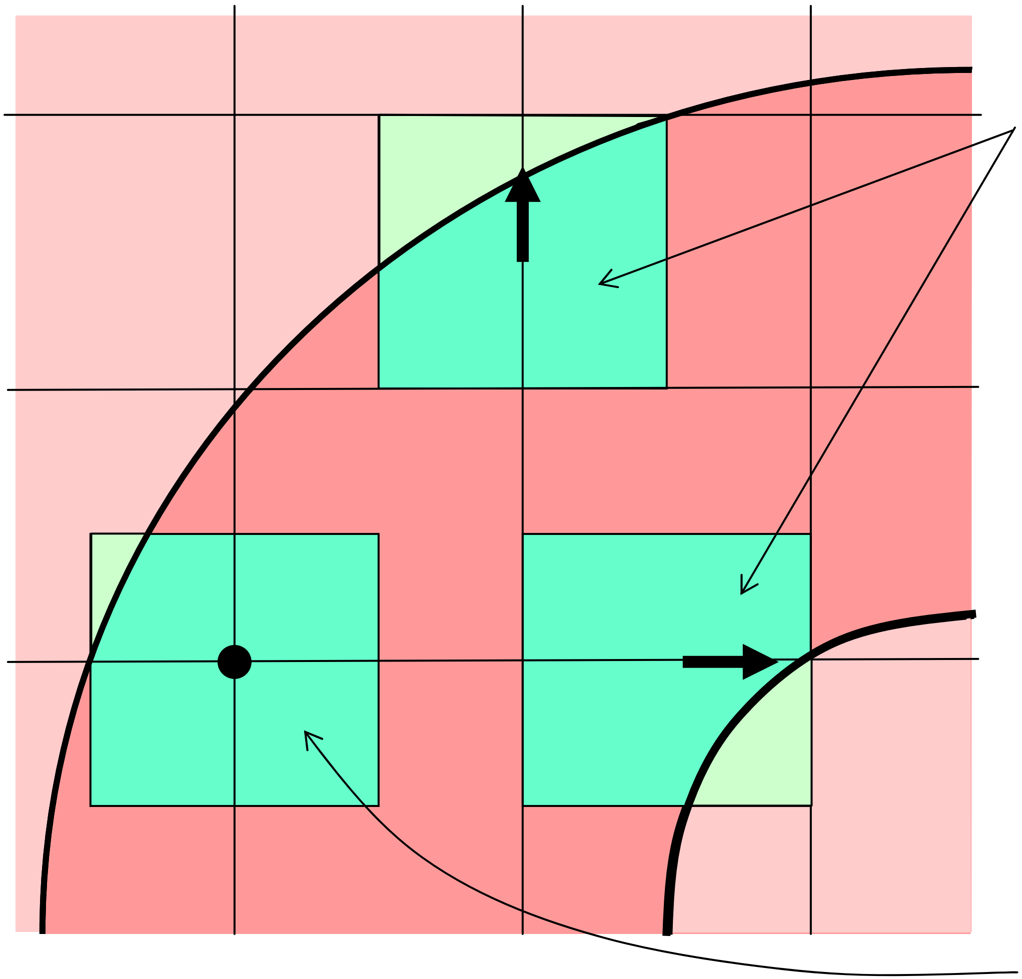

For E fields having components normal to the interface:

ε_{eff}: FD method of Laplace equation

For E fields tangential to the interface:

Tangential BC (E is continuous)

ε_{eff}: geometric average

Measured and Calculated Resonance Frequencies, Linear FDTD

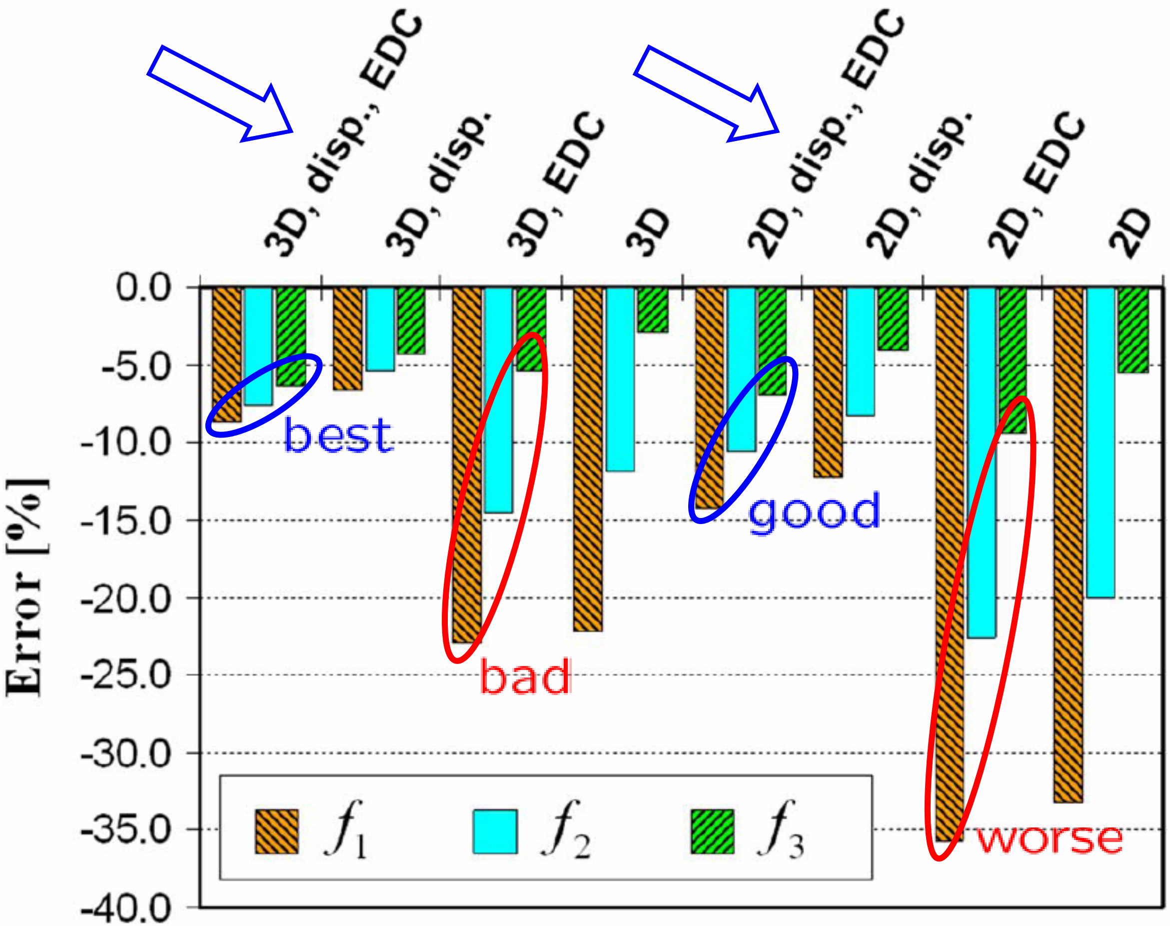

Comparison of measured and calculated resonance frequencies for the different FDTD implementations. The bars indicate the deviation of the resonance frequencies f_1, f_2, and f_3 in percent of the averaged measured FSR $\Delta f^{(\text{meas})} = 2.016$ THz.

Standard FDTD:

- 3D, $2D_{\text{eff. index}}$
- mat. dispersion
- EDC effective ε

Parameters

- $S = 0.8$
- $\Delta t = 0.0465$ fs
  $\Delta x = \Delta z = 25$ nm
  ($\Delta y = 100$ nm)
- parallel cluster
  HP XC6000
  3D/2D
  64/32 CPU
  4 GB /0.5 GB,
  28 h /2.5 h

Koos, C.; Fujii, M.; Poulton, C. G.; Steingrueber, R.; Leuthold, J.; Freude, W.: FDTD-modelling… JQE 42 (2006) 1215–1223

Measured and Calculated FWM Efficiency, Nonlinear Std FDTD

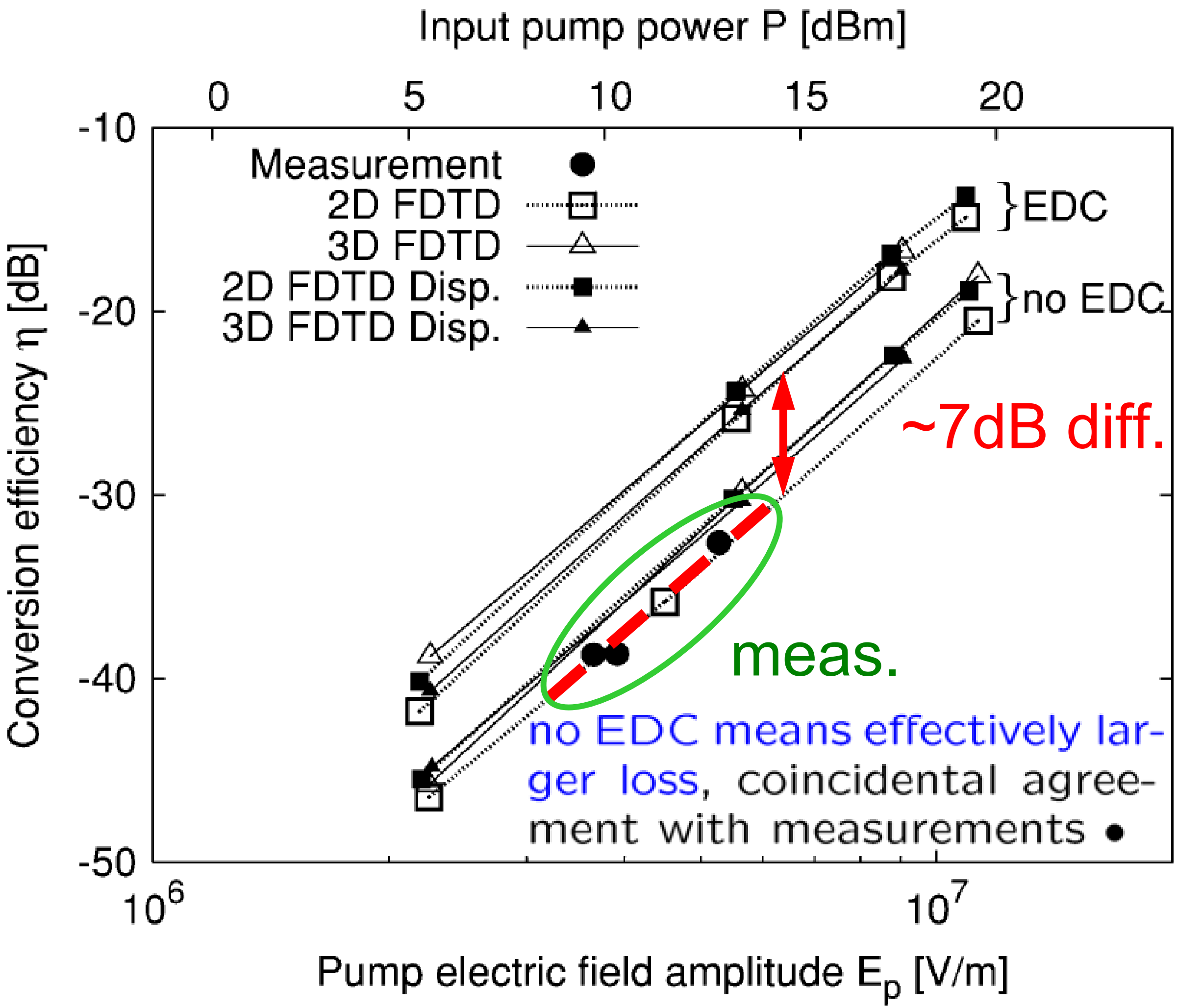

Nonlinear std FDTD

- 3D, 2D$_{\text{eff. index}}$
- mat. dispersion
- EDC effective ε

Parameters

- $S = 0.8$
- $\Delta t = 0.0465\,\text{fs}$
  $\Delta x = \Delta z = 25\,\text{nm}$
  $(\Delta y = 100\,\text{nm})$
- parallel cluster
  HP XC6000
  3D/2D
  64/32 CPU
  4 GB/0.5 GB,
  28 h/2.5 h

Koos, C.; Fujii, M.; Poulton, C. G.; Steingrueber, R.; Leuthold, J.; Freude, W.: FDTD-modelling of dispersive nonlinear ring resonators: Accuracy studies and experiments. IEEE J. Quantum Electron. 42 (2006) 1215–1223

Measured and Calculated FWM Efficiency, Nonlinear Std FDTD

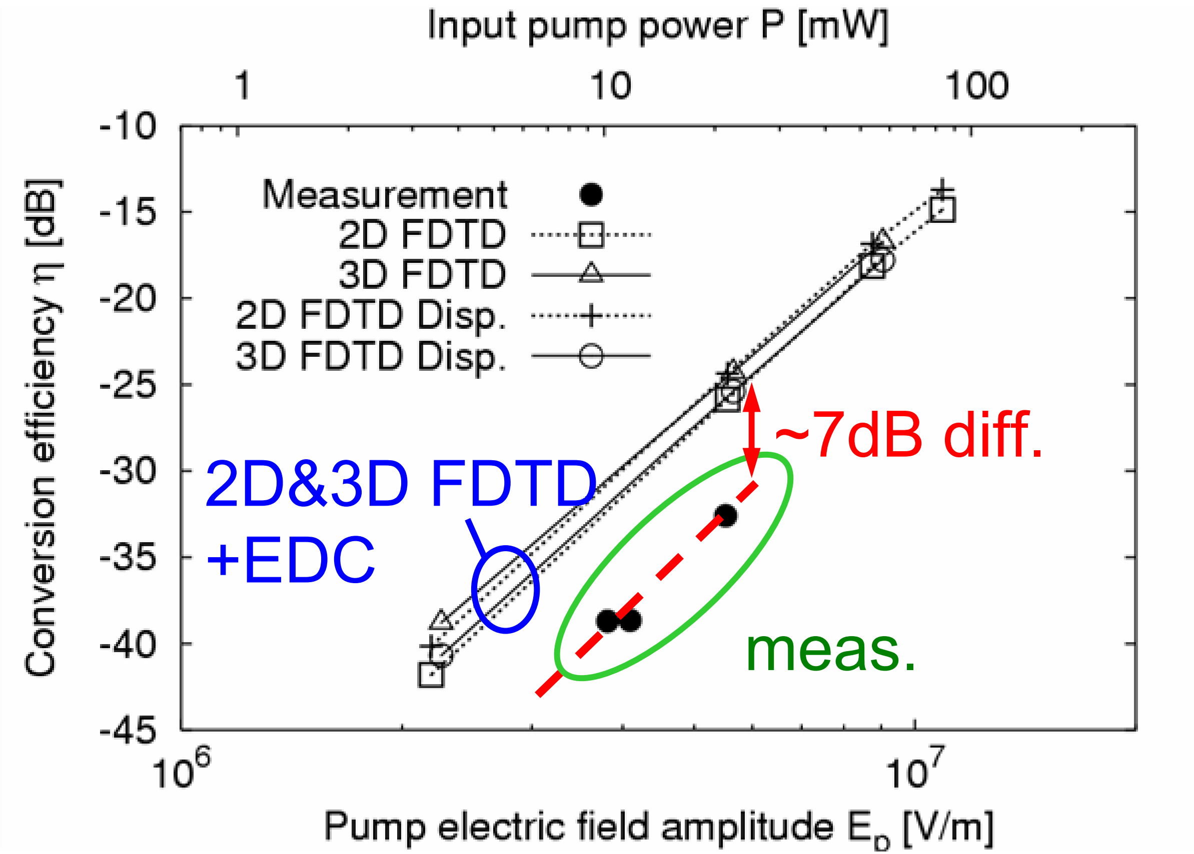

Nonlinear std FDTD

- 3D, $2D_{\text{eff. index}}$
- mat. dispersion
- EDC effective ε

Parameters

- $S = 0.8$
- $\Delta t = 0.0465\,\text{fs}$
  $\Delta x = \Delta z = 25\,\text{nm}$
  $(\Delta y = 100\,\text{nm})$
- parallel cluster
  HP XC6000
  3D/2D
  64/32 CPU
  4 GB/0.5 GB,
  28 h/2.5 h

Koos, C.; Fujii, M.; Poulton, C. G.; Steingrueber, R.; Leuthold, J.; Freude, W.: FDTD-modelling of dispersive nonlinear ring resonators: Accuracy studies and experiments. IEEE J. Quantum Electron. 42 (2006) 1215–1223

Outline

- Wavelets
  - What are they good for?
- Finite-differences in time-domain
  - Yee's leapfrog algorithm
  - Numerical dispersion, stability and accuracy
  - Higher-order finite-differences
  - Method of weighted residuals: Collocation
- Wavelet FDTD
  - Numerical dispersion, stability and accuracy
  - Summary, and what should be further done
  - Dispersive and nonlinear media
- **Application examples in nano-photonics**
  - Waveguide roughness
  - Slow light in a photonic crystal with disorder
  - Four-wave mixing in a microring resonator
  - Switching of a Bragg grating
- Summary and further reading

Simulation of Stopband-Tapered WBG Using NL 2D Std FDTD

$$w = w_0\left(-0.4856\left(\frac{z}{L}\right)^3 + -0.0009\left(\frac{z}{L}\right)^2 + 1\right)\sin(2\pi z / \Lambda)$$

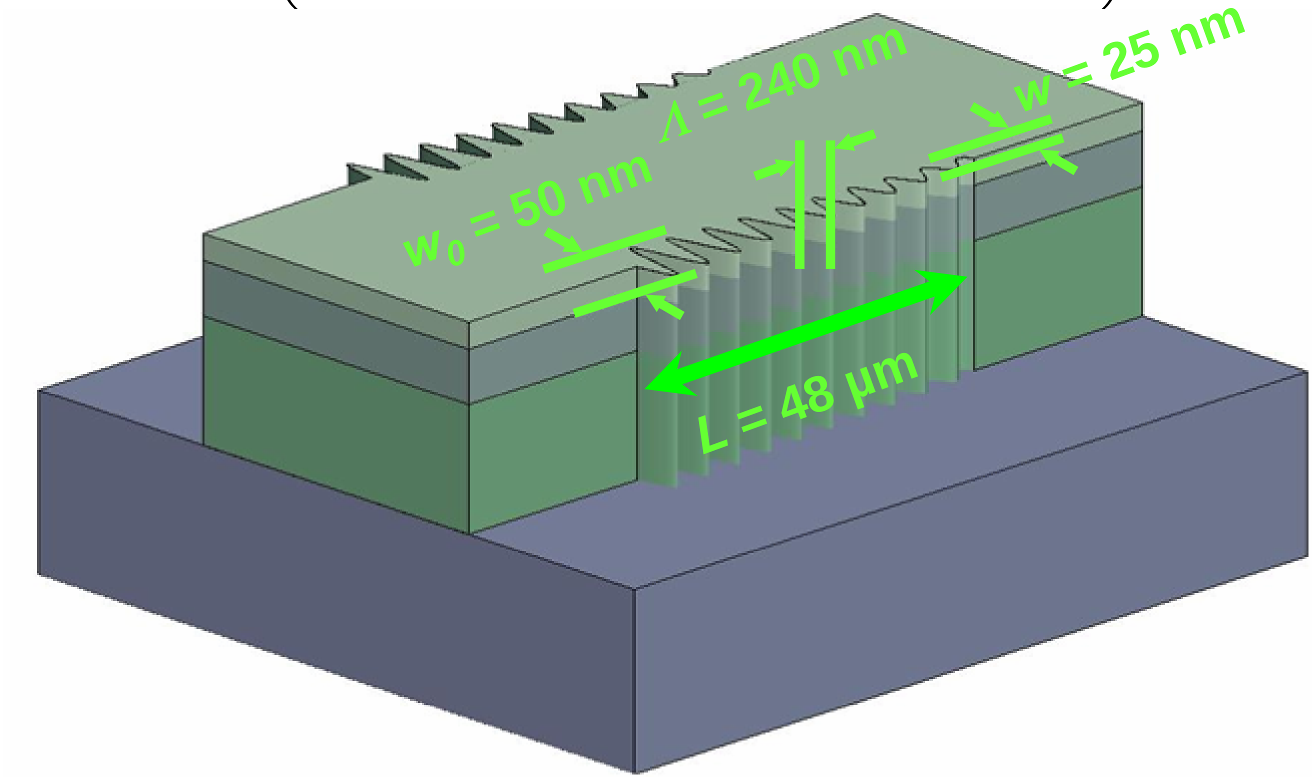

The sidewall modulation amplitude *w* is varied from 50 nm to 25 nm for the total grating with length *L* = 48 µm and period Λ = 0.24 µm (200 periods).

Fujii, M.; Maitra, A.; Poulton, C.; Leuthold, J.; Freude, W.: Non-reciprocal transmission and Schmitt trigger operation in strongly modulated asymmetric WBGs. Opt. Expr. 14 (2006) 12782–12793

Bistability of Stopband-Tapered WBG Using NL 2D Std FDTD

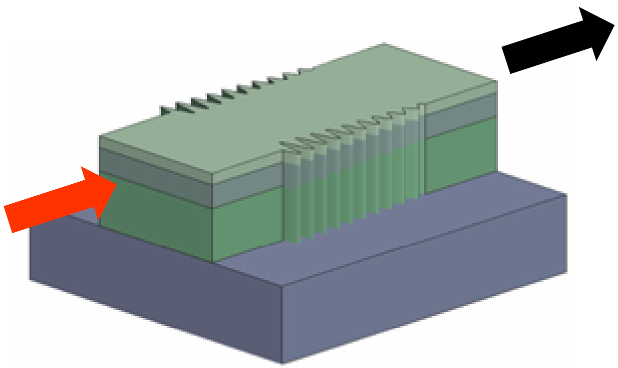

Bistable behaviour in tapered sidewall corrugated structure

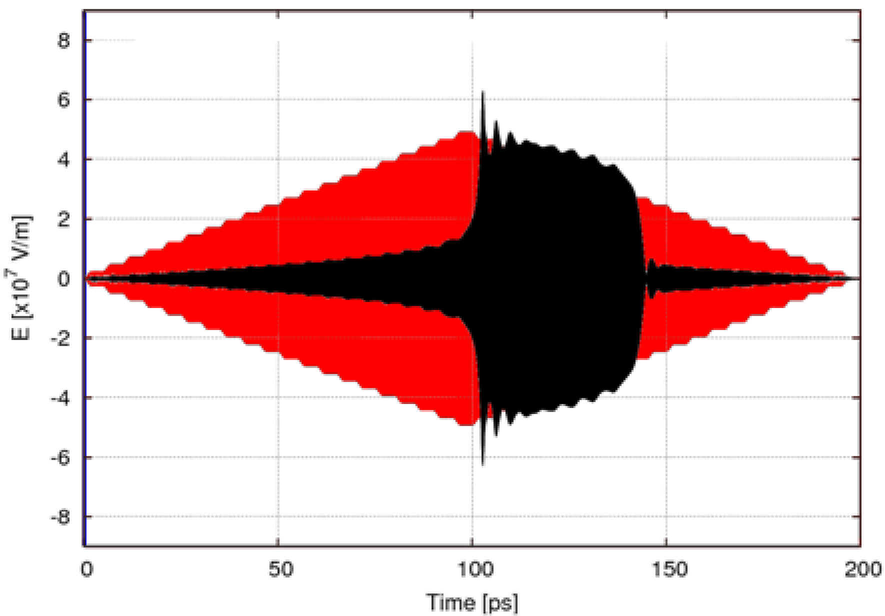

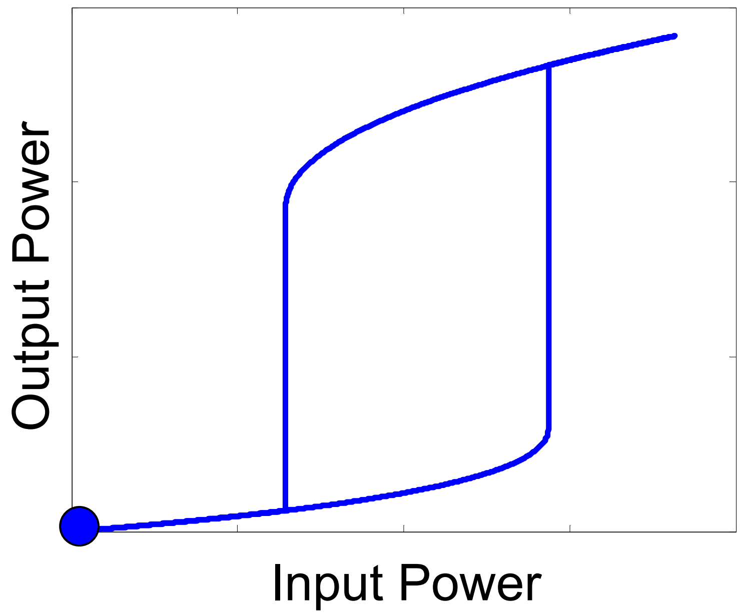

Fujii, M.; Maitra, A.; Poulton, C.; Leuthold, J.; Freude, W.: Non-reciprocal transmission and Schmitt trigger operation in strongly modulated asymmetric WBGs. Opt. Expr. 14 (2006) 12782–12793

Directionality of Stopband-Tapered WBG Using NL 2D Std FDTD

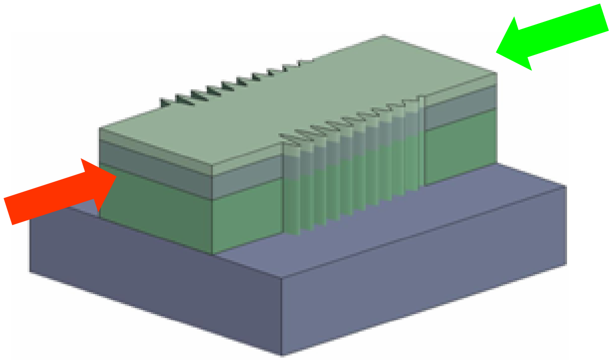

Isolator behaviour in tapered sidewall-corrugated structure

Different up-switching thresholds for LTR & RTL case

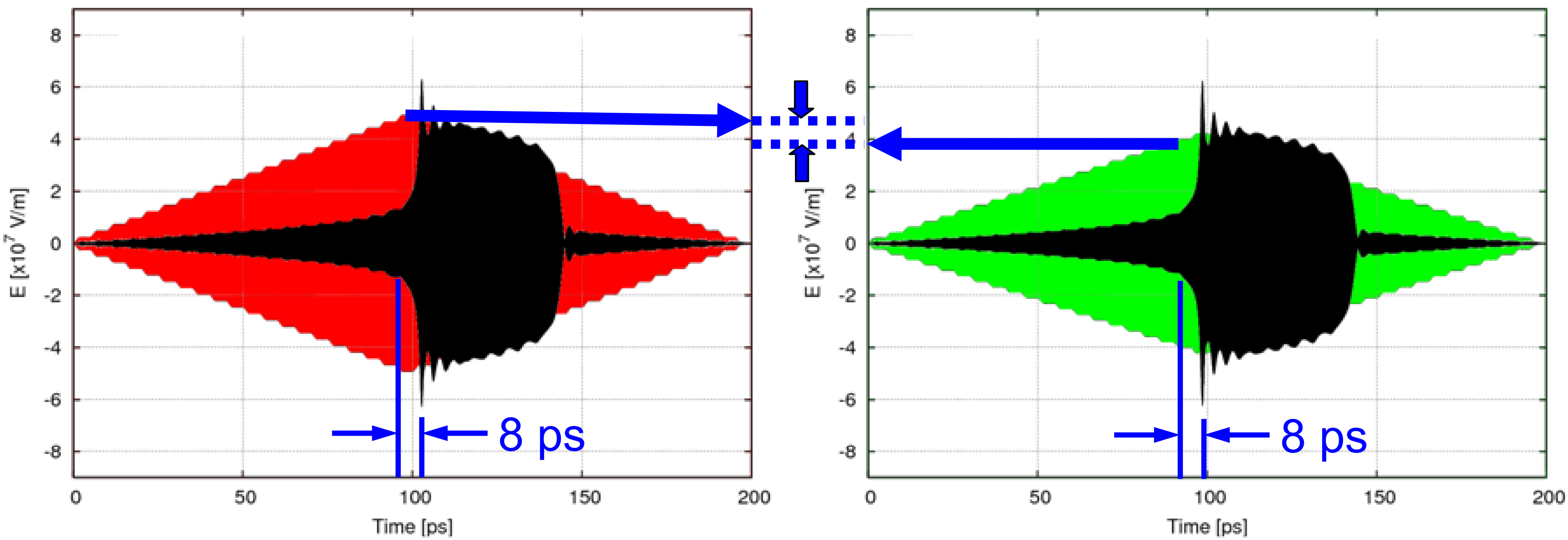

Fujii, M.; Maitra, A.; Poulton, C.; Leuthold, J.; Freude, W.: Non-reciprocal transmission and Schmitt trigger operation in strongly modulated asymmetric WBGs. Opt. Expr. 14 (2006) 12782–12793

Outline

- Wavelets
  - What are they good for?
- Finite-differences in time-domain
  - Yee's leapfrog algorithm
  - Numerical dispersion, stability and accuracy
  - Higher-order finite-differences
  - Method of weighted residuals: Collocation
- Wavelet FDTD
  - Numerical dispersion, stability and accuracy
  - Summary, and what should be further done
  - Dispersive and nonlinear media
- Application examples in nano-photonics
  - Waveguide roughness
  - Slow light in a photonic crystal with disorder
  - Four-wave mixing in a microring resonator
  - Switching of a Bragg grating
- Summary and further reading

Summary

Results:

- Low dispersion for ϕ^{Dp}/ϕ^{DDp} (reduced memory and run time) — *might* be like HFD6
- Equivalence between ϕ and ψ via wavelet transform $\rightsquigarrow$ all dispersion findings also valid for possible MRA

Examples (+ NL DD4 Raman/Kerr):

- Waveguide roughness (DD4 scal fct FDTD)
- Slow light ($0.04\,c$) in PhC with disorder (DD4)
- FWM in a microring (NL FDTD)
- NL Bragg grating (NL FDTD)

What should be done?

- Chose higher-order time difference operator (relatively simple)
- Try MRA with Daubechies ϕ^{Dp} *and* ψ^{Dp}

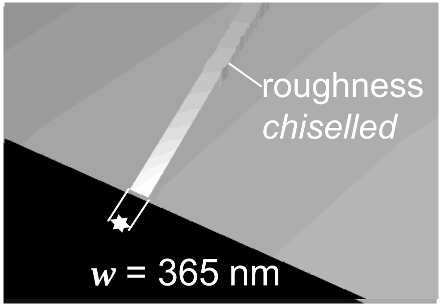

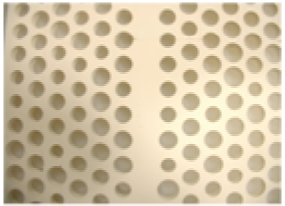

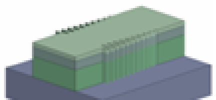

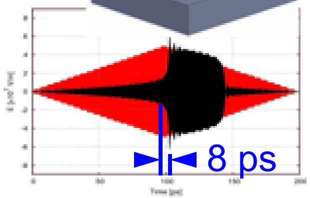

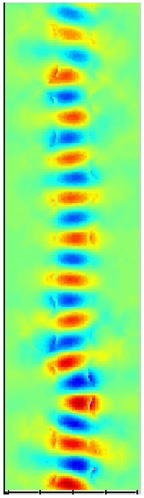

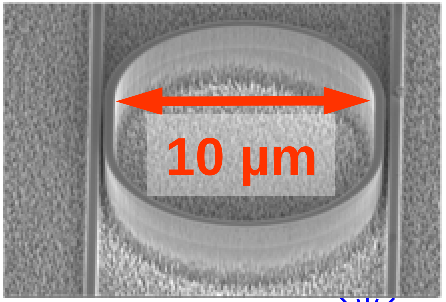

Outline

- Wavelets
  - What are they good for?
- Finite-differences in time-domain
  - Yee's leapfrog algorithm
  - Numerical dispersion, stability and accuracy
  - Higher-order finite-differences
  - Method of weighted residuals: Collocation
- Wavelet FDTD
  - Numerical dispersion, stability and accuracy
  - Summary, and what should be further done
  - Dispersive and nonlinear media
- Application examples in nano-photonics
  - Waveguide roughness
  - Slow light in a photonic crystal with disorder
  - Four-wave mixing in a microring resonator
  - Switching of a Bragg grating
- Summary and further reading (57 citations)

Further Reading (1/10)

Guided-wave modeling

[1] Huang, W. P. (Ed.): Methods for simulation of guided-wave optoelectronic devices: Part II: Waves and interactions. In: PIER 11 — Progress in Elctromagnetic Research, Chief Editor: J. A. Kong. Cambridge (MA): EMW Publishing 1995

[2] Scarmozzino, R.; Gopinath, A.; Pregla, R.; Helfert, S.: Numerical techniques for modeling guided-wave photonic devices. IEEE J. Sel. Topics Quantum Electron. 6 (2000) 150–162

General FDTD methods

[3] Yee, K. S.: Numerical solution of initial boundary value problems involving Maxwells equations in isotropic media. IEEE Trans. Antennas Propag. AP-14 (1966) 302–307

[4] Taflove, A.; Hagness, S. C.: Computational electrodynamics: The finite-difference time-domain method, 2. and 3. Ed. Boston: Artech House 2000 and 2005

Large-scale FDTD modeling

[5] Yu, W.; Liu, Y.; Su, T.; Hunag, N.-T.; Mittra, R.: A robust parallel conformal finite-differente time-domain processing package using the MPI library. IEEE Antennas Propag. Mag. 47 (2005) 39–59

[6] Poulton, C. G.; Koos, C.; Fujii, M.; Pfrang, A.; Schimmel, Th.; Leuthold, J.; Freude, W.: Radiation modes and roughness loss in high index-contrast waveguides. IEEE J. Sel. Topics Quantum Electron. 12 (2006) 1306–1321

Further Reading (2/10)

FDTD Sources: Charging — Sinusoidal — Pulsed modal hard

[7] Taflove, A.; Hagness, S. C.: Computational electrodynamics: The finite-difference time-domain method, 2. Ed. Boston: Artech House 2000. Sect. 5.4 p. 182 ff.; Sect. 5.10 p. 227 ff. (3. Ed. Boston: Artech House 2005)

FDTD staircasing error mitigation

[8] Fujii, M.; Lukashevich, D.; Sakagami, I.; Russer, P.: Convergence of FDTD and wavelet-collocation modeling of curved dielectric interface with the effective dielectric constant technique. IEEE Microw. Compon. Lett. 13 (2003) 469–471

Replacing explicit Yee leapfrogging by *a*lternating *d*irection *i*mplicit scheme

[9] Rao, H.; Scarmozzino, R.; Osgood, Jr., R. M.: An improved ADI-FDTD method and its application to photonic simulations IEEE Photon. Technol. Lett. 14 (2002) 477–479

Further Reading (3/10)

Stability according to the Courant-Friedrichs-Lewy condition

[10] Lakshmikantham, V.; Trigiante, D.: Theory of difference equations: Numerical methods and applications. Boston: Academic Press 1988

[11] Krumpholz, M.; Katehi, L. P. B.: MRTD: new time-domain schemes based on multiresolution analysis. IEEE Trans. Microwave Theory Tech. 44 (1996) 555–571

[12] Tentzeris, E. M.; Robertson, R. L.; Harvey, J. F.; Katehi, L. P. B.: Stability and dispersion analysis of Battle-Lemarié-based MRTD schemes. IEEE Trans. Microwave Theory Tech. 47 (1999) 1004–1013

[13] Taflove, A.; Hagness, S. C.: Computational electrodynamics: The finite-difference time-domain method, 2. Ed. Boston: Artech House 2000. Stability of fourth-order accurate differences: Sect. 4.9.2 pp. 143–147

[14] Fujii, M.; Hoefer, W. J. R.: Interpolating wavelet collocation method of time dependent Maxwell's equations: characterization of electrically large optical waveguide discontinuities. J. Comp. Phys. 186 (2003) 666–689

Further Reading (4/10)

General wavelet theory

[15] Gabor, D.: Theory of communication. J. Inst. Elec. Eng. 93 (1946) 429–457 (*cited after Ref. [187] in [7]*)

[16] Deslauriers, G.; Dubuc, S.: Symmetric iterative interpolation processes. Constr. Approx. 5 (1989) 49–68

[17] Goedecker, S.: Wavelets and their application for the solution of partial differential equations in physics. Lausanne: Presses Polytechniques et Universitaires Romandes 1998

[18] Sarkar, T. K.; Su, C.: A tutorial on wavelets from an electrical engineering perspective, Part 1: Discrete wavelet techniques. IEEE Antennas Prop. Mag. 40 (1998) No. 5 49–70

[19] Sarkar, T. K.; Su, C.; Adve, R.; Salazar-Palma, M.; Garcia-Castilloz, L.; Boix, R. R.: A tutorial on wavelets from an electrical engineering perspective, Part 2: The continuous case. IEEE Antennas Prop. Mag. 40 (1998) No. 6 36–49

[20] Louis, A. K.; Maaß, P.; Rieder, A.: Wavelets. Theorie und Anwendungen, 2. Ed. Stuttgart: Teubner 1998 (in German)

[21] Mallat, S.: A wavelet tour of signal processing, 2. Ed. San Diego: Academic Press 1999

[22] Misiti, M.; Misiti, Y.; Oppenheim, G.; Poggi, J.-M.: Wavelet toolbox user's guide, v. 3.1 (MATLAB release 2006b). Natick (MA): The Mathworks Inc. 2006
`http://www.mathworks.com/access/helpdesk/help/pdf_doc/wavelet/wavelet_ug.pdf`

Further Reading (5/10)

Wavelets for solving partial differential equations

[23] Lakshmikantham, V.; Trigiante, D.: Theory of difference equations: Numerical methods and applications. Boston: Academic Press 1988

[24] Bacry, E.; Mallat, S.; Papanicolaou, G.: A wavelet based spacetime adaptive numerical method for partial differential equations. Math. Model. Numer. Anal. 26 (1992)

[25] Beylkin, G.: On wavelet-based algorithms for solving differential equations. In 'Wavelets: Mathematics and Applications', edited by J. J. Benedetto and M. W. Frazier. Boca Raton: CRC Press 1994. Pages 449–466

[26] Harten, A.: Adaptive multiresolution schemes for shock computations. J. Comput. Phys. 115 (1994) 319–338

[27] Goedecker, S.: Wavelets and their application for the solution of partial differential equations in physics. Lausanne: Presses Polytechniques et Universitaires Romandes 1998

Further Reading (6/10)

Wavelet FDTD leads to low dispersion and coarser grids

[28] Fujii, M.; Hoefer, W. J. R.: Application of wavelet-galerkin method to electrically large optical waveguide problems. IEEE MTT-S Int. Microwave Symposium Digest, vol. TU3E-3 (2000) 239–242

[29] Fujii, M.; Hoefer, W. J. R.: Dispersion of time domain wavelet Galerkin method based on Daubechies compactly supported scaling functions with three and four vanishing moments. IEEE Microwave Guided Wave Lett., 10 (2000) 125–127

[30] Fujii, M.; Hoefer, W. J. R.: Time-domain wavelet Galerkin modeling of two-dimensional electrically large dielectric waveguides. IEEE Trans. Microwave Theory Tech. 49 (2001) 886–892

Wavelet FDTD staircasing error mitigation

[31] Fujii, M.; Lukashevich, D.; Sakagami, I.; Russer, P.: Convergence of FDTD and wavelet-collocation modeling of curved dielectric interface with the effective dielectric constant technique. IEEE Microw. Compon. Lett. 13 (2003) 469–471

Multiscale analysis

[32] Marrone, M.; Mittra, R.: A theoretical study of the stability criteria for hybridized FDTD algorithms for multiscale analysis. IEEE Trans. Antennas Propagat. 52 (2004) 2158–2166

Further Reading (7/10)

Linear wavelet FDTD

[33] Fujii, M.; Hoefer, W. J. R.: A Three-dimensional Haar-wavelet-based multiresolution analysis similar to the FDTD method — Derivation and application. IEEE Trans. Microw. Theory Tech. 46 (1998) 2463–2475

[34] Fujii, M.: A time-domain Haar-wavelet-based multiresolution technique for electromagnetic field analysis. PhD Thesis, University of Victoria 1999

[35] Aidam, A.: Wavelet-Galerkin-Methoden zur Berechnung elektromagnetischer Felder im Zeitbereich. PhD Thesis, University of Munich 1999 (in German, good overview, many references) http://deposit.d-nb.de/cgi-bin/dokserv?idn=959839666&dok_var=d1&dok_ext=pdf&filename=959839666.pdf

[36] Fujii, M.; Hoefer, W. J. R.: Field-singularity correction in 2-D time-domain Haar-wavelet modeling of waveguide components. IEEE Trans. Microw. Theory Tech. 49 (2001) 685–691

[37] Fujii, M.; Hoefer, W. J. R.: Time-domain wavelet Galerkin modeling of two-dimensional electrically large dielectric waveguides. IEEE Trans. Microw. Theory Tech. 49 (2001) 886–892

[38] Fujii, M.; Hoefer, W. J. R.: A wavelet formulation of the finite-difference method: Full-vector analysis of optical waveguide junctions. IEEE J. Quantum Electron. 37 (2001) 1015–1029

[39] Fujii, M.; Hoefer, W. J. R.: Interpolating wavelet collocation method of time dependent Maxwell's equations: characterization of electrically large optical waveguide discontinuities. J. Comp. Phys. 186 (2003) 666–689

[40] Fujii, M.; Freude, W.; Russer, P.: Efficient high-spatial-order FDTD analysis of 3D optical ring resonator filters. 19th Annual Review of Progress in Applied Computational Electromagnetics (ACES'03), Monterey (CA), USA, 24.–28.03.2003, pp. 739–744

Further Reading (8/10)

Nonlinear wavelet FDTD

[41] Kremp, T.; Freude, W.: Fast split-step wavelet collocation method for WDM system parameter optimization. IEEE J. Lightwave Technol. 23 (2005) 1491–1502 (no FDTD, but use of Deslaurier-Dubuc scaling function)

[42] Fujii, M.; Tahara, M; Sakagami, I.; Freude, W.; Russer, P.: High-order FDTD and auxiliary differential equation formulation of optical pulse propagation in 2D Kerr and Raman nonlinear dispersive media. IEEE J. Quantum Electron. 40 (2004) 175–182

[43] Fujii, M.; Omaki, N.; Tahara, M.; Sakagami, I.; Poulton, C.; Freude, W.; Russer, P.: Optimization of nonlinear dispersive APML ABC for the FDTD analysis of optical solitons. IEEE J. Quantum Electron. 41 (2005) 448–454

[44] Fujii, M,; Koos, C.; Poulton, C.; Sakagami, I.; Leuthold, J.; Freude, W.: A simple and rigorous verification technique for nonlinear FDTD algorithm by optical parametric four-wave mixing. Microwave and Optical Technol. Lett. 48 (2006) 88–91

[45] Fujii, M; Koos, C.; Poulton, C.; Leuthold, J.; Freude, W.: Nonlinear FDTD analysis and experimental validation of four-wave mixing in InGaAsP/InP racetrack micro-resonators. IEEE Photon. Technol. Lett. 18 (2006) 361–363

[46] Koos, C.; Fujii, M.; Poulton, C. G.; Steingrueber, R.; Leuthold, J.; Freude, W.: FDTD-modelling of dispersive nonlinear ring resonators: Accuracy studies and experiments. IEEE J. Quantum Electron. 42 (2006) 1215–1223

[47] Fujii, M.; Maitra, A.; Poulton, C.; Leuthold, J.; Freude, W.: Non-reciprocal transmission and Schmitt trigger operation in strongly modulated asymmetric WBGs. Opt. Expr. 14 (2006) 12782–12793

Further Reading (9/10)

Boundary conditions

[48] Berenger, J. P.: A perfectly matched layer for the absorption of electromagnetic waves. J. Comp. Phys. 114 (1994) 185–200

[49] Taflove, A.; Hagness, S. C.: Computational electrodynamics: The finite-difference time-domain method, 2. Ed. Boston: Artech House 2000. Chapter 7

[50] Fujii, M.; Russer, P.: A nonlinear and dispersive APML ABC for the FD-TD Methods. IEEE Microw. Wireless Compon. Lett. 12 (2002) 444–446

[51] Fujii, M.; Omaki, N.; Tahara, M.; Sakagami, I.; Poulton, C.; Freude, W.; Russer, P.: Optimization of nonlinear dispersive APML ABC for the FDTD analysis of optical solitons. IEEE J. Quantum Electron. 41 (2005) 448–454

Further Reading (10/10)

Periodic boundary conditions

[52] Kittel, C.: Introduction to solid state physics, 3rd ed. New York: John Wiley & Sons 1966 (Blochs theorem: Chapter 9 p. 259 ff.)

[53] Myers, H. P.: Introductory solid state physics. New Delhi: Viva Books Private Ltd. 1998 (Blochs theorem: Sect. 7.6 p. 190 ff.)

[54] Morse, P. M.; Feshbach, H.: Methods of theoretical physics, Band 1 und 2. New York: McGraw-Hill 1953 (Floquet theorem: Vol. 1 Sect. 5.2 p. 557)

[55] Ko, W. L.; Mittra, R.: Implementation of Floquet boundary condition in FDTD for FSS analysis. IEEE APS Int. Symp. Dig., June 28-July 2 (1993), vol. 1, pp. 14–17

[56] Harms, P.; Mittra, R.; Ko, W.: Implementation of the periodic boundary condition in the finite-difference time-domain algorithm for FSS structures. IEEE Trans. Antennas Prop. 42 (1994) 1317–1324

[57] Turner, G.; Christodoulou, C.: Broadband periodic boundary condition for FDTD analysis of phased array antennas. IEEE APS Int. Symp. Dig., June 21–26 (1998), vol. 2, pp. 1020–1023

End of Heraeus Presentation

Additional material: Periodic boundary conditions

Periodic Boundary Conditions (PBC)

PBC equivalently describe an infinite structure, comprising the elementary domain ("unit cell" size D_x, D_y, D_z), which is translated and thereby infinitely repeated in all directions with a so-called lattice vector $\vec{R} = n_x D_x \vec{e}_x + n_y D_y \vec{e}_y + n_z D_z \vec{e}_z$ (integers $n_{x,y,z}$).

Bloch's theorem (Floquet theorem in microwaves) states that in a periodic medium the eigenmodes have the property:

$$\vec{E}_{\vec{k}}(\vec{r}) = \vec{u}_{\vec{k}}(\vec{r})\,\mathrm{e}^{-\mathrm{j}\,\vec{k}\cdot\vec{r}}, \qquad \vec{H}_{\vec{k}}(\vec{r}) = \vec{v}_{\vec{k}}(\vec{r})\,\mathrm{e}^{-\mathrm{j}\,\vec{k}\cdot\vec{r}}$$

$$\vec{u}_{\vec{k}}(\vec{r} + \vec{R}) = \vec{u}_{\vec{k}}(\vec{r}), \qquad \vec{v}_{\vec{k}}(\vec{r} + \vec{R}) = \vec{v}_{\vec{k}}(\vec{r})$$

Consequence (assume $n_{x,y,z} = 1$ for primitive vector $\vec{R}$):

$$\Rightarrow \quad \vec{E}_{\vec{k}}(\vec{r} + \vec{R}) = \vec{E}_{\vec{k}}(\vec{r})\,\mathrm{e}^{-\mathrm{j}\,\vec{k}\cdot\vec{R}}, \qquad \Rightarrow \quad \vec{H}_{\vec{k}}(\vec{r} + \vec{R}) = \vec{H}_{\vec{k}}(\vec{r})\,\mathrm{e}^{-\mathrm{j}\,\vec{k}\cdot\vec{R}}$$

Only if $k_x D_x$, $k_y D_y$, $k_z D_z$ happen to equal 2π, then the phasors $\vec{E}_{\vec{k}}(\vec{r} + \vec{R})$, $\vec{H}_{\vec{k}}(\vec{r} + \vec{R})$ do *not* experience a phase shift.

Kittel, C.: Introduction to solid state physics, 3rd ed. New York: John Wiley & Sons 1966 (Bloch's theorem: Chapter 9 p. 259 ff.)
Myers, H. P.: Introductory solid state physics. New Delhi: Viva Books Private Ltd. 1998 (Bloch's theorem: Sect. 7.6 p. 190 ff.)
Morse, P. M.; Feshbach, H.: Methods of theoretical physics, Band 1 und 2. New York: McGraw-Hill 1953 (Floquet theorem: Vol. 1 Sect. 5.2 p. 557)

Periodic Boundary Conditions — Analytic Signal

Analytic signal $\underline{\Psi}(t,\vec{r}\,) = \Psi(t,\vec{r}\,) + \mathrm{j}\,\Psi_i(t,\vec{r}\,)$ with real part $\Psi(t,\vec{r}\,)$ and imaginary part $\Psi_i(t,\vec{r}\,)$. Has causal spectrum $\underline{\breve{\Psi}}(f<0)=0$.

Hilbert transform connects real and imaginary parts (spatial dependency dropped, principal value integral $\mathcal{P}\!\int$):

$$\Psi_i(t) = -\frac{1}{\pi}\mathcal{P}\!\int_{-\infty}^{+\infty}\frac{\Psi(t')}{t'-t}\,\mathrm{d}t', \qquad \Psi(t) = \frac{1}{\pi}\mathcal{P}\!\int_{-\infty}^{+\infty}\frac{\Psi_i(t')}{t'-t}\,\mathrm{d}t'$$

Plane wave, real A and $\vec{k} = k_x\,\vec{e}_x + k_y\,\vec{e}_y + k_z\,\vec{e}_z$, $|\vec{k}|^2 = (n\omega_0/c)^2$:

$$\underline{\Psi}(t,\vec{r}\,) = A\exp[\mathrm{j}(\omega_0 t - \vec{k}\cdot\vec{r}\,)] = \underbrace{A\cos(\omega_0 t - \vec{k}\cdot\vec{r}\,)}_{\Psi(t,\vec{r}\,)} + \mathrm{j}\,\underbrace{A\sin(\omega_0 t - \vec{k}\cdot\vec{r}\,)}_{\Psi_i(t,\vec{r}\,)}$$

$\underline{\Psi}(t,\vec{r}\,) = \underline{A}(t,\vec{r}\,)\exp[\mathrm{j}(\omega_0 t - \vec{k}\cdot\vec{r}\,)]$ represents actual real signal $\Psi(t,\vec{r}\,)$. Average frequency $f_0 = \omega_0/(2\pi)$.

"Slowly" varying complex amplitude $\underline{A}(t,\vec{r}\,) \to \breve{\Psi}(f,\vec{r}\,)$ concentrated at $f = \pm f_0$, no spectral overlap at $f=0$.

Periodic Boundary Conditions — Formulation

Analytic signal $\underline{\Psi}(t,\vec{r}) = A(t,\vec{r})\,\exp[\mathrm{j}(\omega_0 t - \vec{k}\cdot\vec{r})]$. Real part $\Psi(t,\vec{r}) = E_q(t,x,y,z), H_q(t,x,y,z)$ $(q = x,y,z)$ stands for any field component.

PBC and propagation in z-direction only for simplification:

$$\underline{\Psi}(t, z + D_z) = \underline{\Psi}(t,z)\,\exp(-\mathrm{j}\,k_z D_z)$$

Wrap-around update:

$$\underline{\Psi}(t,z) = \underline{\Psi}(t, z + D_z)\,\exp(\mathrm{j}\,k_z D_z)$$

Ingenious idea by Ko and Mittra (1993): Propagate real signal $\Psi(t,\vec{r})$ and imaginary signal $\Psi_i(t,z)$ with parallel FDTD runs. Excitation of unit cell by $A(t,z) = |A(t,z)|\,\exp[\mathrm{j}\,\varphi(t,z)]$ at $z = z_0$:

$$\Psi(t,z_0) = |A(t,z_0)|\cos[\omega_0 t - k_z z_0 + \varphi(t,z_0)]$$
$$\Psi_i(t,z_0) = |A(t,z_0)|\ \sin[\omega_0 t - k_z z_0 + \varphi(t,z_0)]$$

Ko, W. L.; Mittra, R.: Implementation of Floquet boundary condition in FDTD for FSS analysis. IEEE APS Int. Symp. Dig., June 28-July 2 (1993), vol. 1, pp. 14–17.

Periodic Boundary Conditions — Procedure

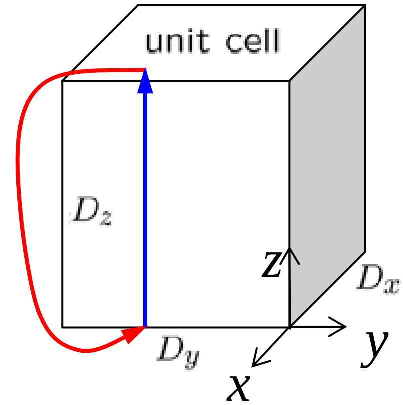

- Excite unit cell at $z = 0$ with $\Psi(t, z), \Psi_i(t, z)$ of modulated plane wave (spectrum near $f = f_0$).
- Propagate initital fields according to FDTD update equations until boundary $z = D_z + \Delta z$.
- Calculate update fields at $z = 0$ by:

$$\Psi(t, 0) = \Re\left\{[\Psi(t, D_z + \Delta z) + \mathrm{j}\, \Psi_i(t, D_z + \Delta z)] \exp(\mathrm{j}\, k_z D_z)\right\},$$

$$\Psi_i(t, 0) = \Im\left\{[\Psi(t, D_z + \Delta z) + \mathrm{j}\, \Psi_i(t, D_z + \Delta z)] \exp(\mathrm{j}\, k_z D_z)\right\}$$

- Repeat updating and wrapping until stationary state is reached.
- Fourier transform stationary time sequence and analyze for resonances (eigenfrequencies) f_ℓ belonging to chosen k_z.
- The spatial distributions associated with the various f_ℓ are the eigenfields or modes of the periodic arrangement.

Ko, W. L.; Mittra, R.: Implementation of Floquet boundary condition in FDTD for FSS analysis. IEEE APS Int. Symp. Dig., June 28–July 2 (1993), vol. 1, pp. 14–17
Harms, P.; Mittra, R.; Ko, W.: Implementation of the periodic boundary condition in the finite-difference time-domain algorithm for FSS structures. IEEE Trans. Antennas Prop. 42 (1994) 1317–1324
Turner, G.; Christodoulou, C.: Broadband periodic boundary condition for FDTD analysis of phased array antennas. IEEE APS Int. Symp. Dig., June 21–26 (1998), vol. 2, pp. 1020–1023